UNIVERSIDADE D
COIMBRA

Adriana António Lemos Gonçalves Malheiro

CROSSTALK BETWEEN PERIVASCULAR ADIPOSE TISSUE AND BLOOD VESSELS IN OBESITY AND TYPE 2 DIABETES

Dissertação no âmbito do Mestrado em Química Medicinal orientada pela Professora Doutora Cristina Maria Tristão Sena e apresentada ao Departamento de Química da Faculdade de Ciências e Tecnologia da Universidade de Coimbra.

Setembro de 2020

Universidade de Coimbra

Faculdade de Ciência e Tecnologia da Universidade de Coimbra

Crosstalk between perivascular adipose tissue and blood vessels in obesity and type 2 diabetes

Adriana António Lemos Gonçalves Malheiro

Dissertação apresentada para provas de Mestrado em Química Medicinal

Trabalho com orientação científica da Professora Doutora Cristina Sena

Setembro de 2020

Agradecimentos

O meu tempo em Coimbra não poderia incluir emoções mais positivas. Este caminho trouxe-me imensas competências em diversas áreas, não só no âmbito profissional como, também, a nível pessoal. No entanto, não poderia deixar de agradecer às pessoas abaixo, que me direcionaram para um futuro melhor.

À Professora Doutora Cristina Sena pela atenção que me deu desde o primeiro dia, por toda a disponibilidade, pelos ensinamentos científicos e, igualmente importantes, humanos. No fundo, por me acolher e por me ter feito sentir concretizada com este projeto.

Ao Marcelo por ter trazido ideias e conhecimentos novos ao laboratório mas, acima de tudo, por ser uma força extra e a razão de boas gargalhadas que vou lembrar com carinho.

À Eduarda e à Joana, que deram um brilho especial à nossa casa.

Ao André, por ter suportado as minhas crises durante este ano tão intenso e por me dar 128 razões para ser melhor.

À Valentina que sempre esteve atenta e a par das minhas novidades e, mesmo estando na ilha distante, só me falhou nos abraços.

Agradeço à minha mãe, ao Leo e ao Pedro, que me deram muito a pensar que davam pouco, que sempre me fizeram perseguir os meus sonhos e sem os quais eu não teria tido coragem de entrar neste projeto. Desculpo-me, no entanto, pelos momentos ausentes e fica a promessa de que darei o meu melhor para vos compensar.

À restante família e amigos, agradeço a paciência nos dias mais difíceis, o amor transmitido e as distrações, que só me fizeram bem. Não poderia sentir-me mais orgulhosa por ter cada um de vós na minha vida.

Para o meu António todas as palavras são poucas. Agradeço por todas as surpresas e todos os minutos livres em que fez de tudo para me encher o coração de bons momentos e memórias, por nunca me deixar baixar a cabeça e pelo orgulho que sente, revestido de amor. O uso do aditivo "e", independentemente das vezes que está presente, não faz jus a todo o apoio diário que recebo. Tudo de bom e de mau que este projeto teve associado foi suportado e erguido por nós. Não teria sido o mesmo sem a sua presença. Agradeço por... ser único.

Dedico este trabalho ao meu irmão, que é o melhor de mim.

Table of contents

List of ilustrations

List of tables

Abbreviations

ACh	acetylcholine
ADMA	asymmetric dimethylarginine
ADRF	adipocyte-derived relaxing factor
AGE	advanced glycation-end product
AI	atherogenic index
ALT	aspartate transaminase
Ang II	angiotensin II
AST	alanine transaminase
ATP	adenosine triphosphate
BAT	brown adipose tissue
BH_4	tetrahydrobiopterin
BSA	bovine serum albumin
CAMs	cell adhesion molecules
CD31	cluster of differentiation 31
CEL	carboxyethyl-lysine
CML	carboxymethyl-lysine
COX	cyclooxygenase
DAB	3,3'- diaminobenzidine
DAG	diacylglycerol
DKA	diabetic ketoacidosis
DM	diabetes *mellitus*
DNA	deoxyribonucleic acid

eNOS	endothelial nitric oxide synthase
ET-1	endothelin-1
FA	fatty acid
FAS	fatty acid synthesis
FFAs	free fatty acids
FMN	flavin mononucleotide
FPG	fasting plasma glucose
Gamma-GT	gamma-glutamyl transferase
GLUT-4	glucose transporter type 4
GPx	glutathione peroxidase
GSH	glutathione
GTT	glucose tolerance test
HDL	high-density lipoprotein
HFD	high-fat diet
HbA1c	glycated hemoglobin
HHS	hyperosmolar hyperglycemic state
HIF-1α	hypoxia-inducible factor-1 alpha
HSL	hormone-sensitive lipase
H_2O_2	hydrogen peroxide
ICAMs	intercellular adhesion molecules
IGF	insulin-like growth factor
IL	interleukins
Indo	indomethacin
iNOS	inducible nitric oxide synthase

IR	insulin receptor
IRS	insulin receptor substrates
ITT	insulin tolerance test
L-arg	L-arginine
LDL	low-density lipoprotein
L-NAME	N^{ω}-Nitro-L-arginine
MAPK	mitogen-activated protein kinase
MG	methylglyoxal
NADH	nicotinamide adenine dinucleotide
NADPH	nicotinamide adenine dinucleotide phosphate
NFE	nitrogen-free extract
NF-κB	factor nuclear kappa B
NO	nitric oxide
NOS	nitric oxide synthase
OGTT	oral glucose tolerance test
$ONOO^-$	peroxynitrite
O_2	molecular oxygen
PAI-1	plasminogen activator inhibitors
PBS	phosphate-buffered saline (pH=7.4)
PDGF	platelet-derived growth factor
PECAM-1	platelet endothelial cell adhesion molecule
PGI2	prostacyclin
PHE	phenylephrine
PI3K	phosphoinositide 3-kinase

PKB	protein kinase B
PKC	protein kinase C
PVAT	perivascular adipose tissue
RAGE	receptor for advanced glycation-end product
ROS	reactive oxygen species
SEM	standard error of the mean
SNP	sodium nitroprusside
SOD	superoxide dismutase
STZ	streptozotocin
TAGs	triacylglycerols
TGF	transforming growth factor
TLR4	Toll-like receptor 4
TNF-α	tumor necrosis factor-alpha
tPA	tissue plasminogen activator
TxA2	thromboxane A2
UCP-2	uncoupling protein-2
uPA	urokinase-type plasminogen activator
VCAMs	vascular cell adhesion molecules
VEGF	vascular endothelial growth factor
VLDLs	very low-density lipoproteins
VSMCs	vascular smooth muscle cells
vWF	von Willebrand factor
W	Wistar
WAT	white adipose tissue

Resumo

A diabetes *mellitus* (DM) é uma patologia metabólica com uma prevalência crescente na sociedade ocidental. A DM é caracterizada por hiperglicémia resultante de defeitos na secreção ou ação de insulina, ou ambos. Por conseguinte, a hiperglicémia crónica está associada, a longo prazo, a danos, disfunção e falha de vários órgãos. A diabetes encontra-se intimamente associada a disfunção endotelial, aterosclerose, dislipidemia e obesidade. A resistência à insulina, que acompanha a obesidade e a diabetes tipo 2, é uma condição na qual as células apresentam resistência à ação da insulina e não são capazes de absorver glicose da corrente sanguínea que, desta forma, conduz a hiperglicémia.

Nos últimos anos, o tecido adiposo perivascular (do inglês, PVAT) tem captado a atenção da comunidade científica devido às suas funções endócrinas e parácrinas como constituinte da parede dos vasos sanguíneos. Desempenha, ainda, um papel fundamental no desenvolvimento de doenças cardiovasculares. Em condições fisiológicas, este tecido sintetiza uma série de moléculas que contribuem para a regulação do tónus vascular e da inflamação local, devido ao equilíbrio entre substâncias vasodilatadoras, como o óxido nítrico, e vasoconstritoras, como a endotelina-1. Por outro lado, em situações patológicas, o PVAT aumenta de volume, torna-se disfuncional e leva a várias complicações micro e macrovasculares.

Este trabalho utiliza dois modelos animais diferentes, com o propósito de estudar o impacto de dietas ocidentais hipercalóricas (dieta rica em gordura e dieta gorda com metilglioxal) no PVAT e avaliar a disfunção endotelial associada. O primeiro modelo animal estuda o impacto da diabetes tipo 2 no PVAT e suas implicações vasculares. O segundo modelo permite fazer uma avaliação de uma dieta rica em gordura com metilglioxal no PVAT e estudar o seu impacto vascular. De facto, os nossos resultados sugerem que a dieta gorda, por si só, induz não só insulinorresistência, como também um grau de disfunção do PVAT bastante considerável. Surpreendentemente, mostrámos alguma similaridade entre os modelos em termos da perda do efeito anticontrátil do tecido adiposo perivascular.

Palavras-chave: diabetes tipo 2, disfunção endotelial, tecido adiposo perivascular, óxido nítrico, endotelina-1.

Abstract

Diabetes *mellitus* (DM) is a metabolic pathology with increasing prevalence in the western society. DM is characterized by hyperglycemia resulting from defects in insulin secretion or action, or both. Therefore, chronic hyperglycemia is, in long-term, associated with damage, dysfunction and failure of various organs. Diabetes is closely linked to endothelial dysfunction, atherosclerosis, dyslipidemia and obesity. Insulin resistance, which accompanies obesity and type 2 diabetes, is a condition in which cells are resistant to insulin action and are unable to absorb glucose from the bloodstream and, thus, lead to hyperglycemia.

Over the last years, perivascular adipose tissue (PVAT) has emerged as an active component of the blood vessel wall, with endocrine and paracrine functions, that regulates vascular homeostasis and that plays a role on the pathogenesis of cardiovascular diseases. In physiological conditions, this tissue synthetizes a variety of adipokines that contribute to regulation of vascular tone and local inflammation, due to the balance between nitric oxide and endothelin-1. On the other hand, in vascular pathologies, PVAT increases in volume, becomes dysfunctional and leads to a series of physiological complications.

This work utilizes two different models with expectations to bring new insights on the field. These two models were used to study the impact of western hypercaloric diets (high-fat diet and fat diet with methylglyoxal) on PVAT and endothelial function. The first animal model evaluates the impact of type 2 diabetes on PVAT and its vascular implications. The second model allows an assessment of a diet rich in fat and methylglyoxal in PVAT to study its vascular outcome. In fact, our results suggest that the fat diet alone induces not only insulin resistance, but also a considerable degree of PVAT dysfunction. Surprisingly, we showed some similarity between the models in terms of the loss of the anticontractile effect of perivascular adipose tissue.

Key words: type 2 diabetes, endothelial dysfunction, perivascular adipose tissue, nitric oxide, endothelin-1.

Chapter 1

Introduction

Chapter 1: Introduction

1.1. Diabetes *mellitus*

Diabetes *mellitus* is a chronic and metabolic disease that occurs either when the pancreas does not produce enough insulin, as in type 1 diabetes, or when the body cannot effectively use the insulin it produces, as in type 2 diabetes. In 2019, approximately 463 million adults were globally diagnosed with diabetes, a number that leans towards to 700 million until 2045. In fact, diabetes is one of the fastest growing health challenges of the 21st century that has nearly tripled over the past 20 years. In addition, the prevalence of this disease in adults, in Portugal, is, at the beginning 2020, 14,2 % (International Diabetes Federation 9th ed., 2019). Moreover, according to the World Health Organization, diabetes was considered the seventh cause of death in 2016.

In diabetes, the hallmark is hyperglycemia due to a disorder in insulin secretion, insulin action, or both. Insulin is the hormone which reduces the glucose level in the blood by binding to insulin receptors, located in cell membranes, in various insulin-responsive tissues (Wilcox, 2005). When activated, the insulin receptors cause vesicles containing glucose transporters (GLUT-4, in skeletal muscle and adipose tissue) to fuse with the plasma membrane, allowing this sugar to be transported into the cell. However, in this pathology, there is a reduction in glucose uptake by tissues, leading to increased levels of glucose outside the cells (Mueckler and Thorens, 2013).

There are several ways to diagnose diabetes, including glycated hemoglobin (HbA1c), fasting plasma glucose (FPG) and oral glucose tolerance test (OGTT). In fact, it is also possible to determine a pre-diabetic state and, thus, control the patient to prevent further advance of the disease. As red blood cells in the human body survive for 8 to 12 weeks before renewal, measuring HbA1c can be used to reflect average blood glucose levels over that period. Therefore, a value between 5,7 and 6,4 % means prediabetes and greater than 6,5 % reflects a diabetic state. Furthermore, if FPG is higher than 125 mg/dL, that is a diagnosis criteria for diabetes, or, somewhere between 100 and 125 mg/dL, prediabetes. Moreover, the OGTT must be greater than 200 mg/dL to declare diabetes or, in the case of prediabetes, a value between 140 and 199 mg/dL. Finally, a random measure of glucose with a value higher than 200 mg/dL with classic symptoms of hyperglycemia, it is probable that the patient has diabetes (American Diabetes Association, 2020).

1.1.1. The endocrine pancreas: the role of insulin

The pancreas is a gland that consists of two major types of secretory tissue, which reflects its dual function. Moreover, it is involved in blood sugar control and metabolism of the body, as well as secretion of substances which help digestion. While the endocrine pancreas produces hormones that regulate blood sugar, such as insulin and glucagon, the exocrine pancreas, on the other hand, produces enzymes involved in food digestion (Röder *et al.*, 2016). Moreover, the endocrine portion consists of islets of Langerhans, which are scattered between the acini and ducts of the exocrine part of the gland. These islets consist of several cell types, including α, β, δ and, in some islets, PP-cells, which secrete glucagon, insulin, somatostatin and pancreatic polypeptide, respectively (Damjanov, 2008; Figure 1). Furthermore, the hormones produced by the islets of Langerhans are the key regulators of the intermediary metabolism of carbohydrates, lipids and proteins (Xavier, 2018).

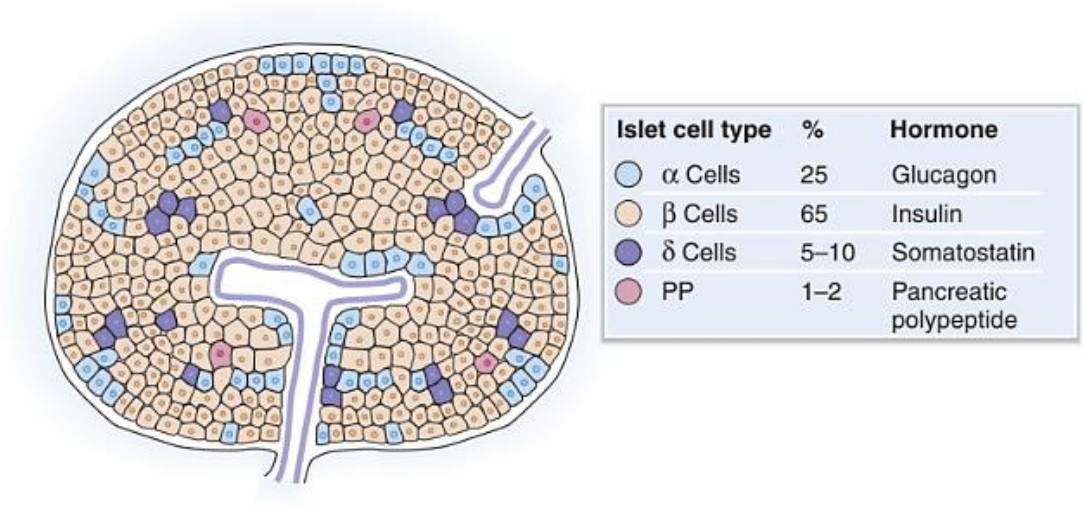

Figure 1: Islets of Langerhans. Insulin-secreting β-cells account for two thirds of all cells in the islets. (Adapted from Damjanov, 2008).

Insulin is formed from proinsulin, through the cleavage of the C peptide, leading to a short polypeptide composed of 51 amino acids, which is arranged in two chains linked together by two disulfide bonds (Damjanov, 2008). Its secretion is stimulated by high blood glucose, amino acids and lipids and by intestinal secretin, which is released during feeding. On the opposite, insulin release is inhibited by epinephrine, somatostatin and decreased food intake. The hormone acts, mainly, on peripheral tissues such as liver, muscle and adipose tissue (Figure 2; Samuel and Shulman, 2016).

At the liver, insulin promotes the storage of glucose in the form of glycogen, while the excess of this carbohydrate is used for the synthesis of lipids, which are stored on hepatocytes in the form of triacylglycerols (TAGs; Rui, 2014). Insulin also affects lipid metabolism by inhibiting ketogenesis and promoting synthesis of very low-density lipoproteins (VLDLs). When VLDLs are released into the bloodstream they are taken up by muscle or fat cells and stored or used for energy production. Finally, insulin stimulates the uptake of amino acids into hepatocytes (Tkacs *et al.*, 2020).

On the other hand, in the muscle, this polypeptide promotes the uptake of glucose from the blood and glycogen synthesis. It also inhibits glycogen phosphorylase to slow down glycogenolysis. Lastly, it stimulates the entry of amino acids into muscle cells and protein synthesis (Röder *et al.*, 2016).

In fat tissue, insulin signaling enhances lipid storage in adipocytes. In fact, it decreases the rate of lipolysis, promotes fatty acids (FA) esterification, therefore stimulating triacylglycerol synthesis. In addition, insulin is also responsible for increasing protein synthesis in the adipose tissue (Czech *et al.*, 2013).

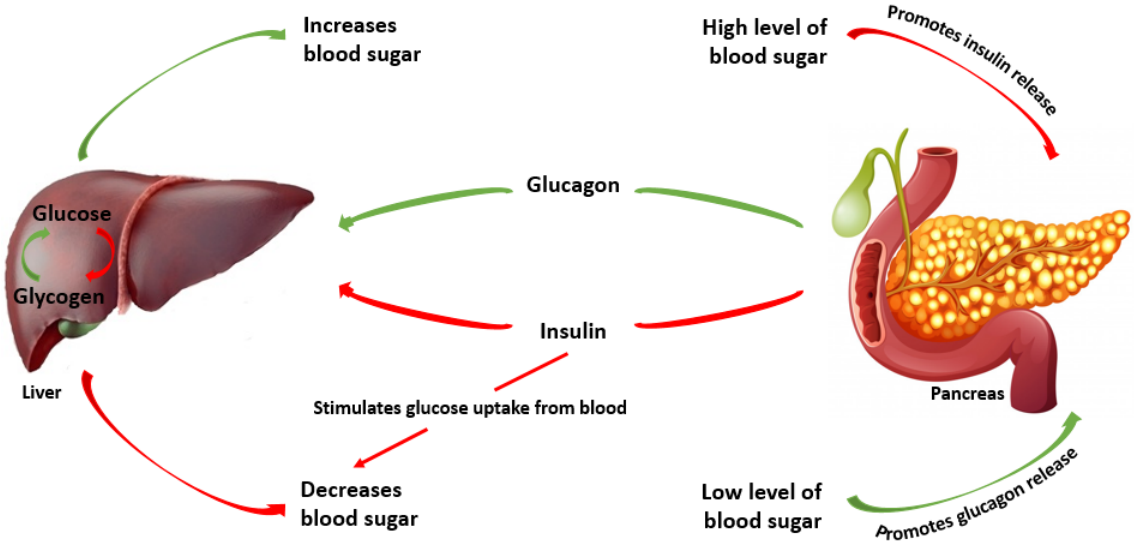

Figure 2: Regulation of blood sugar and balance between hormones insulin and glucagon, stimulating formation or degradation of glycogen, respectively. Besides affecting the liver, insulin stimulates the uptake of glucose by muscles, adipose tissue and kidneys.

1.1.2. Diabetes *mellitus* type 1

Although the highest prevalence is assigned to type 2 diabetes, about 5 to 10 % corresponds to type 1 diabetes (International Diabetes Federation 9th ed., 2019). In type 1 diabetes, much more common in children, the body can't produce insulin to give answer to its needs. The most common etiology is due to a genetic abnormality that causes a loss of self-tolerance among T-cells that specifically targets beta cells antigens, and, thus, type 1 diabetes can also be considered an autoimmune disease (Bluestone *et al.*, 2010).

As insulin is not produced, glucose is not transported into insulin-dependent cells, therefore they cannot generate energy and, in response, adipose tissue starts breaking down fat, a process called lipolysis, and muscle tissue breaks down proteins, also known as proteolysis (Wilcox, 2005). Both effects result in weight loss and such catabolic process causes polyphagia, a condition where patients feel constantly hungry. Even knowing that people with type 1 diabetes are unable to produce their own insulin, they can still respond to the hormone. This way, the treatment for this pathology involves lifelong insulin therapy (American Diabetes Association, 2020).

1.1.3. Diabetes *mellitus* type 2

In type 2 diabetes, the pancreas produces insulin, but there are defects in insulin secretion, insulin action, or both (Cantley and Ashcroft, 2015). In fact, insulin resistance is a condition frequently associated with it, which is characterized by an inability for cells to absorb glucose from the bloodstream due to a lack of sensitivity to insulin. Some risk factors for type 2 diabetes include obesity, lack of exercise and hypertension, although the exact pathologic mechanisms are still being explored. Moreover, as many obese people are not diabetic, we must consider that genetic factors also play a major role in the etiology of type 2 diabetes (Herder and Roden, 2010). Even so, obese people are more likely to develop diabetes, so it can be said that an excess of adiposity may cause the release of free fatty acids (FFAs) and adipokines, which are signaling molecules that can cause inflammation and that might be related to insulin resistance (Jung and Choi, 2014).

In type 2 diabetes, due to insulin resistance, tissues do not respond to regular levels of insulin. Consequently, the normal response from the organism involves producing an increased amount of this hormone, in order to compensate the effect (Guilherme *et al.*, 2008). Therefore, hyperplasia and hypertrophy of β-cells occur. Although, this mechanism of compensation only

works for a short period of time and, after that, physiological complications, such as dysfunction, hypotrophy and hypoplasia, tend to occur, leading to pancreatic β-cells destruction (Cerf, 2013).

Type 2 diabetes is associated with elevated levels of oxidative stress, glycation and endothelial dysfunction, which are further aggravated by diets rich in fats (Morón *et al.*, 2019). High glucose levels in the blood can cause other problems that may be indirectly associated. In fact, when this sugar is filtered in kidneys, some of it can be directed to urine, a process called glycosuria. Consequently, since glucose has an osmotic gradient associated, then water tends to follow it, leading to polyuria and, therefore, to polydipsia, a process referring to the need of water intake due to dehydration (Fayfman *et al.,* 2017).

1.1.4. Complications associated with diabetes

Maintaining blood glucose levels at, or close to, normal can help delay or prevent diabetes complications. In this topic, we can differentiate acute from chronic complications of the disease, which can be the same or different for both types 1 and 2 diabetes (Umpierrez *et al.,* 2002). In general, the acute complications include diabetic ketoacidosis (DKA), hyperosmolar hyperglycemic state (HHS) and, although rare, hypoglycemia due to several diabetes treatments. On the other hand, chronic complications comprise microangiopathy, which are the result of damage in small blood vessels, macrovascular problems and abnormal immune responses (Chawla *et al.,* 2016).

One very serious complication related to type 1 diabetes is, precisely, DKA, that occurs due to the increased level of ketone bodies in blood coming from lipolysis, since tissues breakdown fat. In addition, by the transporter H^+/K^+ ATPase, cells can intake protons in exchange for potassium which, in a case of ketoacidosis, leads to increased level of potassium in the blood. This effect is known as hyperkalemia and it can be related to muscle contraction modifications. In sum, ketoacidosis can easily become severe enough to cause hypotension, shock or even death (Kitabchi *et al.*, 2009).

Unlike type 1 diabetes, hyperinsulinemia occurs in type 2 diabetes. The balance between insulin and glucagon is such that DKA does not usually happen (Wilcox, 2005). Having said that, HHS is much more likely to happen in type 2 diabetes than in type 1 and it causes increased plasma osmolarity and concentration of the blood. As this happens, intracellular water tends to move to circulation, increasing urination and, subsequently, total body dehydration. In addition, this last one can be a dangerous complication, especially for the brain, since it can lead to mental status changes (Umpierrez *et al.,* 2002).

Overtime, diabetes can cause damage in microvasculature. Regarding microangiopathies, the most common are retinopathy, neuropathy and nephropathy. This last one regards severe damages in afferent and efferent arterioles and the glomerulus itself, in the kidney, which can lead to nephrotic syndrome and, ultimately, the need for dialysis (Madsen and King, 2013). In arterioles is common to find hyaline deposits in the endothelium, a process called hyaline arteriolosclerosis, which makes the vessel hard and inflexible. In capillaries, the basement membrane can thicken and make it harder for oxygen to get into the tissues, causing hypoxia (Cade, 2008).

Macrovascular problems, in turn, when associated with atherosclerosis, are mostly related to cardiovascular disease. The most common complications are cerebrovascular disease, coronary artery disease and strokes, which are the major contributors to morbidity and mortality for patients with diabetes (Petrie *et al.*, 2018; Leon and Maddox, 2015).

1.2. Obesity

Obesity is a medical condition mostly caused by excessive intake of food, lack of physical activity and genetic susceptibility, which has been increasing overtime. In fact, worldwide obesity has nearly tripled since 1975 and, in 2016, 39 % of adults were overweight and 13 % were obese. Moreover, in 2019, about 38 million children under the age of 5 were overweight or obese (World Health Organization, 2020).

Obesity is characterized by the enlargement of adipose tissue, that is associated with a hypertrophy of fat cells, hyperplasia, or a combination of the two (Longo *et al.*, 2019). This state of overweight carries many complications, including cardiovascular diseases, insulin resistance and type 2 diabetes, due to an unbalanced or, more likely, an overproduction of pro-inflammatory adipokines and FFAs (Villarroya *et al.*, 2018).

Adipokines, or adipocytokines, are cell signaling proteins secreted by the adipose tissue. Leptin, tumor necrosis factor-alpha (TNF-α) and a few interleukins are examples of adipokines that are oversecreted in obesity and type 2 diabetes, due to the increased volume of adipose tissue, dysfunction and inflammation (Park and Ahima, 2015). On the other hand, adiponectin is one of the adipokines that has a basal secretion lower than the normal levels. In fact, the majority of oversecreted adipokines are, indeed, harmful and related to inflammatory processes. Obesity is, therefore, regarded as a state of systemic, chronic, low-grade inflammation linked to insulin resistance (Itoh *et al.*, 2011).

In obesity, the adipose tissue secretes several chemotactic factors, which are responsible for stimulating cell migration, to induce macrophage infiltration. Furthermore, macrophages enhance the inflammatory changes through the crosstalk with parenchymal adipocytes (Itoh et al., 2011). For example, the macrophage-derived TNF-α induces the release of saturated fatty acids from adipocytes via lipolysis, which, in turn, induces inflammatory changes in macrophages via Toll-like receptor 4 (TLR4). Such a paracrine loop between adipocytes and macrophages constitutes a vicious cycle, thereby accelerating adipose tissue inflammation (Surmi and Hasty, 2008). The interaction between adipocytes and macrophages results in intense upregulation of pro-inflammatory adipokines and significant downregulation of anti-inflammatory adipokines, which leads to the development of obesity-related complications in multiple organs, such as hepatic steatosis, a condition where excess fat accumulate in the liver, and atherosclerosis (Jung and Choi, 2014).

1.3. Adipose tissue

The adipose tissue is a metabolically dynamic organ responsible for the storage of energy in the form of lipids. Although, it was recently described also as an endocrine organ capable to synthesize various biologically active compounds that regulate metabolic homeostasis (Villarroya *et al*., 2018). As it is involved in regulatory processes through all endocrine, paracrine and autocrine signals, the adipose tissue affects the liver, pancreas, skeletal muscle, immune system and endothelium, among others. There are several types of adipose tissue, including brown adipose tissue (BAT), white adipose tissue (WAT) and beige. Perivascular adipose tissue (PVAT), an ectopic fat depot directly adherent to blood vessels, is one of the many adipose tissue depots of the body (Hildebrand *et al.*, 2018).

BAT is characterized by an increased number of mitochondria and an extensive vascularization, which provides the brown color to the tissue. Its main role lies on generating energy in the form of heat (thermogenesis) by oxidizing fatty acids, instead of storing it and supply to other cells (Ravussin and Galgani, 2015). Brown adipocytes have a polygonal shape with an oval and centered nucleus on a large cytoplasm that contains multiple and small lipid droplets. In addition, it appears that BAT activity protects the organism against hyperglycemia and hyperlipidemia by draining circulating metabolic substrates for oxidation (Coelho *et al*., 2013).

On the other hand, WAT stores fat, maintains the body temperature and, among other, produces cytokines, hormones and growth factors. White adipocytes have variable shape with a peripheral and flat nucleus on a thin cytoplasm that contains a single large lipid drop. Unlike BAT, WAT is poorly vascularized and innervated, although, both require endocrine and neural

communication with the brain (Hernández *et al.*, 2016). A well-defined balance between fat synthesis (lipogenesis) and fat breakdown (lipolysis) is very important to maintain homeostasis. Lipogenesis occurs, mostly, on cytosol of hepatocytes and adipocytes. Moreover, it is regulated by insulin and the nutrition state of the organism (Saponaro *et al.*, 2015). On the other hand, lipolysis is inhibited by insulin and activated by epinephrine and glucagon. In addition, HSL (Hormone-Sensitive Lipase) is triggered, in the adipose tissue, to promote the hydrolysis of triacylglycerol in glycerol and fatty acids (Duncan *et al.*, 2010). The β-oxidation of fatty acids, on mitochondria, is the following catabolic pathway, in which results acetyl coenzyme A, therefore used as a substrate in several reactions, and ATP (Houten and Wanders, 2010).

1.3.1. Perivascular adipose tissue

Due to its specific location and function, we can identify PVAT with BAT- and WAT--like features. This tissue surrounds large arteries and veins, small and resistance vessels, and skeletal muscle microvessels. Although, other pulmonary and the cerebral vasculature are free of PVAT (Brown *et al*., 2014; Gil-Ortega *et al.*, 2015). Large vessels are separated from PVAT by an anatomical barrier rich in collagen bundles, elastin networks, vascular smooth muscle cells (VSMCs), fibroblasts, autonomic nerve endings and *vasa vasorum*. In small vessels and microvessels, however, PVAT is an integral part of the vascular wall without laminar structures or any organized barrier separating PVAT from the adventitia (Xia and Li, 2016). In this case, perivascular tissue is believed to cause stronger effects on the vessel wall than the factors released by WAT, either by direct diffusion, via *vasa vasorum* or via small conduits. Its main function relies in providing mechanical support to the vessels and regulating vascular tension and torsion (Dam *et al.*, 2017).

For a long time, the effect and function of PVAT was neglect. Although, there are, nowadays, many reasons to believe that this tissue releases biologically active molecules that comprehend both endocrine and paracrine effects on vessels (Szasz and Webb, 2012). In physiological conditions, PVAT has beneficial effects on the vessels because it attenuates agonists-induced vasoconstriction by releasing vasoactive molecules, including hydrogen peroxide, angiotensin, adiponectin, nitric oxide and leptin. Therefore, it can be stated that perivascular adipose tissue has anticontractile properties (Dam *et al.*, 2017).

In order to study the mechanism of action of substances secreted by PVAT, it was taken, for starter, the example of adipokines. Although a large number of these cytokines are known as vasoactive, there is one that plays a major role in vasoregulation (Xia and Li, 2016). The adipocyte-derived relaxing factor (ADRF), not yet identified, has been shown to relax arteries by

opening voltage-dependent K^+ channels (K_v) on membranes of smooth muscle cells (Gollasch, 2012). Acting through the same mechanism, it is also considered the NO, which can be stimulated by angiotensin 1-7 that, in turn, is released by PVAT. Moreover, adiponectin is a hormone secreted by perivascular adipose tissue which, from multiple mechanisms, induces vasodilation (Maenhaut and Voorde, 2011). Leptin is a very important hormone produced by adipocytes, mainly WAT, that regulates hunger and energy expenditure. In fact, leptin also regulates neuroendocrine function and immune responses. Furthermore, it is a vasorelaxant agent produced by PVAT that acts through different mechanisms (Park and Ahima, 2015).

Like the other adipose tissues, PVAT expands in obesity due to cellular hypertrophy, immune cell infiltration and extracellular matrix overproduction. As a result, not only the anticontractile effect is lost, but there is also hypoxia (possibly due to hypertrophy of the cells with consequently reduction of angiogenesis), oxidative stress and overproduction of pro-inflammatory adipokines, other cytokines and chemokines by infiltrated immune cells. Moreover, these substances contribute to atherosclerosis development (Figure 3; Qi *et al.*, 2018).

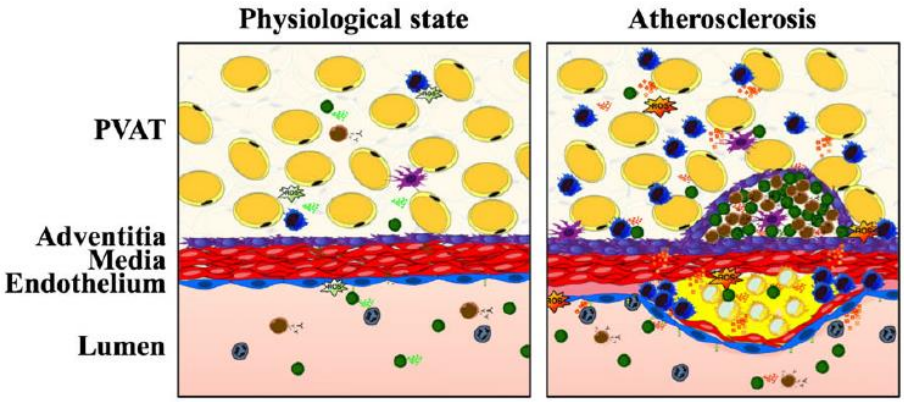

Figure 3: Role of PVAT and vascular compartments in the normal physiological state (left panel) and in the development of vascular pathology atherosclerosis (right panel), with accumulation of inflammation-related molecules in the adventitia layer (Adapted from Nosalski and Guzik, 2017). PVAT- perivascular adipose tissue.

It appears that PVAT may take on different extents of BAT- or WAT-like phenotypes in response to temperature, nutrition status and obesity. This flexibility is associated with distinct extents of macrophage infiltration and pro-inflammatory signaling (Hernández *et al.*, 2016). In fact, the extent of BAT-like phenotype in PVAT is, more likely, meant to protect the vasculature from inflammation by reducing the secretion of pro-inflammatory signals. Moreover, the secretion of presumed vasoprotective signals (adipokines secreted by BAT) may help protect vascular function against atherosclerosis (Qi *et al.*, 2018). Although, the general capacity of PVAT with BAT- like features is reduced as obesity induces its whitening process (Villarroya *et al.*, 2018; Hildebrand *et al.*, 2018). Furthermore, the phenotype of thoracic PVAT resembles BAT, whereas abdominal PVAT is more like WAT (Brown *et* al., 2014; Villarroya *et al.*, 2018).

1.3.2. Insulin resistance

Insulin, as explained before, is a peptide hormone that consists of two chains. Its receptor (IR) is a dimer with two identical subunits: two α subunits, that move together to form the binding site for one molecule of insulin, and two β subunits, which are two domains of protein kinase. At the time the receptor is activated, the phosphorylation of tyrosine residues takes place, in which results a cascade of phosphorylation of signaling proteins, such as insulin-receptor substrates (IRS; Berg *et al.*, 2012).

Classically, insulin signaling results in vasodilation by increasing nitric oxide (NO) production and its bioavailability. However, in conditions of insulin resistance, it promotes vasoconstriction and vascular proliferation (Manrique *et al.*, 2014). Two signaling pathways of insulin must be considered: the pathway dependent of phosphoinositide 3-kinase (PI3K), which mediates insulin's metabolic and vascular actions; and the pathway dependent of mitogen-activated protein kinase (MAPK), which mediates insulin's mitogenesis and cell growth actions (Boucher *et al.*, 2014).

There are two classes of serine/threonine kinases which are known to act downstream of PI3K, namely the serine/threonine kinase AKT, also known as protein kinase B (PKB), and protein kinase C (PKC). The expression of AKT in adipocytes results in increased glucose transport and persistent transport of GLUT4 to cell membranes (Liao and Hung, 2010). Moreover, AKT also phosphorylates the enzyme that synthesizes nitric oxide (NOS), leading to an increased action and production of NO, resulting in vasodilation (Pessin and Saltiel, 2000). On the other hand, activation of MAPK pathway induces vasoconstriction by increasing secretion of endothelin-1 (ET-1), stimulating the expression of adhesion molecules such as VCAM-1 and E-selectin, and inducing production of reactive oxygen species (ROS). Together, and duly balanced, these two pathways maintain vascular homeostasis and regulate the vascular response to insulin (Potenza *et al.*, 2009). In pathological conditions, however, it is noticed that the activity of the PI3K pathway is reduced, contrasting with the MAPK pathway, which has increased activity (Walker *et al.*, 2013).

Insulin resistance occurs when normal circulating concentrations of the hormone are insufficient to regulate these processes appropriately (Figure 4; Wilcox, 2005). Thus, by definition, insulin resistance is a defect in signal transduction and it is associated with metabolic abnormalities that include glucotoxicity, lipotoxicity and inflammation due to an increased concentration of FFAs, glycerol, hormones, cytokines and pro-inflammatory substances, that also lead to endothelial dysfunction (Muniyappa and Sowers, 2013).

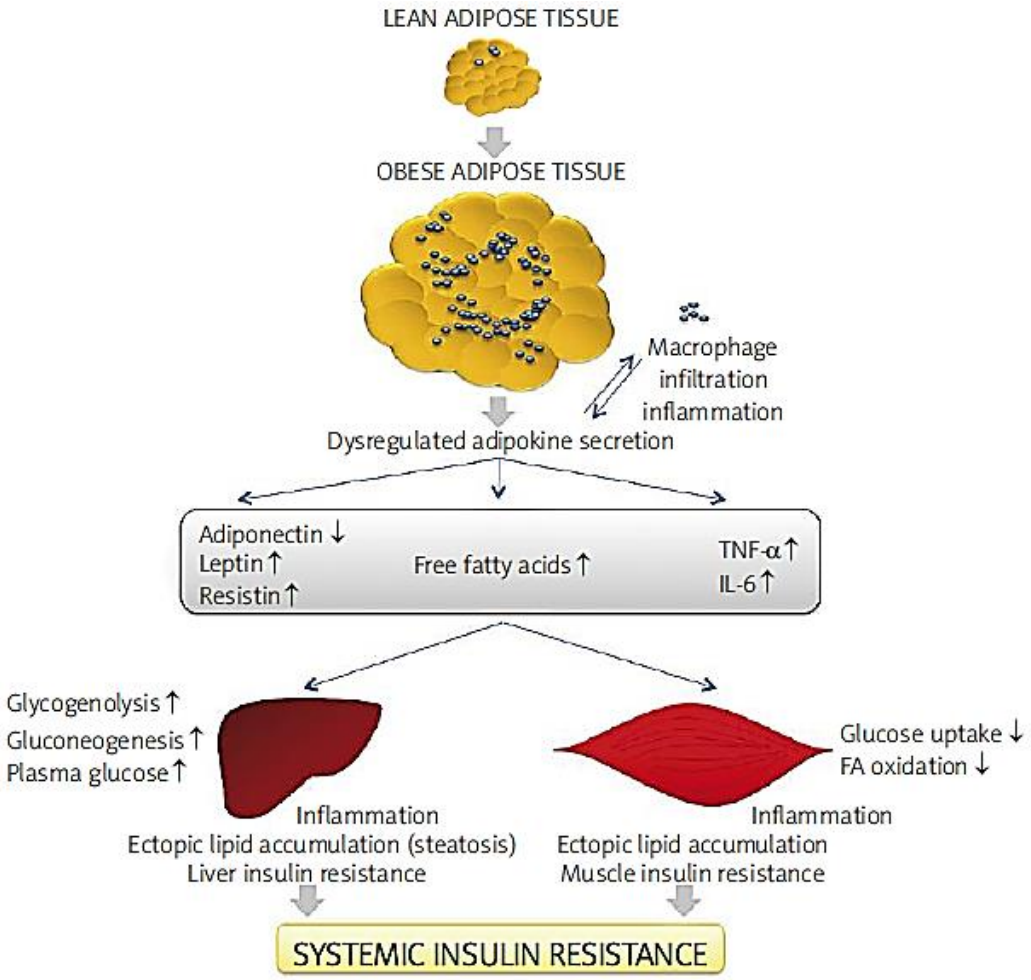

Figure 4: Systemic insulin resistance due to expansion of adipose tissue, which leads to impaired secretion of adipokines, therefore creating a chronic state of general inflammation. (Adapted from Coelho *et al.*, 2013). TNFα- tumor necrosis factor-alpha. IL-6- interleukin 6.

On a healthy subject, there is a continuous feedback relationship between β-cells and the insulin-sensitive tissues. If adipose tissue, liver, and muscles demand glucose, this will lead to increased insulin supply by β-cells. Any unbalance in this process results in a dysregulation of glucose levels and the development of a metabolic disorder (Ormazaval *et al.*, 2018). If β-cells are healthy, there is an adaptive response to insulin resistance, which leads to the maintenance of normal levels of glucose. By contrast, when pancreatic β-cells are impaired, abnormal glucose tolerance or abnormal fasting glucose may develop, and it may even be followed by the development of type 2 diabetes (Al-Goblan *et al.*, 2014).

1.4. Endothelium

The endothelium is a monolayer of endothelial cells facing the interior of blood and lymphatic vessels, forming an interface between the lumen and the vessel wall (Genge *et al.*, 2019). Endothelial cells not only act as a barrier, but they can also adjust the vascular tone, by acting on smooth muscle cells, produce factors related to coagulation and fibrinolysis, regulate adhesion and permeability and control cell growth and differentiation. Nevertheless, these cells activity slightly differ in large conduit vessels, resistance vessels, pre-capillary arterioles and capillaries (Potenza *et al.*, 2009).

Concerning the modulators of the vascular tone, we must consider vasodilators and vasoconstrictors. The most relevant vasodilator, in large blood vessels, is nitric oxide, which is produced by endothelial nitric oxide synthase (eNOS) under conditions like shear stress and due to signaling molecules, such as bradykinin, vascular endothelial growth factor (VEGF), insulin and serotonin (Michel and Vanhoutte, 2010). Besides NO, products of the arachidonic acid metabolism, generated by cyclooxygenase (COX) system, also participate in vasodilation. Prostacyclin (PGI2) is a prostaglandin with vasodilating properties associated with regulation of local blood flow (Majed and Khalil, 2012). On the other hand, some vasoconstrictor factors produced by endothelial cells are angiotensin II (Ang II), thromboxane A2 (TxA2) and, the most vasoactive peptide, endothelin-1. Moreover, any dysregulation of ET-1 synthesis, release or activity is associated with vascular complications. In fact, together with a disruption on NO bioavailability, ET-1 may be involved in endothelial dysfunction (Kolluru *et al.*, 2011).

The endothelium produces both anti-coagulant and pro-coagulant factors. Inhibition of the clotting process and fibrinolysis are regulated essentially by three endothelial-derived factors: thrombomodulin, which reduces blood coagulation by converting thrombin to an anti-coagulant enzyme (Yau *at al.*, 2015); urokinase-type plasminogen activator (uPA), which activates plasmin and triggers a proteolytic cascade that, depending on the physiological environment, participates in thrombolysis or extracellular matrix degradation; and tissue plasminogen activator (tPA), that catalyzes the conversion of plasminogen to plasmin (Deryugina and Quigley, 2012). To promote coagulation, the most important molecules are von Willebrand factor (vWF), which function holds for binding to other proteins and help in platelet adhesion to wound sites; plasminogen activator inhibitors (PAI-1), which is the principal inhibitor of tPA and urokinase; and platelet tissue factor, a protein responsible for converting prothrombin to thrombin (Hinsbergh, 2012).

Regarding adhesion and permeability, many molecules produced by endothelial cells are able to regulate these properties. E-selectins are a family of endothelial cell adhesion molecules (CAMs) that play an important role in inflammation and mediate the adhesion of tumor cells to

endothelial cells, by binding to E-selectin ligands on the tumor cells (Barthel *et al.*, 2008). In addition, intercellular adhesion molecules (ICAMs) and vascular cell adhesion molecules (VCAMs) are important in inflammation, immune responses and in intracellular signaling events, since they bind immune cells to the vascular endothelium (Galley and Webster, 2004). Finally, platelet endothelial cell adhesion molecule (PECAM-1), also known as CD31, is a cell adhesion molecule which is required for leukocyte trans-endothelial migration under most inflammatory conditions (Privratsky *et al.*, 2010).

1.4.1. Endothelial dysfunction

The term endothelial dysfunction refers to a condition in which the endothelium loses its physiological properties. In fact, the pathogenesis is quite extensive but, above all, the reduction of NO bioavailability is the most important contributor factor for endothelial damage in the setting of diabetes *mellitus* and insulin resistance (Kubisz *et al.*, 2015). This decline may result from decreased eNOS protein expression, reduced or insufficient amounts of eNOS substrates and/or co-factors, or accelerated NO degradation (Potenza *et al.*, 2009).

Additionally, endothelial dysfunction is characterized by reduced vasodilation, hemodynamic dysregulation, impaired fibrinolytic ability, enhanced turnover, overproduction of growth factors, increased expression of adhesion molecules and inflammatory genes, excessive generation of ROS, increased oxidative stress and, consequently, enhanced permeability of the cell layer (Sena *et al.*, 2013). A dysfunctional endothelium is the starting point to initiate vascular dysfunction, leading to several pathologic conditions including and micro and macrovascular complications, such as atherosclerosis (Sena *et al.*, 2018).

1.4.2. Causes and mechanisms underlying endothelial dysfunction

Metabolic conditions like hyperglycemia, excess FFAs release and insulin resistance in diabetes can independently participate in endothelial dysfunction, oxidative stress, low-grade inflammation and platelet hyperactivity by triggering several intracellular mechanisms (Zhang *et al.*, 2012).

a. Hyperglycemia

The state of hyperglycemia induces oxidative stress mainly because increased glycolysis results in higher NADH production and increased electron transfer through the electron transport chain on mitochondria. This results in accumulation of several intermediates, which can transfer

an electron to molecular oxygen to form $O_2^{\bullet-}$ (Figure 5; Romero *at al.*, 2014). This highly reactive compound can react with NO to form peroxynitrite ($ONOO^-$), which has harmful effects on vascular function, including lipid peroxidation, protein nitrosylation and DNA fragmentation (Aprioku, 2013). Like a cycle, $ONOO^-$ can react with the eNOS co-factor, tetrahydrobiopterin (BH_4). With insufficient concentrations of BH_4, eNOS becomes uncoupled and transfers electrons to molecular oxygen instead of L-arginine, to produce superoxide rather than NO (Zhang *at al.*, 2013).

In addition, the hyperglycemic state is related to increased concentration of diacylglycerol (DAG) by the activation of phospholipase C, D or from *de novo* synthesis. This molecule is responsible for the activation of PKC isoforms which, in turn, inhibit the activity of the PI3K/PKB pathway, thereby limiting subsequent phosphorylation of eNOS and, consequently, NO production in response to insulin (Boucher *et al.*, 2014). Moreover, PKC-dependent activation of NAD(P)H oxidase is also a significant source of $O_2^{\bullet-}$ in diabetes, due to increased superoxide anion production from the mitochondrial electron transport chain (Potenza *et al.*, 2009).

Furthermore, hyperglycemia is the initiating event in the formation of advanced glycation-end products (AGEs), a group of modified proteins, lipids, and nucleic acids formed by non-enzymatic reaction between sugars and amines (Luévano-Contreras *et al.*, 2017). Accumulation of AGEs alters the functional properties of matrix components and mediates cellular changes. Thereby, binding of AGEs to their receptor, RAGE, increases intracellular enzymatic superoxide production and promotes macrophages-mediated inflammation in the vessel wall (Singh *et al.*, 2014). Furthermore, AGEs decrease NO bioavailability and eNOS expression by accelerating eNOS mRNA degradation. Moreover, by activation of NF-κB (factor nuclear kappa B) pathways, AGEs also enhance the expression of ET-1 in endothelial cells, therefore altering the balance between NO and ET-1 to favor vasoconstriction and endothelial dysfunction (Liu *et al.*, 2017).

Finally, glucotoxicity induces a low-grade pro-inflammatory condition, manifested with increased activation of pro-inflammatory transcription factor NF-κB and subsequent amplified expression of pro-inflammatory cytokines, including TNF-α, several interleukins (IL), adhesion molecules and other factors regulating apoptosis and cell proliferation (Collier *et al.*, 2008).

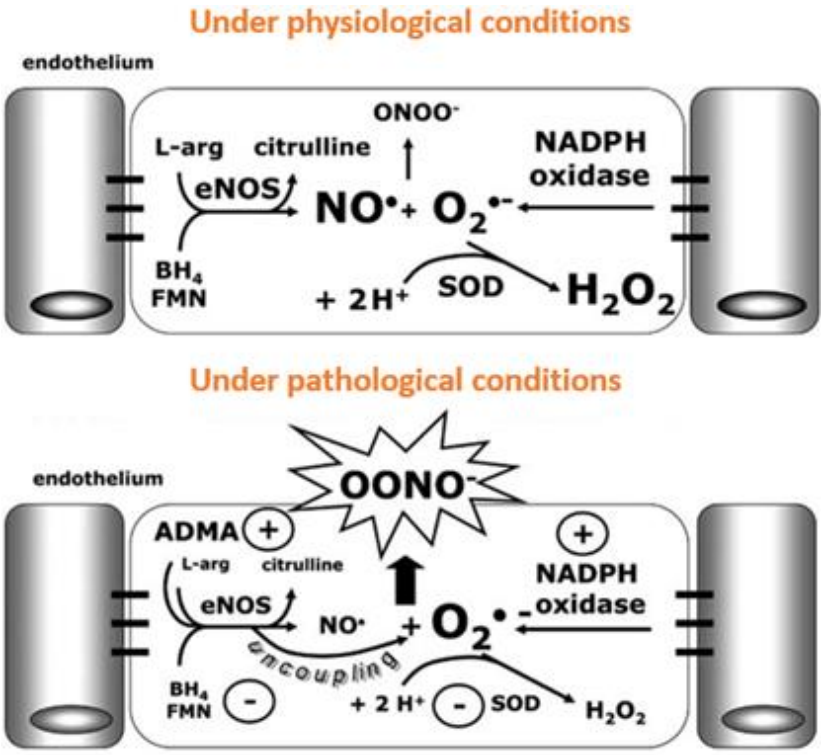

Figure 5: Redox reaction balance in endothelial cells under both physiological and pathological conditions. When production of superoxide anion exceeds the physiological scavenging ability of endothelial cells, this highly reactive intermediate reacts with NO to form peroxinitrite, strong oxidants that alter structure and function of several cellular components (Adapted from Potenza *et al.*, 2009). $ONOO^-$- peroxynitrite. L-arg- L-arginine. eNOS- endothelial nitric oxide synthase. BH_4- tetrahydrobiopterin. FMN- flavin mononucleotide. NAD(P)H- nicotinamide adenine dinucleotide phosphate. $NO^•$- radical nitric oxide. $O_2^{•-}$- superoxide anion. SOD- superoxide dismutase. H_2O_2- hydrogen peroxide. ADMA- asymmetric dimethylarginine.

b. Free fatty acids

Excessive release from adipose tissue and diminished uptake by skeletal muscles increase circulating levels of FFAs in diabetes. Lipotoxicity by FFAs may impair endothelial function by increasing the production of ROS, pro-inflammatory signaling and activation of PKCs (Martins *et al.*, 2012). Furthermore, FFAs induce ROS production on vasculature via mitochondrial uncoupling and by increasing the expression and protein content of NADPH oxidases. These species, reacting with NO, lead to the production of peroxynitrite that damage endothelial cells, like in the hyperglycemic state (Newsholme *et al.*, 2007).

Indeed, overexpression of uncoupling protein-2 (UCP-2) improves the impaired vascular relaxation and endothelial cell apoptosis induced by ROS-mediated FFA toxicity. Increased ROS in response to FFAs also activates NF-κB, which, further, stimulates the production of other pro-inflammatory cytokines, including TNF-α and IL-6 (Boden *et al.*, 2005).

Increased oxidation of fatty acids, derived, in part, from insulin resistance leads to oxidative stress in diabetic macrovasculature, while in microvascular ROS are derived mainly from intracellular hyperglycemia. In both cases, under diabetic conditions, oxidative stress seems to be the common mechanism that triggers vascular dysfunction (Pitocco *et al.*, 2013). Progressive and long-term vascular complications of diabetes include cardiovascular disease, chronic renal failure, retinal damage, neuropathy and poor wound healing (Bento *et al.*, 2010).

c. Insulin resistance

Metabolic insulin resistance, as previously mentioned, refers to a decreased ability of insulin to promote glucose uptake in skeletal muscle and adipose tissue and to suppress gluconeogenesis. Normally, insulin stimulates NO production in endothelial cells by activating eNOS via PI3K pathway (Wilcox, 2005). In a state of insulin resistance, this pathway is impaired, and the production of NO is diminished. Instead, insulin resistance results in activation of MAPK pathway, therefore increasing secretion of endothelin-1 and, consequently, inducing vasoconstriction. Moreover, the insulin resistance state also enhances PAI-1 and CAMs expression (Muniyappa and Sowers, 2013).

In addition to the direct effects of insulin resistance on the endothelium, it also stimulates VSMC proliferation and migration and, in adipose tissue, it is associated with excessive release of FFAs, which evokes pathogenic gene expression through PKC activation and increased oxidative stress (Sena *et al.*, 2013). Ultimately, insulin resistance and type 2 diabetes are associated with low-grade inflammation, as shown on Figure 4, being reflected in increased serum levels of TNF-α, IL-6, ET-1 and PKC, also related to endothelial dysfunction (Natali *et al.*, 2006).

1.4.3. Advanced glycation-end products

Advanced glycation-end products, as mentioned before, result from non-enzymatic modification of proteins and lipids by sugars. Diabetic patients usually have higher AGE levels when compared to healthy individuals. Under physiological conditions, endogenous formation of AGEs occurs slowly and affects predominantly long-life molecules, which is also why it is associated with the aging process and age-related diseases, such as cardiovascular complications of diabetes, neurodegenerative diseases and connective tissue disorders (Fournet *et al.*, 2018). Furthermore, these products tend to accumulate continuously on vessel walls and they are present in the intima, media and adventitia, prevalently in diabetes (Rodrigues *et al*., 2014).

AGEs are a very heterogeneous group of molecules. Since the discovery of the first glycated protein, glycated hemoglobin in diabetes, numerous other AGEs have been detected (Gkogkolou and Böhm, 2012). Carboxymethyl-lysine (CML), pentosidine and carboxyethyl--lysine (CEL) are some examples of glycation end-products. A very important AGEs precursor, methylglyoxal (MG), is a 1,2-dicarbonyl compound which is generated either endogenously by cell metabolism, glucose oxidation and lipid peroxidation, or by degradation of carbohydrates in foods (Nigro *et al.*, 2019). Such highly reactive dicarbonyl attacks lysine, arginine and cysteine residues of long-life proteins, like collagens, to form irreversible AGEs (Sena *et* al., 2012).

Besides glycation, this compound may also interact with RAGE, initiating intracellular signaling pathways that lead to activation of NF-κB and, therefore, to inflammation and cell death. These receptors, when binding AGEs, contributes to age- and diabetes-related chronic inflammatory diseases, such as atherosclerosis, asthma, arthritis, myocardial infarction, nephropathy, retinopathy and neuropathy (Bongarzone *et al.*, 2017).

Glycation, for example, increases glycoconjugates and fibrosis in adipose tissue, which complicates its pathways of adaptation to hypoxia, angiogenesis and expandability. Thereby, accumulation of glycated products during adipose tissue expansion is associated with impaired insulin signaling and decreased adiponectin secretion (Rodrigues *et al*., 2017). Moreover, these factors contribute for systemic alterations, namely decreased glucose tolerance, hyperinsulinemia, increased FFAs and skeletal muscle insulin resistance (Ormazabal *et al.*, 2018). Furthermore, the major matrix proteins, like collagen, elastin, vitronectin and laminin, are targets to be glycated via formation of crosslinks. Additionally, this crosslinking increases the extracellular matrix area, which results in increased stiffness of the vasculature (Sena *et al.*, 2012).

Although also possible through other ways, AGEs impair endothelium-dependent vascular relaxation mainly by reducing the bioavailability and activity of NO. Several mechanisms by which AGEs block or reduce NO activity have been proposed. The first one refers to a rapid chemical reaction. The second mechanism proposes that AGEs reduce not only eNOS protein expression but also the half-life of eNOS mRNA through an increased rate of mRNA degradation (Rashid *et* al., 2004). Lastly, the third mechanism suggests that AGEs impair NO production by binding to their receptors, which causes a decrease in serine phosphorylation of eNOS, resulting in deactivation of this enzyme (Xu *et al.*, 2003). In addition, other mechanisms may be also involved since it has been observed that AGEs decrease PGI2 production and increase ET-1 expression in endothelial cells (Majed and Khalil 2012).

a. Methylglyoxal

MG is a highly reactive α-oxoaldehyde mainly formed as a byproduct of glycolysis and its production is enhanced by exposure of cells to high glucose levels (Figure 6). In addition, methylglyoxal can also be originated from the breakdown of TAGs and proteins. Nevertheless, under physiological conditions, the glyoxalase system, that requires catalytic amount of reduced glutathione (GSH), degrades MG into D-lactate and keeps plasma MG levels low. An excess of MG formation is related to several disturbances in the organism (Kalapos, 1999).

As mentioned before, AGEs attenuate the angiogenesis process, therefore leading to tissue hypoxia. In fact, previous studies showed that MG leads to destabilization of hypoxia-inducible factor-1α (HIF-1α), which is a key regulator of the vascular endothelial growth factor, by decreasing its transcriptional activity which, consequently, leads to decreased levels of VEGF. Therefore, it can be said that increased production of MG is likely to be a link between hyperglycemia and destabilization of HIF-1α (Bento *et al.*, 2010). On the other hand, methylglyoxal increases the expression of angiopoietin-2 (Ang II), which is essential for destabilization of cell connections in order to allow VEGF-induced proliferation (Yao *et al.*, 2007). Moreover, the function of Ang 2 appears to be highly dependent on the presence of the vascular endothelial growth factor. In fact, increased levels of Ang 2 in the presence of low concentrations of VEGF were shown to result in endothelial cell death and vessel regression (Bento *et al.*, 2010).

Finally, it can be assumed that hyperglycemia, by increasing the intracellular levels of MG, is likely to disrupt the VEGF-Ang 2 balance, resulting in activation of the apoptotic cascade and decreasing proliferation of endothelial cells, leading to characteristic features of the early stages of diabetic vascular complications, such as alteration of endothelium morphology and loss of vascular integrity (Bento *et al.*, 2010).

Besides hampering angiogenesis, MG also increases angiotensin II receptor expression, which may intensify the signal to increase blood pressure. The consequences in the adipose tissue, for example, appear to be hypoxia, macrophage recruitment, hypoadiponectinemia and increased plasma FFAs which, altogether, are related to insulin resistance (Rodrigues *et al.*, 2017).

Elevated levels of MG have been shown to affect glutathione. In fact, GSH levels are apparently reduced in the plasma, pancreas, adipose tissue, and skeletal muscle in conditions of elevated MG levels (for instance diabetes). Since it plays a central role in activating the glyoxalase system, a reduction in GSH level decreases MG degradation, increase its levels and sets up a vicious cycle (Dhar *et al.*, 2011). In addition, an excess of MG inactivates other antioxidant enzymes, leading to general oxidative stress. Furthermore, it induces ROS and AGEs overproduction, that can harm mitochondrial function, and NF-κB activation, that promotes

inflammation in vascular smooth muscle cells. As it decreases NO bioavailability, MG is naturally connected with vasoconstriction and consequent increase of the blood pressure (Zhang *et al.*, 2017).

At the end, according to Dhar *et al.*, 2011, methylglyoxal is able to elevate fasting plasma glucose and reduce insulin levels, since it decreases the insulin secreting capacity of the pancreas, therefore being responsible for impaired β-cell function. Moreover, MG seems to be a mediator of high glucose-induced insulin resistance and type 2 diabetes that is becoming a serious health problem in the western world. Additionally, chronic hyperglycemia and related MG formation originate AGE accumulation, leading to progression of diabetic nephropathy and increased risk of renal failure, as well as other macrovascular complications (Rodrigues *et al.*, 2014).

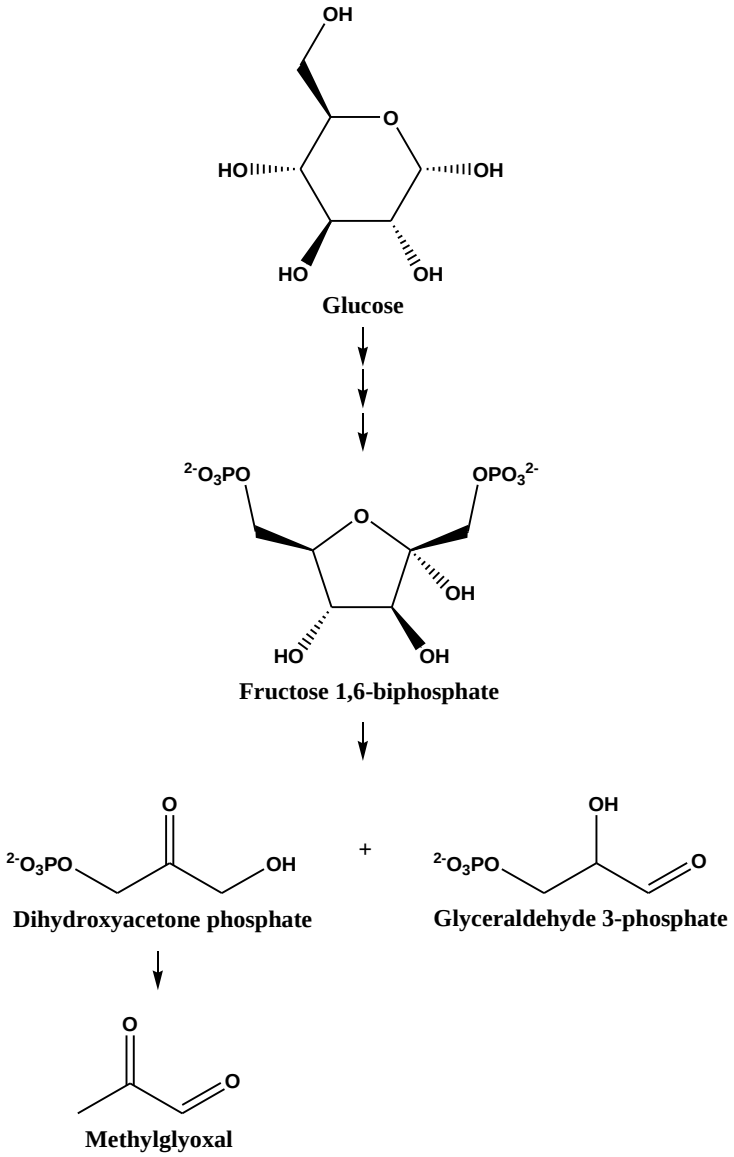

Figure 6: Glycolysis is one of the possible pathways from which MG is formed. By the action of the enzyme aldolase, the opened form of fructose 1,6-biphosphate is cleaved and it originates two isomers. The conversion of dihydroxyacetone phosphate to methylglyoxal is accomplished by the enzyme methylglyoxal synthase.

1.5. Aim of the project

This work pretends to study the impact of western type diets (high-fat diet and fat diet with methylglyoxal) and of type 2 diabetes on PVAT and associated endothelial regulation. Only recently has become clear that this adipose tissue is critical for the regulation of endothelial function in both physiological and pathological conditions. Thus, our aim is to comprehend the potential pathogenic effect of PVAT on the vasculature and its long-term effects.

This research complies two different models dividing the animals in four different groups, not only to study, directly, type 2 diabetes, but also to examine the complications associated with it. Therefore, in the first model, we induced type 2 diabetes in Wistar rats through a new method developed by compiling various protocols from different authors. This way, we fully describe this model of type 2 diabetes. In contrast, the second model focus on the endothelial and PVAT-dysfunction caused by accumulation of glycation-end products, which have been related to diabetes-associated vascular complications.

Our expectations rely on the switch from beneficial to harmful effect of the perivascular adipose tissue when damaged by diabetes and diabetes-like vascular lesions.

Chapter 2

Materials and Methods

Chapter 2: Materials and Methods

2.1. Materials

The reagents used to prepare the solutions and the immunohistochemical kit, as well as the reagents not mentioned on the next list, were bought with the highest quality available to Sigma-Aldrich (USA), Merch (Darmstad, Germany) and Panreac Química SA (Spain).

Glucose 30 %	**BBraun, Portugal**
Insulin (Humulin Regular 100 UI/mL)	**Lilly, EUA**
Saline Solution (0,9 %)	**Alifar, Portugal**
Albumin Bovine Fraction V	**NZYTech, Portugal**
Monoclonal Anti-Insulin Antibody	**Sigma-Aldrich, USA**
Glycergel Mounting Medium	**Agilent Dako, USA**

Table 1: Other reagents used in the study.

2.2. Experimental animal procedures

For this work were used male Wistar (W) rats obtained from the local breeding colony at the Faculty of Medicine, University of Coimbra (Portugal). The animals were kept under standard conditions of 24°C, 50-60 % of humidity and 12-hour periods light and darkness. All animals were allowed free access to water and food, both normal and high-fat diet (A03 + 20 % cocoa butter + 1,25 % cholesterol), with composition described in Table 2.

In order to study three different models, the animals were divided in four groups: 1- control group fed with normal diet (WC_0); 2- group fed with HFD (WHFD); 3- WHFD group injected with streptozotocin (WHFDSTZ); and 4- WHFD treated with methylglyoxal (WHFDMG).

		Normal Diet (A03)	High-Fat Diet (A03 + 20 % cocoa butter + 1,25 % cholesterol)
kcal/kg		3395	4585
% of nutrients	Proteins	21,4	16,9
	Fat	5,1	25,2
	NFE	52,0	41,0

Table 2: Composition of the food used in this study, acquired from Safe Augy, France. NFE- nitrogen-free extract.

Animals fed with HFD started the diet with two months-old. For the STZ-induced diabetes model, after two months, and with two weeks in between, three intraperitoneal injections of STZ (35 mg/kg) were given to the animals. In the second model, the MG-treated group, the animals were submitted to an increasing dose of 50 to 75 mg/kg (in the first two weeks) of MG in drinking water (daily given), for three months (Figure 7).

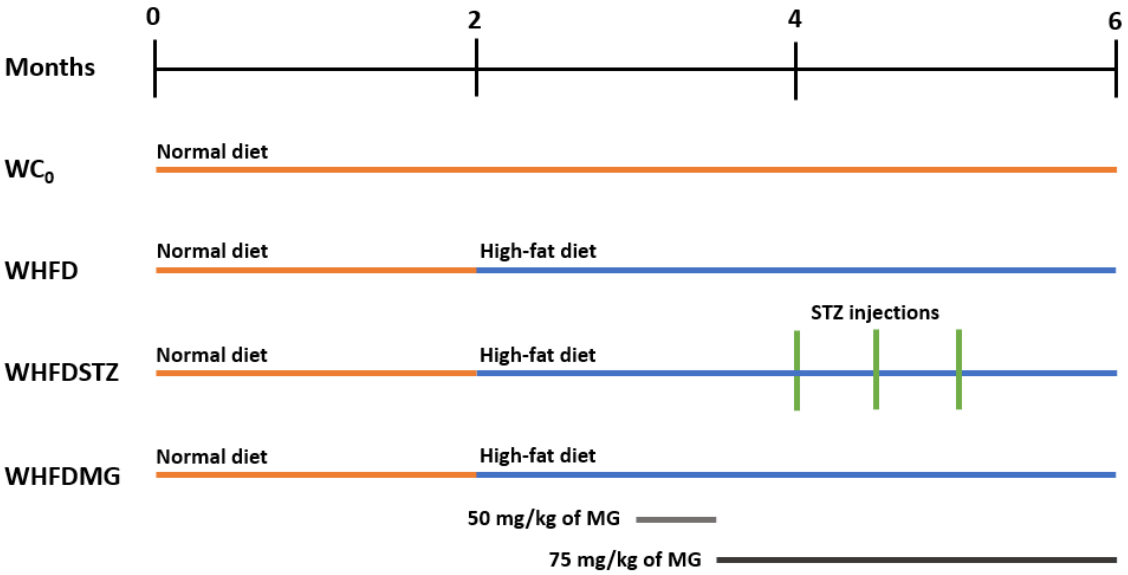

Figure 7: Timetable regarding the treatment to all Wistar rats. WC_0- Wistar rats control group. WHFD- Wistar rats fed with high-fat diet. WHFDSTZ- Wistar rats fed with high-fat diet and injected with streptozotocin. WHFDMG- Wistar rats fed with high-fat diet and treated with methylglyoxal.

2.2.1. Body weight and biochemical measurements

The body weight was measured every week after the animals started the high-fat diet, as well as the measurement of glycemia, both random and after an overnight fasting, on WHFD and WHFDSTZ groups. The procedure was made with a drop of blood from the tail vein by a glucose--oxidase method, using a glucometer (Glucometer-Elite-Bayer, Portugal S.A.) and compatible reactive test strips.

We performed intraperitoneal insulin tolerance test (ITT) and glucose tolerance test (GTT) one week before the animal sacrifice and a week apart. For the ITT, the animals were fasten for 6 hours and a solution of insulin was injected (Humulin Regular; $0.25\ U.mL^{-1}.kg^{-1}$) diluted in saline. After administration, glycemia was measured at 15, 30, 45, 60 and 120 minutes, using the glucose-oxidase method described before. For the GTT, the animals were fasten overnight and given an injection of glucose (Glucose 30 %, BBraun, Portugal; 1,75 g/kg). The glycemia was measured 1 and 2 hours after the administration, as previously.

After an overnight fasting, animals were anaesthetized with ketamine/chlorpromazine [ketamine chloride (75 $mg.kg^{-1}$, i.m., Parke-Davis, Ann Arbor, MI, USA) and chlorpromazine chloride (2.65 $mg.kg^{-1}$, i.m., Lab. Vitória, Portugal)]. Blood was collected by heart puncture at the end of treatment for biochemical measurements. The blood was centrifuged at 3000 x g at 4 °C for 15 minutes. Both serum and plasma were divided in aliquots and kept as -80 °C for additional studies.

2.2.2. Animal sacrifices

All animals were sacrificed with six months-old by cervical dislocation for further studies. The care and the procedures were in accordance with the Portuguese Law on Experimentation with Laboratory Animals, which is based on the principles of laboratory animal care as adopted by the EC Directive 86/609/EEC for animal experiments.

After a 15 h fast, glycemia measurements and body weight was obtained. The animals were then anaesthetized with ketamine/chlorpromazine and killed by cervical dislocation. The different tissues (liver and thoracic aorta) were weighed, snap frozen and stored at -80 ºC. The aortas and PVAT were excised and used as described below. The physiological buffer used, Krebs-Henseleit solution contains chemical compounds that mimic the extracellular environment and, therefore, is what we use for rinsing the organs and for *ex-vivo* studies. The solution is composed by 118.6 mM of NaCl, 4.7 mM of KCl, 1.18 mM of $MgSO_4$, 1.18 mM of KH_2PO_4,

11.0 mM of glucose, 25.0 mM of $NaHCO_3$ and 1.6 mM of $CaCl_2$. The pH is maintained at 7.4 and the solution, at room temperature, is submitted to a constant flux of gas of 95 % of O_2 and 5 % of CO_2.

The thoracic and abdominal aorta, along with connective and adipose tissues surrounding, are cautiously extracted and saved in Krebs-Henseleit solution. The aorta is, then, divided according to its anatomical location. Two segments of the thoracic aorta are prepared to be set-up in the myograph: one with and the other without the perivascular tissue. The remaining artery is separated from the PVAT and all the fragments are saved individually at -80 °C. In addition, one of the segments of the aorta may be kept in formaldehyde for further studies.

2.2.3. Studies of isometric contraction

The segments, of about 4mm, of the thoracic aorta are placed in the individual cameras of the myograph (DMT 620-M, Denmark), with Krebs-Henseleit solution. Once the biological material is connected to the strength signal transducer (PowerLab 8/35, ADInstruments) we establish the basal tension at, approximately, 1 g for 45 minutes.

The procedure starts with an induced contraction with phenylephrine (PHE), a α-1 adrenergic agonist, followed by a dose-response to acetylcholine (ACh) with increasing and cumulative concentrations from 1 nM to 10 mM. This step plays an important role, as a control, for the following testing compounds, as a qualitative measurement of the contractile response and the consequent endothelium-dependent vasodilation on smooth muscle cells. It is, therefore, critical to evaluate the primary endothelium dysfunction.

After the basal solution is changed, it is followed by an incubation of 15 minutes with N^{ω}-Nitro-L-arginine (L-NAME). This compound is a non-selective inhibitor of nitric oxide synthase (NOS) and, therefore, a vasoconstriction factor. A new incubation with L-NAME+PHE is followed, for 15 minutes, with the aim to inhibit NOS. One more time, the endothelium dysfunction is tested with a dose-response to ACh with the same concentrations as mentioned before. At the end, the Krebs-Henseleit solution will wash out the products and reestablish the basal values in the artery.

The next step of the procedure involves indomethacin (Indo), which is an inhibitor of cyclooxygenase, an enzyme that catalyzes the production of prostaglandins. In turn, prostaglandins are produced in many tissues and they are powerful locally acting vasodilators, as well as inhibitors of platelets aggregation. The study of this other pathway will help understand

the specific effect of the NO-independent vasodilation, excluding any other source of vasodilators. Therefore, this step involves incubation with L-NAME+Indo followed by L-NAME+Indo+PHE and, at the end, the dose-response to ACh.

After replacing these products for Krebs-Henseleit solution, the response to endothelin-1 is evaluated. Concentrations from 25 nM to 1 μM of this endothelium-dependent vasoconstrictor are added to the solution, cumulatively, in intervals of 10 minutes to test its mediated response. Afterwards, the solution is removed and replaced by Krebs-Henseleit solution.

At last, after pre-constriction with phenylephrine, increasing concentrations of sodium nitroprusside (SNP) are added, from 1 nM to 200 μM, also cumulative. This compound has potent vasodilating effects as a result of its breakdown to NO and, therefore, it is used to evaluate the response of the endothelium-independent vasorelaxation.

2.2.4. Studies of immunohistochemistry

This study includes the immunologic analysis, on the type 2 diabetes model, of pancreas extracted from the three groups of animals in study. For such purpose, right after the sacrifice, the organ was stored in 10% formaldehyde buffered solution. Subsequently, a few sections were cut into 3-mm sections and stained with hematoxylin/eosin using standard techniques (a process made at the Centro Hospitalar da Universidade de Coimbra), while other sections were used to stain insulin secretion from the pancreas.

Tissue sections of pancreas were washed in xylene for 5 minutes, for three times, to deparaffinize, and submitted to a decreasing concentration gradient of ethanol (100, 70 and 30 %), for three minutes each, to re-hydrate. After washing with purified water, samples were kept at 90 °C with antigen retrieval, for 10 minutes at the microwave. This last step is important to expose the epitopes that, in further steps, will react and, then, fix the primary antibody.

Once the slides were, again, at room temperature, we used hydrogen peroxide, to eliminate endogenous peroxidases, three times for two minutes each. After washing with PBS 1x + 0,1 % Tween, the tissue was incubated, for one hour, with PBS 1x + 1 % BSA + 10 % of goat serum, in order to block nonspecific binding of proteins and antibodies to reactive surfaces and non-specific binding sites. The next step included overnight incubation with the primary antibody (monoclonal anti-insulin antibody) diluted in PBS 1x + 1 % BSA.

After washing three times with PBS 1x, for 2 minutes, the sections were incubated with the secondary antibody from the immunohistochemical kit (goat anti-rabbit IgG secondary antibody), for one hour. Subsequently, and after washing three times with PBS 1x, the incubation with the enzyme streptavidin took place, because the complex streptavidin-biotin is very resistance and, therefore, it can be used to attach various biomolecules.

In the next step, slides were washed with PBS 1x four times for 2 minutes, followed by incubation, for 2 minutes, with DAB to stain cells. Since DAB is insoluble in the most commonly used reagents, it allows the subsequent treatment of the tissue section. After washing with tap water, five times for 2 minutes, the tissue was incubated, for 4 minutes, with hematoxylin to stain nucleus with a purple-blue color. Finally, tissue sections were mounted with glycergel mounting medium and analyzed under the microscope.

2.2.5. Statistical analysis

All data were analyzed by standard computer programs (Graph-Pad Prism PC Software version 3.0, ANOVA) and are expressed as mean ± SE. group). Significant differences were evaluated using either the t-test or ANOVA. $P < 0.05$ was considered significant. Dose–response curves were fitted by nonlinear regression with simplex algorithm. Relaxation responses were given as the percentage of phenylephrine preconstruction. Comparisons of dose–response curves were evaluated by two-way ANOVA for repeated measures followed by Bonferroni post hoc test for individual comparisons.

Chapter 3

Results

Chapter 3: Results

3.1. High-fat low-dose STZ-induced type 2 diabetic animal model

3.1.1. Body weight

For this study, three groups of animals were used: the control group (WC_0), which was fed with normal diet, the group fed with high-fat diet (WHFD) and the group fed with high-fat diet and treated with streptozotocin (STZ), which was fed with high-fat diet (WHFDSTZ). The groups WHFD and WHFDSTZ started the high-fat diet at two months-old, to prevent adaptation to the diet. Additionally, three injections of STZ were given to WHFDSTZ group, after the fourth month, with two weeks in between, with the purpose of partially destroying the beta cell mass and induce type 2 diabetes. Therefore, it is crucial to monitor the body weight during this period.

Analyzing the body weight, we can verify that both control Wistar and Wistar fed with high-fat diet have a constant increasing weight profile and that WHFD has the highest value of body weight (Table 3). Between these two groups, it is possible to notice the greatest difference at five months-old (p<0,001).

Although increasing until the fourth month, Wistar rats treated with STZ lost weight in the last two months. For three months, there is no record of significant difference of weight neither between WHFDSTZ and WC_0 nor between WHFD and WHFDSTZ. However, right before the STZ treatment started, at four months-old, we notice a statistically significant difference when compared to the control group (p<0,01), as well as when compared to the WHFD group (p<0,05). Indeed, as the treatment with streptozotocin started, the animals appear to have a significant loss in body weight. At five months-old, the weight of WHFDSTZ is closer to the WC_0 group (p<0,01) than to the high-fat Wistar rats (p<0,001). At six months-old, the WHFDSTZ group presents a significant lower body weight when compared to the other two groups (p<0,001), probably due to the toxic effects streptozotocin (Figure 8).

Body Weight (g)			
	WC_0 (n=18)	**WHFD (n=18)**	**WHFDSTZ (n=8)**
3 months	-	367 ± 6,13	378 ± 6,68
4 months	436 ± 5,10	424 ± 10,30	386 ± 8,55 $^{**\phi}$
5 months	460 ± 6,49	515 ± 3,59 §§§	368 ± 10,06 $^{**\phi\phi\phi}$
6 months	515 ± 14,28	532 ± 12,75	359 ± 8,39 $^{***\phi\phi\phi}$

Table 3: Body weight profile of all groups of Wistar rats used in this section of the study, expressed in g. Data are mean ± SEM (standard error of the mean; n=8-18). $^{\phi}$ p<0,05 in comparison with WHFD; $^{\phi\phi\phi}$ p<0,001 in comparison with WHFD; ** p<0,01 in comparison with WC_0; *** p<0,001 in comparison with WHFD; §§§ p<0,001 in comparison with WC_0. Data about the weight at 3 months-old from WC_0 group is not available.

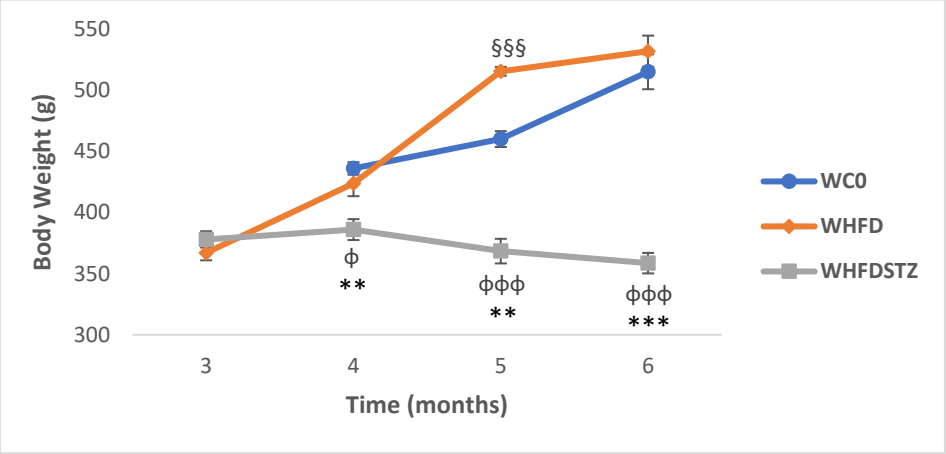

Figure 8: Evolution of body weight at 3, 4, 5 and 6 months-old, expressed in g. Data are mean ± SEM (standard error of the mean; n=8-18). $^{\phi}$ p<0,05 in comparison with WHFD; $^{\phi\phi\phi}$ p<0,001 in comparison with WHFD; ** p<0,01 in comparison with WC_0; *** p<0,001 in comparison with WC_0; §§§ p<0,001 in comparison with WC_0. Data about the weight at 3 months-old from WC_0 group is not available.

3.1.2. Lipid profile

a. Serum cholesterol levels and atherogenic index

As animals were fed with high-fat diet, it is convenient to evaluate their blood lipid profile. For such purpose, after the sacrifice the blood serum was collected and analyzed.

Concerning HDL levels after four months of an increased lipid intake, the group of WHFD presents significant lower levels when compared to the control group (p<0,001). As expected, in terms of total cholesterol, it is possible to notice a slight enhancement (Figure 9B), due to an increased value of non-HDL cholesterol (Table 4).

Similarly, the levels of total cholesterol are increased in WHFDSTZ, with a significant difference from both WC_0 (p<0,01) and WHFD (p<0,05) groups. Interestingly, it may be noticed a slight rise on HDL cholesterol (Figure 9A) levels when compared to WHFD (p<0,01), although, the ratio between HDL and total cholesterol levels proves a decrease in HDL turnover, typical of diabetes.

	WC_0 (n=12)	WHFD (n=15)	WHFDSTZ (n=7)
HDL Cholesterol (mg/dL)	49 ± 1,51	23 ± 1,07 §§§	51 ± 6,15 ^{ϕϕ}
Total Cholesterol (mg/dL)	83 ± 3,53	112 ± 15,68	276 ± 45,33 ^{**ϕ}

Table 4: Serum cholesterol levels, expressed in mg/dL. Data are mean ± SEM (standard error of the mean; n=7-15). ^{ϕ} p<0,05 in comparison with WHFD; ^{ϕϕ} p<0,01 in comparison with WHFD; ** p<0,01 in comparison with WC_0; §§§ p<0,001 in comparison with WC_0.

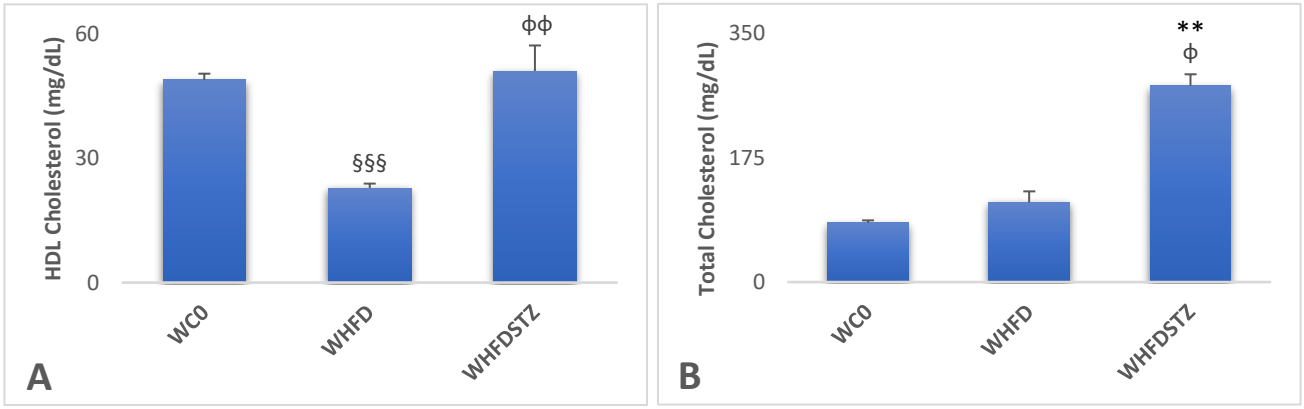

Figure 9: Serum cholesterol levels of the three groups of study, expressed in mg/dL. Data are mean ± SEM (standard error of the mean; n=7-15). ^{ϕ} p<0,05 in comparison with WHFD; ^{ϕϕ} p<0,01 in comparison with WHFD; ** p<0,01 in comparison with WC_0; §§§ p<0,001 in comparison with WC_0.

Representing the relationship between HDL and total cholesterol, the atherogenic index (AI; given by the ratio total cholesterol/HDL) is a strong marker to predict the risk of atherosclerosis. As expected, it is higher in animals fed with high-fat diet than those fed with normal diet (Figure 10). Therefore, there is a prominent difference of AI between WHFD and the control group (p<0,001). Concerning the group treated with streptozotocin, it complies a statistically difference from both WHFD (p<0,05) and WC_0 (p<0,001), as expected from the results observed in HDL and total cholesterol levels. Therefore, we may assume that the WHFDSTZ group presents an atherogenic risk, due to the cholesterol profile, not to mention the type 2 diabetes that we induced on those animals.

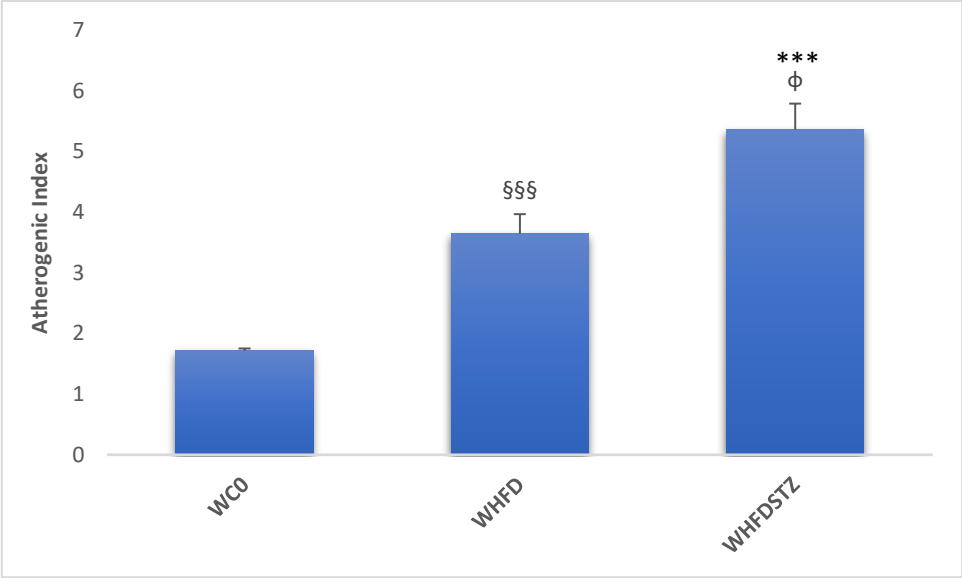

Figure 10: Atherogenic index of the three groups of study. Data are mean ± SEM (standard error of the mean; n=5-12). $^{\phi}$ p<0,05 in comparison with WHFD; *** p<0,001 in comparison with WC_0; §§§ p<0,001 in comparison with WC_0.

b. Triglycerides and phospholipids

As part of the lipid profile, triglycerides were analyzed and, as expected, there is a substantial increase in WHFD and WHFDSTZ rats when compared to the control group. In fact, the diabetic model presents the highest value of triglycerides level, as shown on Table 5.

In terms of phospholipids, it can be noticed that there is a slight increase on WHFD comparing to WC_0. Nonetheless, the values observed in STZ-treated rats are significantly higher than both control and high-fat diet Wistar rats (p<0,01), presumably due to the role that the induced diabetes plays in hepatic steatosis.

	WC_0 (n=11)	WHFD (n=12)	WHFDSTZ (n=8)
Triglycerides (mg/dL)	75 ± 5,69	86 ± 10,13	92 ± 9,73
Phospholipids (mg/dL)	137 ± 4,80	142 ± 6,19	345 ± 47,08 $^{**\phi\phi}$

Table 5: Triglycerides and phospholipids levels, expressed in mg/dL. Data are mean ± SEM (standard error of the mean; n=8-12). $^{\phi\phi}$ p<0,01 in comparison with WHFD; ** p<0,01 in comparison with WC_0.

3.1.3. Liver function tests

a. Transaminase levels and AST/ALT ratio

Levels of both liver enzymes alanine transaminase (ALT) and aspartate transaminase (AST) were measured and their ratio calculated through the formula AST/ALT.

As a specific marker of liver damage, extracted from serum, ALT (Figure 11A) is significantly increased in WHFD group when compared to the control (p<0,001) and, similarly, so does the WHFDSTZ group (p<0,01). In addition, the diabetic model group also appears to have significant differences from the WHFD group (p<0,01).

Moreover, as a marker of other inflammatory processes, AST levels (Figure 11B) are also important to determine liver damage. Relating WHFD group with the control (Table 6), it is possible to understand that there is a slight, although significant (p<0,05), difference on this transaminase level. Similarly, STZ-treated Wistar rats show an increased value of AST (p<0,05) when compared to the other two groups. The increment in transaminases is consistent with the steatosis observed in the Wistar rat livers fed with high-fat diet.

The hepatocellular injury may be reflected on the ratio of these two enzymes (Figure 11C), which is significantly decreased (p<0,001) on WHFDSTZ.

	WC_0 (n=12)	WHFD (n=14)	WHFDSTZ (n=5)
ALT (U/L)	50 ± 2,22	64 ± 3,11 §§§	1654 ± 209,93 ^{**ϕϕ}
AST (U/L)	114 ± 5,45	141 ± 12,54 §	1698 ± 354,11 ^{*ϕ}
ratio	2,28	2,22	0,98 ^{***ϕϕϕ}

Table 6: Transaminases levels, expressed in U/L, and corresponding ratio, given by the formula AST/ALT. Data are mean ± SEM (standard error of the mean; n=5-14). ^{ϕ} p<0,05 in comparison with WHFD; ^{ϕϕ} p<0,01 in comparison with WHFD; ^{ϕϕϕ} p<0,001 in comparison with WHFD; * p<0,05 in comparison with WC_0; ** p<0,01 in comparison with WC_0; *** p<0,001 in comparison with WC_0; § p<0,05 in comparison with WC_0; §§§ p<0,001 in comparison with WC_0.

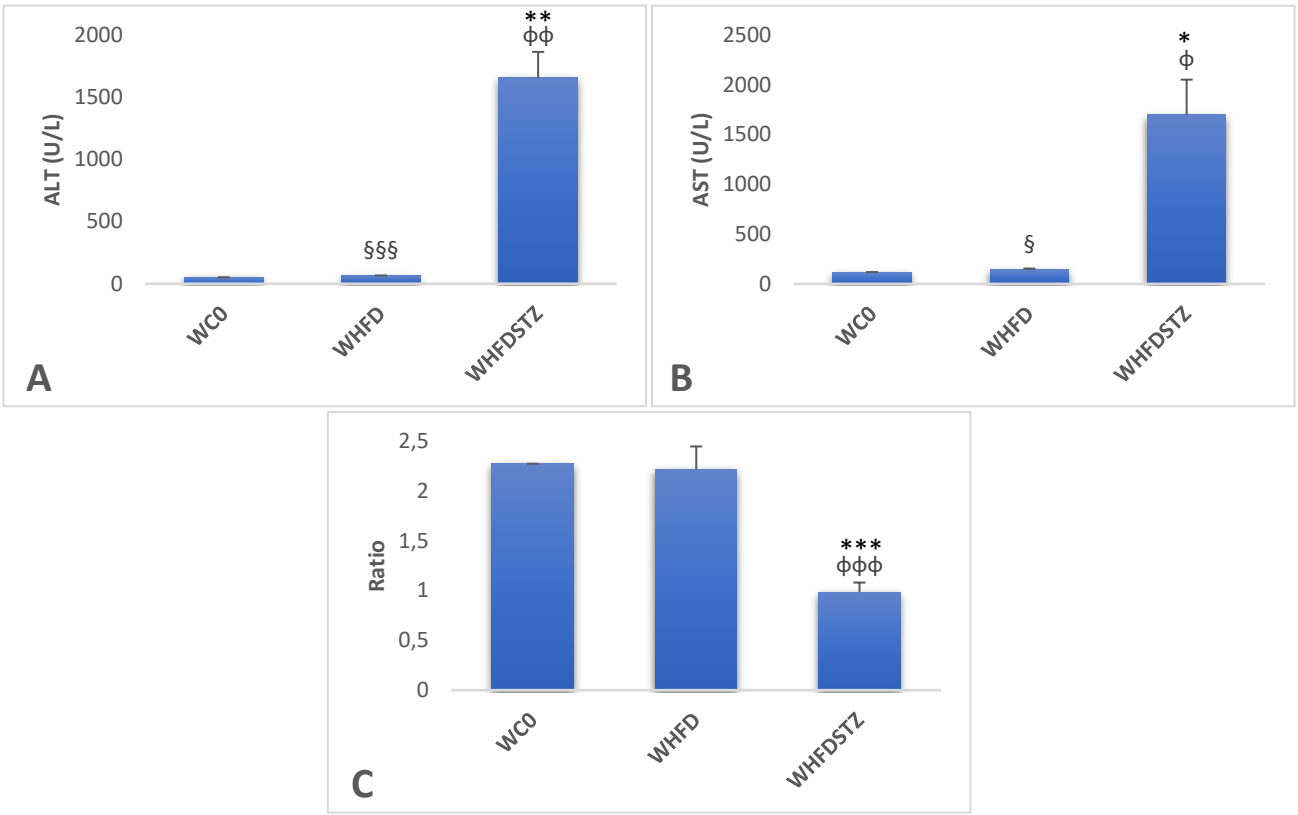

Figure 11: Transaminases levels, expressed in U/L, and corresponding ratio, given by the formula AST/ALT, of the three groups of study. Data are mean ± SEM (standard error of the mean; n=5-14). ^{ϕ} p<0,05 in comparison with WHFD; ^{ϕϕ} p<0,01 in comparison with WHFD; ^{ϕϕϕ} p<0,001 in comparison with WHFD; * p<0,05 in comparison with WC_0; ** p<0,01 in comparison with WC_0; *** p<0,001 in comparison with WC_0; § p<0,05 in comparison with WC_0; §§§ p<0,001 in comparison with WC_0.

b. Levels of alkaline phosphatase and gamma-GT

The enzyme alkaline phosphatase, a biomarker of liver damage, is significantly increased in WHFDSTZ group when compared to both WC_0 and WHFD (p<0,001; Figure 12A), corroborating the previous data. Furthermore, the difference of food itself seems to be enough to cause significant differences in this enzyme, as shown when associating WHFD to WC_0 (p<0,001).

Similarly, the gamma-glutamyl transferase level, also reflecting the pathological condition in the liver (Figure 12B), in STZ-treated group is higher than the control (p<0,01) and the WHFD rats (p<0,01), meaning hepatotoxicity caused by streptozotocin along with the increased intake of fats (Table 7).

	WC_0 (n=12)	WHFD (n=14)	WHFDSTZ (n=5)
Alkaline Phosphatase (U/L)	84 ± 5,69	172 ± 18,51 §§§	449 ± 27,87 ^{***ϕϕϕ}
Gamma-GT (U/L)	1	1,11 ± 0,11	3,33 ± 0,49 ^{**ϕϕ}

Table 7: Values of alkaline phosphatase and gamma-GT, expressed in U/L. Data are mean ± SEM (standard error of the mean; n=5-14). ^{ϕϕ} p<0,01 in comparison with WHFD; ^{ϕϕϕ} p<0,001 in comparison with WHFD; ** p<0,01 in comparison with WC_0; *** p<0,001 in comparison with WC_0; §§§ p<0,001 in comparison with WC_0.

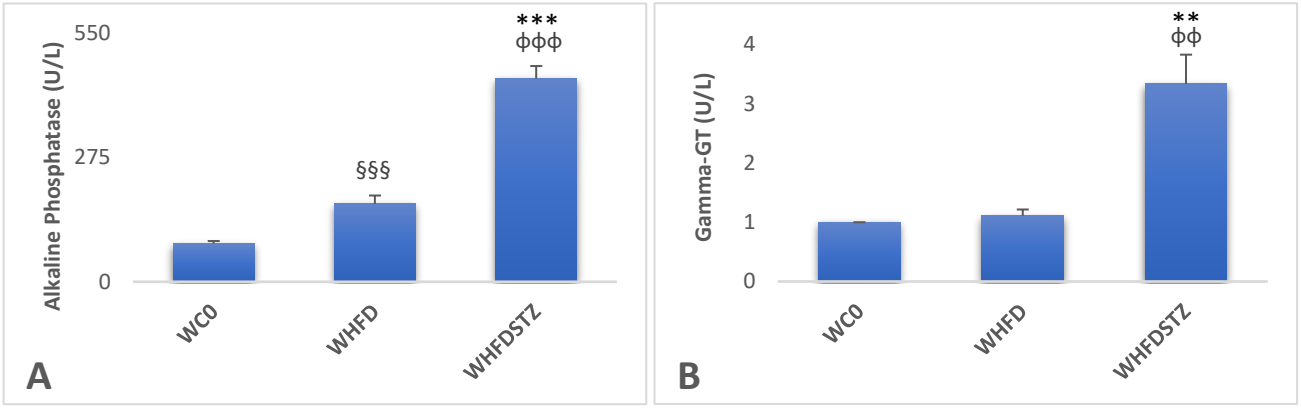

Figure 12: Levels of alkaline phosphatase and gamma-GT, expressed in U/L, of the three groups of study. Data are mean ± SEM (standard error of the mean; n=5-14). ^{ϕϕ} p<0,01 in comparison with WHFD; ^{ϕϕϕ} p<0,001 in comparison with WHFD; ** p<0,01 in comparison with WC_0; *** p<0,001 in comparison with WC_0; §§§ p<0,001 in comparison with WC_0.

3.1.4. Glycemia levels

As the study is about type 2 diabetes, the glucose levels are important to determinate. To do so, we accompanied both randomly measured and fasting glycemia, in order to monitor the degree of hyperglycemia correlated to the stage of damage induced on β-cells. Furthermore, it seems to be important to study, every month, the progress of such destruction since the treatment started (Table 8).

It is possible to observe that STZ-treated Wistar rats do not have an immediate glycemia level increase after the first injection of streptozotocin (Figure 13A and 13A'). Although, it is quite outstanding after the second (Figure 13B) and the third one (Figure 13C), comprising a significant increase when compared to the WHFD group (p<0,001).

Naturally, the fasting glycemia levels are lower than the random, nevertheless, they both confirm the diabetic state (>126 and >200 mg/dL for fasting and random glycemia, respectively). Although increasing until the fifth month (p<0,001; Figure 13B'), there is a stabilization, and even a slight decrease, of fasting glycemia on the last month (p<0,01; Figure 13C'). More revealing to realize when measured after approximately 12 hours of fasting, these data, along with the loss of weight, expresses the stabilization of the diabetic condition.

	WHFD (n=13)	WHFDSTZ (n=6)	
4 months	117 ± 6,69	123 ± 16,41	**Random Glycemia (mg/dL)**
5 months	114 ± 2,69	580 ± 13,33 ϕϕϕ	
6 months	102 ± 2,22	559 ± 25,92 ϕϕϕ	
4 months	89 ± 2,47	96 ± 23,42	**Fasting Glycemia (mg/dL)**
5 months	88 ± 1,36	340 ± 23,24 ϕϕϕ	
6 months	76 ± 2,53	287 ± 35,04 ϕϕ	

Table 8: Levels of both random and fasting glycemia, expressed in mg/dL, measured for three months. Data are mean ± SEM (standard error of the mean; n=6-13). ϕϕ p<0,01 in comparison with WHFD; ϕϕϕ p<0,001 in comparison with WHFD.

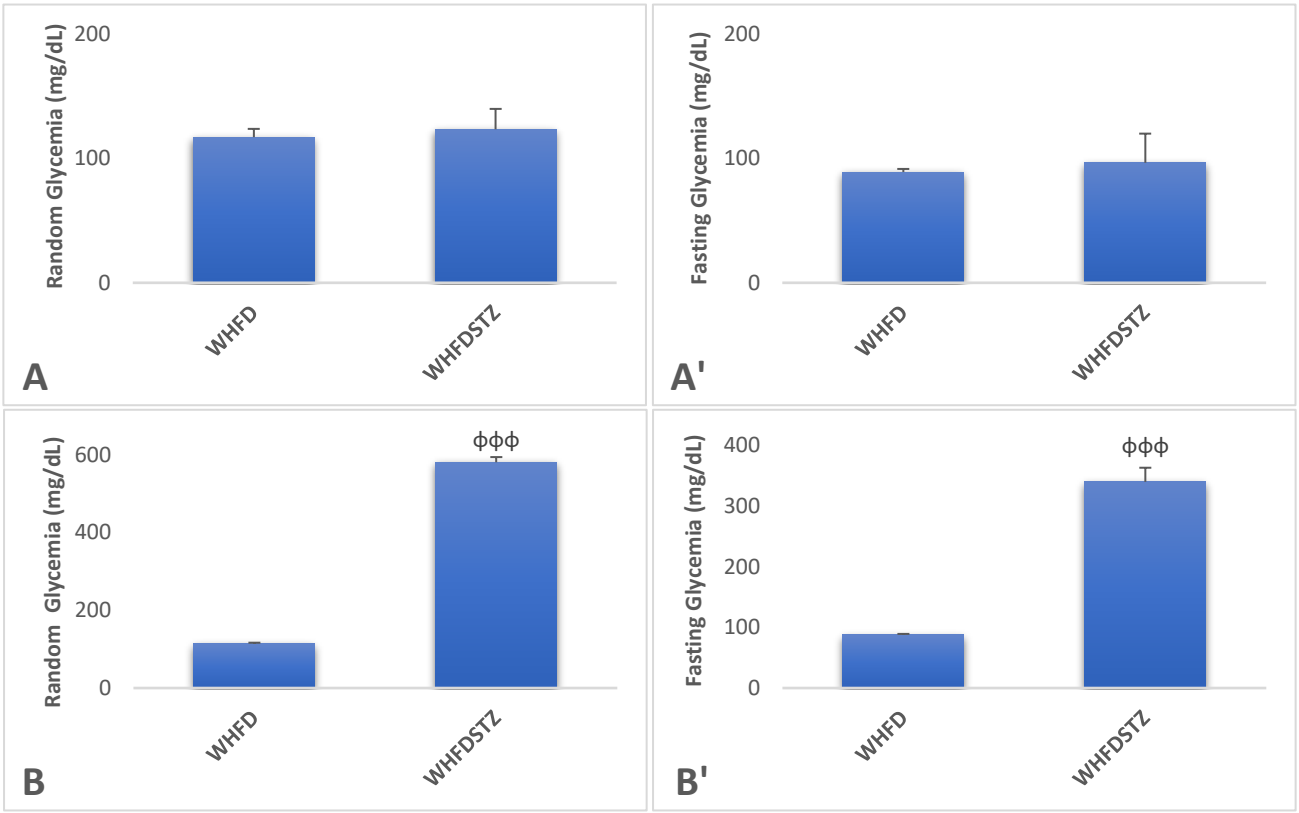

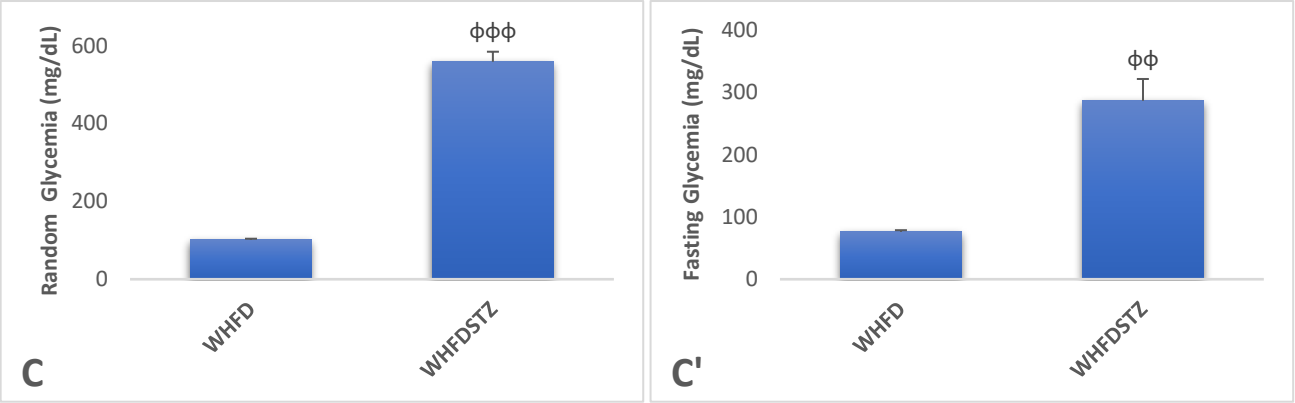

Figure 13: Levels of both random and fasting glycemia, expressed in mg/dL, of the two groups fed with high-fat diet, measured for three months. Data are mean ± SEM (standard error of the mean; n=5-14). $^{\phi\phi}$ p<0,01 in comparison with WHFD; $^{\phi\phi\phi}$ p<0,001 in comparison with WHFD.

3.1.5. Glucose Tolerance Test (GTT) and Insulin Tolerance Test (ITT)

Insulin resistance is an inherent feature of type 2 diabetes and, therefore, it is crucial for the present study. These two tests, performed one week before the sacrifices and a week apart, are proof of the glucose intolerance and insulin resistance state in this animal model, respectively. The GTT is given to determine how quickly glucose is cleared from the blood and it is quite important to prove an impaired beta cell function. Similarly, the ITT is used to evaluate the insulin sensitivity on type 2 diabetes.

For the first test, GTT, the WC_0 group is the control model of glucose tolerance, therefore fulfilled the expected metabolic profile, since it indicates proper glucose utilization.

As expected, the high-fat diet, by itself, creates a certain degree of glucose intolerance, showed by statistically significant differences (Table 9), when compared to the control group, with normal diet, at the beginning of the test (fasting glucose; p<0,05) and two hours after the glucose load (glucose level 2 h after a load; p<0,01).

In respect to the diabetic model, it was no surprise the result obtained (Figure 14), since it demonstrated a great variance from both groups (p<0,001) at 0 and 60 minutes. The difference, from both WC_0 and WHFD, observed two hours after the injection (p<0,01) is in accordance with our expectations. At that time, a glycemia higher than 200 mg/dL and a clearance profile that slow indicates glucose intolerance. The area under the curve is significantly higher in WHFD (263 ± 15.9) and WHFDSTZ (989 ± 46.2) compared with WC_0 group (220 ± 6.2).

Glycemia (mg/dL)			
Time (min)	**WC_0 (n=11)**	**WHFD (n=14)**	**WHFDSTZ (n=4)**
0	66 ± 1,13	74 ± 2,82 §	317 ± 8,23 $^{***\phi\phi\phi}$
60	138 ± 5,14	165 ± 13,30	563 ± 21,62 $^{***\phi\phi\phi}$
120	98 ± 2,99	118 ± 5,88 §§	536 ± 51,46 $^{**\phi\phi}$

Table 9: Glucose tolerance test, where glycemia is expressed in mg/dL. Data are mean ± SEM (standard error of the mean; n=4-14). $^{\phi\phi}$ p<0,01 in comparison with WHFD; $^{\phi\phi\phi}$ p<0,001 in comparison with WHFD; ** p<0,01 in comparison with WC_0; *** p<0,001 in comparison with WC_0; § p<0,05 in comparison with WC_0; §§ p<0,01 in comparison with WC_0.

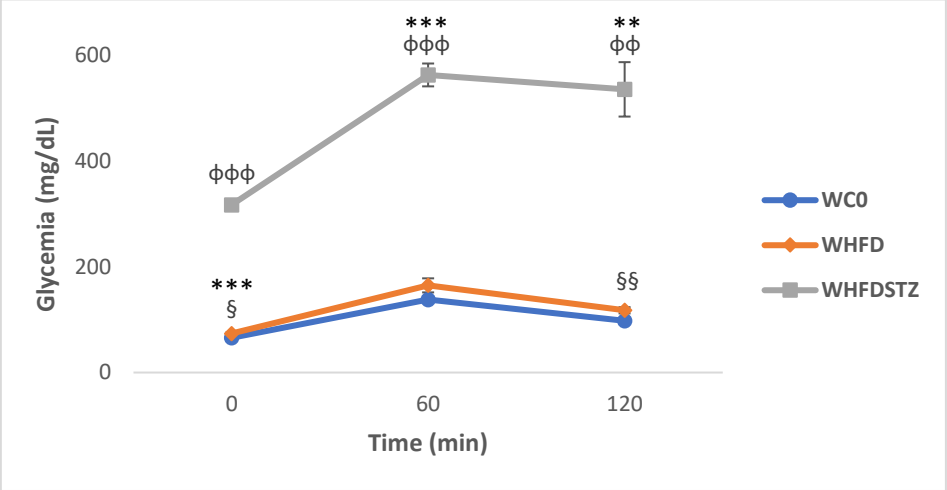

Figure 14: Glucose tolerance test of the three groups in study, where glycemia is expressed in mg/dL. Data are mean ± SEM (standard error of the mean; n=4-14). $^{\phi\phi}$ p<0,01 in comparison with WHFD; $^{\phi\phi\phi}$ p<0,001 in comparison with WHFD; ** p<0,01 in comparison with WC_0; *** p<0,001 in comparison with WC_0; § p<0,05 in comparison with WC_0; §§ p<0,01 in comparison with WC_0.

In the insulin tolerance test, the degree to which blood glucose concentrations fall following insulin administration represent the efficiency of insulin action. It is liable to see the significant difference from the WHFD to WC_0 at the beginning and after 15 minutes of the test (p<0,001). At 30 minutes there is still a slight increment in the glucose levels (p<0,01), but it is only after 45 minutes that we observe equal levels of glucose between the two groups (Table 10).

When it comes to the STZ-treated group, we can observe that this group is, clearly, insulin resistant. As so, we notice a continuous decrease of glycemia level with curves (Figure 15) clearly distant from the other two groups (p<0,001). Even so, the glucose clearance from the blood quite delayed. Moreover, it is just at 2 hours after the insulin injection that the decline is the most evident.

Glycemia (mg/dL)			
Time (min)	**WC_0 (n=9)**	**WHFD (n=11)**	**WHFDSTZ (n=4)**
0	81 ± 1,80	93 ± 2,30 §§§	387 ± 8,14 ^{***ϕϕϕ}
15	75 ± 1,07	93 ± 1,45 §§§	390 ± 5,72 ^{***ϕϕϕ}
30	65 ± 1,87	80 ± 3,52 §§	378 ± 13,69 ^{***ϕϕϕ}
45	66 ± 2,72	68 ± 2,85	362 ± 11,73 ^{***ϕϕϕ}
60	65 ± 2,15	65 ± 2,95	317 ± 17,83 ^{***ϕϕϕ}
120	67 ± 2,30	63 ± 3,06	235 ± 32,60 ^{*ϕ}

Table 10: Insulin tolerance test, where glycemia is expressed in mg/dL. Data are mean ± SEM (standard error of the mean; n=4-11). ^{ϕ} p<0,05 in comparison with WHFD; ^{ϕϕϕ} p<0,001 in comparison with WHFD; * p<0,05 in comparison with WC_0; *** p<0,001 in comparison with WC_0; §§ p<0,01 in comparison with WC_0; §§§ p<0,001 in comparison with WC_0.

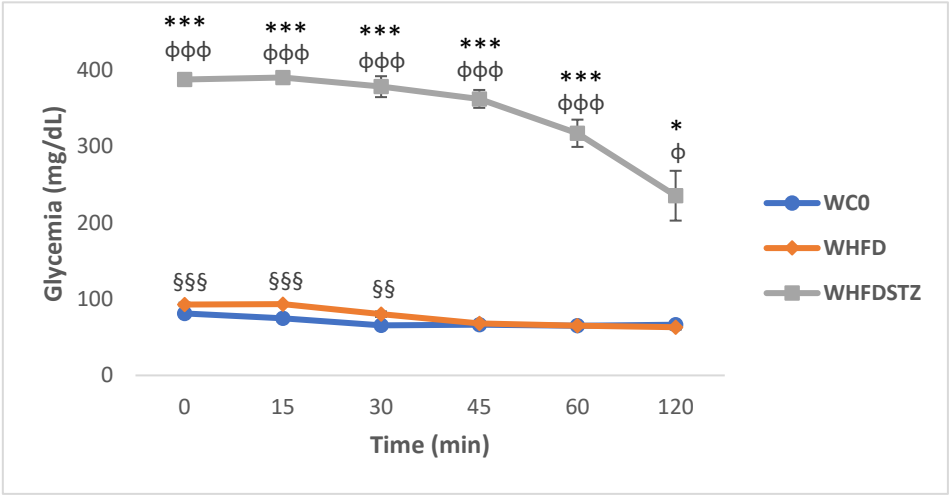

Figure 15: Insulin tolerance test of the three groups in study, where glycemia is expressed in mg/dL. Data are mean ± SEM (standard error of the mean; n=4-11). ^{ϕ} p<0,05 in comparison with WHFD; ^{ϕϕϕ} p<0,001 in comparison with WHFD; * p<0,05 in comparison with WC_0; *** p<0,001 in comparison with WC_0; §§ p<0,01 in comparison with WC_0; §§§ p<0,001 in comparison with WC_0.

3.1.6. Isometric tension studies

The following studies of isometric tension intend to demonstrate the effect of the treatment with HFD and HFD+STZ at the vascular level, in thoracic aorta. Therefore, three parts of the subsequent protocol were performed to evaluate the endothelium and smooth muscle cells response to different vasodilator factors, both dependent and independent from the endothelium, and one part is meant to evaluate their response to a contractile factor. The comparison of HFD-fed animals with WC_0 will give us quantitative and qualitative information about the degree of endothelium dysfunction. At first, the vasodilation dependent from the endothelium was examined. The procedure involves contraction with phenylephrine (PHE), a α-1 adrenergic agonist, followed by a dose-response to increasing concentrations of acetylcholine (ACh). In fact, the control group shows a vascular relaxation of about 80 % (Figure 16). In contrast, WHFD group has about 10 % less relaxation (p<0,01 and p<0,001) and lower sensitivity to ACh, with a shift in the dose-response to the right.

When it comes to WHFDSTZ, the profile of the curve is quite different from the others, since after the fifth concentration of ACh, the tissue does not seem to relax in response to higher doses of this vasodilator, showing a statistically significant difference from the other groups (p<0,01 on the fifth concentration, in comparison with WC_0, and p<0,001 in general). In conclusion, the maximum relaxation observed for the STZ-treated group is about 50 %, indicating endothelium dysfunction, as it will be discussed later.

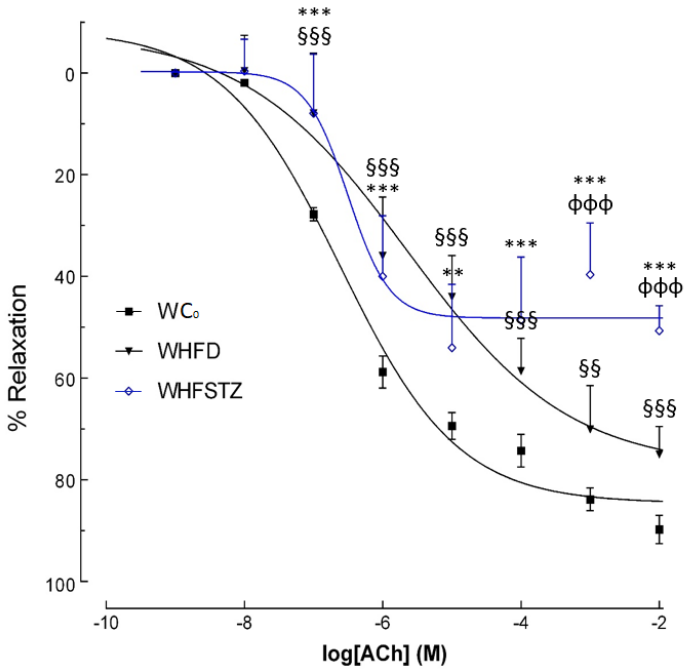

Figure 16: Dose-response curves to ACh of the three groups in study after contraction with PHE. Data are mean ± SEM (standard error of the mean; n=4-12). $^{\phi\phi\phi}$ p<0,001 in comparison with WHFD; ** p<0,01 in comparison with WC_0; *** p<0,001 in comparison with WC_0; §§ p<0,01 in comparison with WC_0; §§§ p<0,001 in comparison with WC_0.

To evaluate the role of perivascular adipose tissue on endothelial function, aortic rings were mounted with and without PVAT. On Figure 17, we first compare the control group with the group fed with HFD. In fact, there are no significant differences on WC_0 with and without PVAT. Moreover, the curve of WC_0+PVAT shows a tendency to about 5 % more relaxation than WC_0-PVAT. Therefore, there are no significant differences to note on these curves.

Concerning the WHFD group, we can observe that the curve regarding the presence of PVAT has a profile which indicates that, after the fourth concentration of ACh, the tissue does not respond to any increased concentration of the relaxing factor, leaving WHFD+PVAT with a maximum relaxation of 50 %. In comparison with the absence of perivascular adipose tissue, there is a variance between the curves of about 25 %, with differences of $p<0,01$, on third and sixth concentrations, and $p<0,001$, on seventh and eighth concentrations. In addition, there are also statistically significant differences from the control group with PVAT ($p<0,01$ on the fourth concentration and $p<0,001$ after the fifth concentration).

Moreover, there are some differences between WC_0+PVAT and WHFD-PVAT, and WC_0-PVAT and WHFD+PVAT, yet we do not intend to compare groups with distinct conditions, since the perivascular adipose tissue creates a different environment for the tissue.

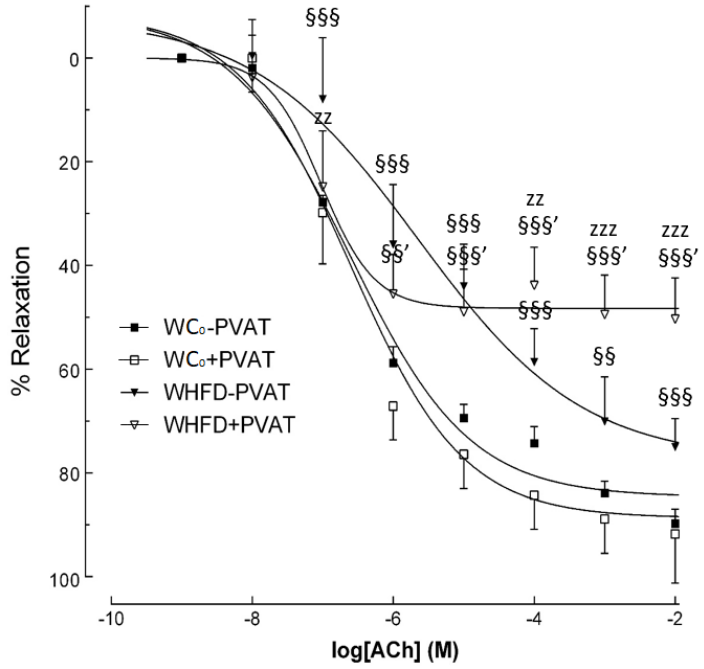

Figure 17: Dose-response curves to ACh of WC_0 and WHFD after contraction with PHE. Data are mean ± SEM (standard error of the mean; n=4-12). §§ $p<0,01$ in comparison with WC_0-PVAT; §§§ $p<0,001$ in comparison with WC_0-PVAT; $^{§§`}$ $p<0,01$ in comparison with $WC_0$+PVAT; $^{§§§`}$ $p<0,001$ in comparison with WC_0+PVAT; ^{zz} $p<0,01$ in comparison with WHFD-PVAT; ^{zzz} $p<0,001$ in comparison with WHFD-PVAT.

Including now the data regarding the STZ-treated group, we observe a reduced relaxation. While the aorta clean from the adipose tissue shows, as mentioned before, a maximum relaxation of 50 %, the presence of PVAT decreases such percentage to 30 % (Figure 18). After the fourth concentration of ACh, the variances between the presence and absence of perivascular adipose tissue are quite significant (p<0,01 and p<0,001). There is, approximately, a reduction of approximately 20 % in maximum relaxation in response to ACh due to the presence of the perivascular adipose tissue (WHFDSTZ+PVAT) when compared to its absence (WHFDSTZ-PVAT). The profile of the dose-response curve of the WHFDSTZ+PVAT group demonstrates a decreased sensibility for acetylcholine, such as, after the fourth added concentration, there is no response to it. Therefore, these data indicate a major endothelium dysfunction.

The comparison of WHFDSTZ with WHFD shows that the statistically significant difference on aortas without PVAT is quite noteworthy (p<0,001 on the last two concentrations), as well as the aortas with the perivascular tissue (p<0,01 for the fifth, sixth and last concentrations, and p<0,001 for the third, fourth and seventh concentrations). To note, data regarding any comparison with the WC_0 is not expressed on the graph simply because we would like to compare the HFD-fed animals, which have similar curve profiles. Although, it is noticed a very high discrepancy compared to the STZ-treated group.

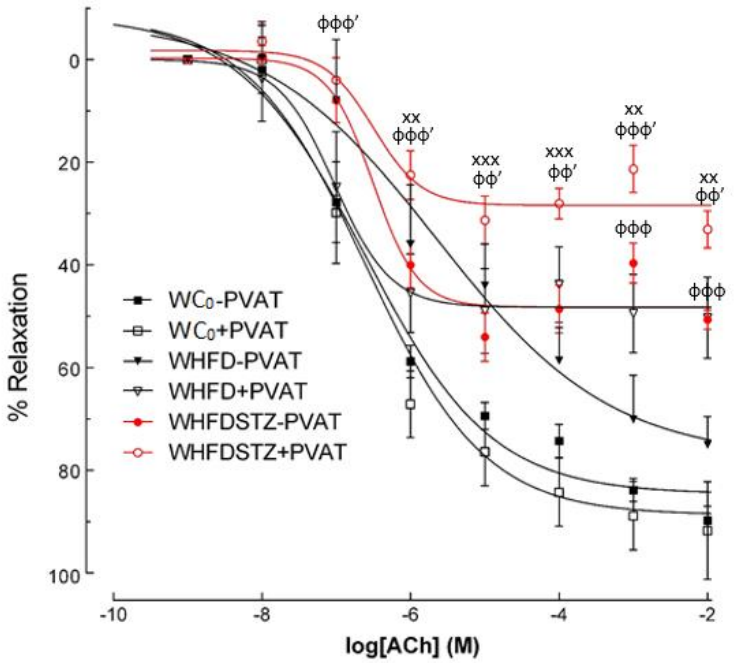

Figure 18: Dose-response curves to ACh of the three groups in study after contraction with PHE. Data are mean ± SEM (standard error of the mean; n=4-12). $^{\phi\phi\phi}$ p<0,001 in comparison with WHFD-PVAT; $^{\phi\phi'}$ p<0,01 in comparison with WHFD+PVAT; $^{\phi\phi\phi'}$ p<0,001 in comparison with WHFD+PVAT; ^{xx} p<0,01 in comparison with WHFDSTZ-PVAT; ^{xxx} p<0,001 in comparison with WHFDSTZ-PVAT.

Concerning the endothelium-independent vasodilation to evaluate vascular smooth muscle integrity, the method included contraction with phenylephrine, followed by a dose-response to a powerful nitric oxide donor, sodium nitroprusside (SNP).

All three groups fulfil the prognostic: the vasodilation was almost total (Figure 19). As the compound is very potent and its action quite extensive, the expected results were, indeed, a full relaxation of the artery. Observing the curves on the control group, WC_0+PVAT appears to have a slightly faster relaxation compared to WC_0-PVAT, which is the expected result, since the perivascular adipose tissue integrity is intact and, consequently, its anticontractile effect can be noticed. Although, a small statistically significant difference between these two curves was observed on the fourth concentration (p<0,01).

Similarly, the curves of WHFD-PVAT and WHFD+PVAT also have the same profile as those from the control group, where the presence of PVAT requires less concentration of SNP for the same percentage of relaxation of WHFD-PVAT. Although, the maximum vasodilation is achieved by the aorta without the perivascular adipose tissue. In addition, there are some significant differences between the curves along the dose-response (p<0,05 on the third concentration and p<0,001 in general). Also, some points reveal the variance from the control group, in both absence (p<0,01 on the seventh concentration) and presence of PVAT (p<0,05 on third and eighth concentrations).

In respect to the STZ-treated group, we observe a different behavior of the curves when compared to the two other groups. In this case, WHFDSTZ-PVAT has a rapid reaction to SNP, while the response of WHFDSTZ+PVAT is delayed. In fact, data indicates some statistically significant differences between these two curves (p<0,05 on the second and p<0,001 on third, fourth and fifth concentrations). Comparing to WC_0, there are differences between the curves with the absence (p<0,05 on the second and p<0,001 on following concentrations) and the presence of PVAT (p<0,05 on sixth and seventh concentrations). Likewise, comparing to WHFD, there are also differences in the absence (p<0,05 on the sixth and p<0,001 on third, fourth and fifth concentrations) and the presence of PVAT (p<0,05 only on the sixth and p<0,001 on third, seventh and eighth concentrations).

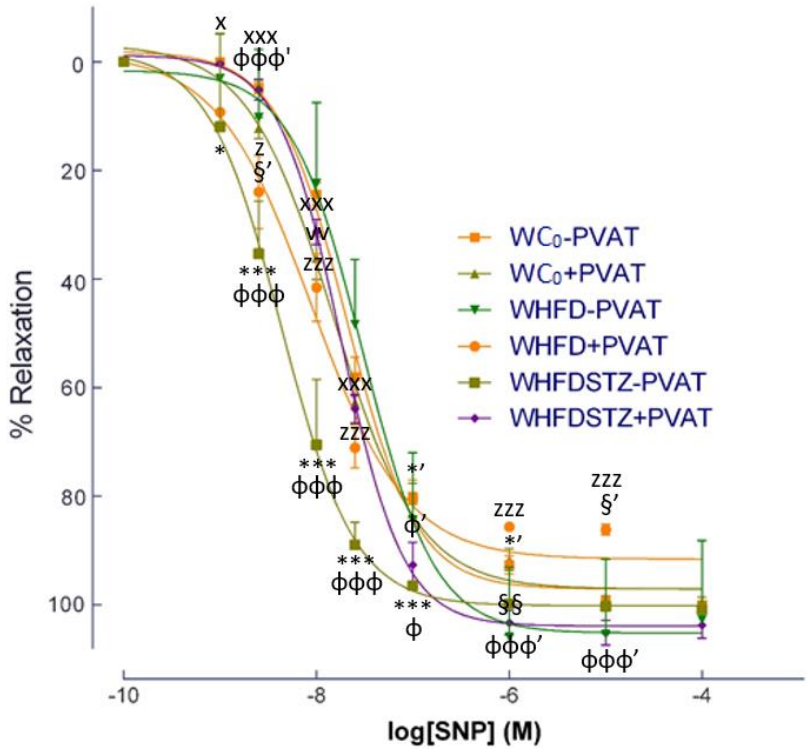

Figure 19: Dose-response curves to SNP of the three groups in study after contraction with PHE. Data are mean ± SEM (standard error of the mean; n=4-12). $^{\phi}$ p<0,05 in comparison with WHFD-PVAT; $^{\phi\phi\phi}$ p<0,001 in comparison with WHFD-PVAT; $^{\phi'}$ p<0,05 in comparison with WHFD+PVAT; $^{\phi\phi\phi'}$ p<0,001 in comparison with WHFD+PVAT; * p<0,05 in comparison with WC_0-PVAT; *** p<0,001 in comparison with WC_0-PVAT; $^{*'}$ p<0,05 in comparison with WC_0+PVAT; §§ p<0,01 in comparison with WC_0-PVAT; $^{\S'}$ p<0,05 in comparison with WC_0+PVAT; ^{vv} p<0,01 in comparison with WC_0+PVAT; ^{x} p<0,05 in comparison with WHFDSTZ-PVAT; ^{xxx} p<0,001 in comparison with WHFDSTZ-PVAT; ^{z} p<0,05 in comparison with WHFD-PVAT; ^{zzz} p<0,001 in comparison with WHFD-PVAT.

Next, we studied the effect of L-NAME, an inhibitor of the enzyme NOS, incubated with indomethacin, a cyclooxygenase inhibitor, with the purpose to evaluate the vasodilation independent of direct actions of NO and prostaglandins, especially PGI2 (Figure 20). To note, the increase, in almost every point, of contraction between the first and the second concentration is due to the prevailing contractile conditions of L-NAME, Indo and PHE, which are not revertible by the first addition of a small concentration of ACh.

The WC_0-PVAT group presents a constant relaxation, providing us the expected dose-response to acetylcholine after contraction with phenylephrine, on an environment with L-NAME and indomethacin. Nevertheless, some differences can be noticed when studying the WC_0+PVAT curve. In fact, the perivascular adipose tissue leads to a late response to ACh, demonstrating that it is affected by L-NAME and indomethacin (p<0,01 on the fourth concentration). Similarly, the behavior of the curves on WHFD rats shows that PVAT is affected by the substances used on this study and, consequently, affects smooth muscle relaxation. In fact,

it does not appear to have any relaxation at all, creating statistically significant differences with the curve WHFD-PVAT (p<0,05 on the third and p<0,001 on the following concentrations). In fact, there are also points where the difference is important when comparing to WC_0-PVAT (p<0,01 on the seventh concentration) and to WC_0+PVAT (p<0,05 on third and last concentrations).

Regarding the STZ-treated group, we see that the curve regarding the absence of PVAT demonstrates a constant relaxation, similar to the control group, although having some differences (p<0,05 on the second concentration and p<0,001 from the third to the sixth concentrations). In the same way, WHFDSTZ+PVAT does not seem to have any relaxation until the last added concentration on ACh, just like WC_0+PVAT (p<0,05 on sixth and seventh concentrations, which are the only significant differences between these two groups). Additionally, there are many differences when comparing WHFDSTZ to WHFD, in both absence (p<0,05 and p<0,001) and presence of the perivascular adipose tissue (p<0,05 and p<0,001). Moreover, differences between WHFDSTZ-PVAT and WHFDSTZ+PVAT can be noticed on the second (p<0,05) and following concentrations (p<0,001).

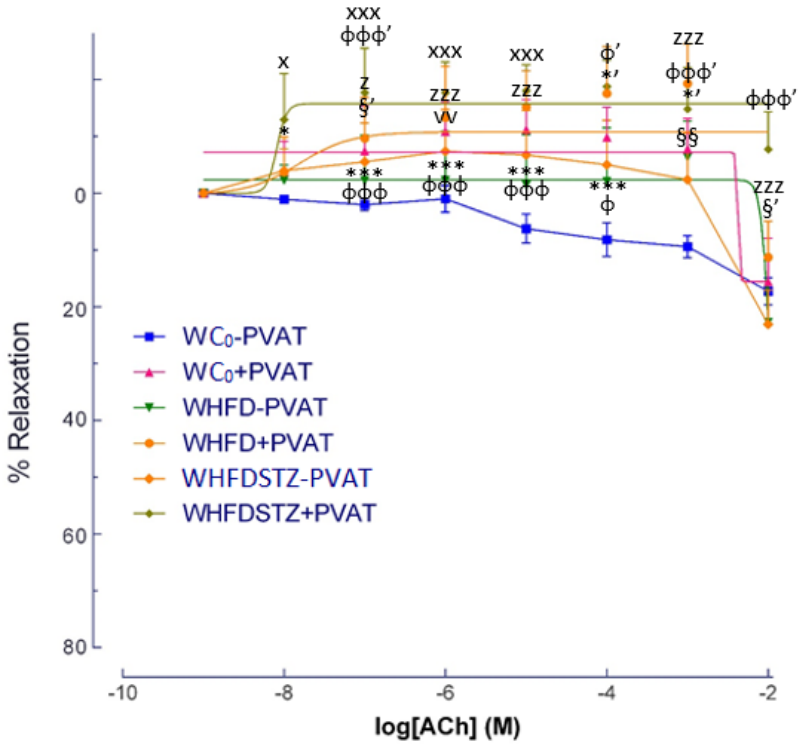

Figure 20: Dose-response curves to ACh of the three groups in study after incubation with L-NAME+Indo and contraction with PHE. The results include standard deviation as ± SEM (n=4-12). $^{\phi}$ p<0,05 in comparison with WHFD-PVAT; $^{\phi\phi\phi}$ p<0,001 in comparison with WHFD-PVAT; * p<0,05 in comparison with WC_0-PVAT; *** p<0,001 in comparison with WC_0-PVAT; §§ p<0,01 in comparison with WC_0-PVAT; $^{\phi'}$ p<0,05 in comparison with WHFD+PVAT; $^{\phi\phi\phi'}$ p<0,001 in comparison with WHFD+PVAT; $^{*'}$ p<0,05 in comparison with WC_0+PVAT; $^{\S'}$ p<0,05 in comparison with WC_0+PVAT; ^{vv} p<0,01 in comparison with WC_0-PVAT; ^{x} p<0,05 in comparison with WHFDSTZ-PVAT; ^{xxx} p<0,001 in comparison with WHFDSTZ-PVAT; ^{z} p<0,05 in comparison with WHFD-PVAT; ^{zzz} p<0,001 in comparison with WHFD-PVAT.

At last, a study of the vasoconstriction was performed, through a dose-response to the potent vasoconstrictor endothelin-1 (ET-1).

Analyzing the behavior of the curves on the control group (Figure 21), we can verify that WC_0-PVAT has a higher contraction than WC_0+PVAT, as expected due to the anticontractile effect of this tissue. Yet, some differences between these curves in the presence and the absence of perivascular adipose tissue can be appointed for third, fourth and fifth concentrations (p<0,001).

Similarly, the group fed with high-fat diet demonstrates a higher contraction level on the aorta with PVAT than on the one without the tissue, also showing some difference between the curves (p<0,001 on fourth and last concentrations). Although, WHFD-PVAT can contract slightly more than WC_0-PVAT, possibly because subjects with diet rich in lipids have higher production of contractile substances, thus it is not significantly different.

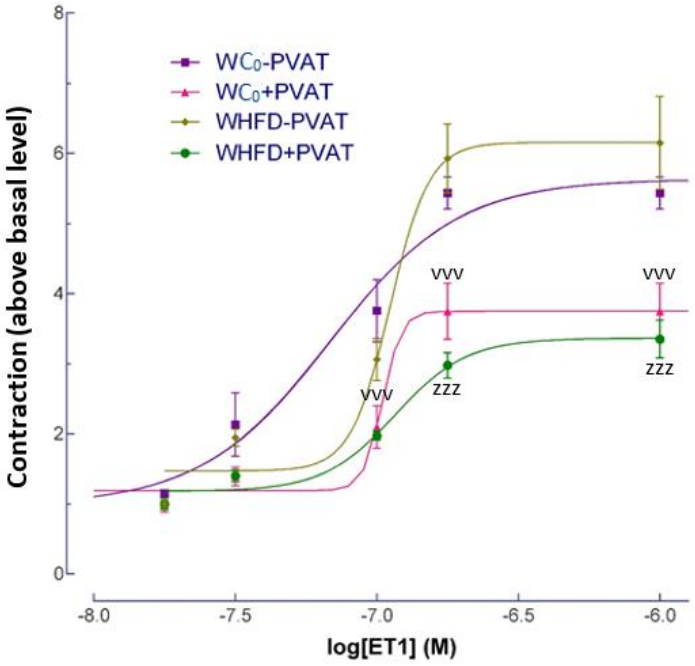

Figure 21: Dose-response curves to ET-1 of WC_0 and WHFD. Data are mean ± SEM (standard error of the mean; n=4-12). ^{vvv} p<0,001 in comparison with WC_0-PVAT; ^{zzz} p<0,001 in comparison with WHFD-PVAT.

In the same way, when adding WHFDSTZ to the comparison (Figure 22), we can predict that, as a type 2 diabetes model fed with HFD, the organism itself has higher production of contractile factors when compared to WHFD. For this motive, the curve observed in WHFDSTZ-PVAT seems reasonable. In fact, the WHFDSTZ+PVAT curve reaches a maximum contraction higher than WC_0+PVAT but quite proximal to WHFDSTZ-PVAT, demonstrating that the perivascular adipose tissue does not have so much anticontractile effect. Nonetheless, a significant difference was observed when comparing the curves WHFD+PVAT to WHFDSTZ+PVAT (p<0,05).

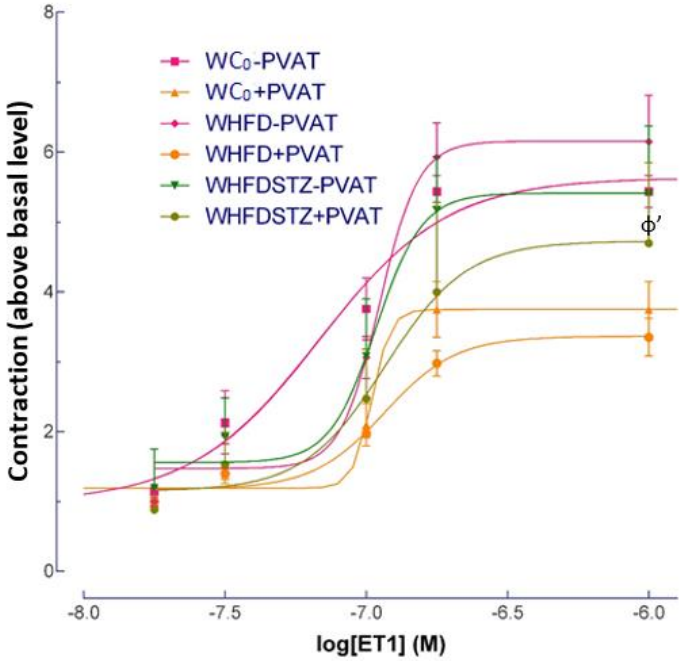

Figure 22: Dose-response curves to ET-1 of the three groups in study. Data are mean ± SEM (standard error of the mean; n=4-12). $^{\Phi'}$ p<0,05 in comparison with WHFD+PVAT.

3.1.7. Immunohistochemistry studies

To prove the effects of the high-fat diet and the treatment with streptozotocin on the islets of Langerhans, we performed immunohistochemistry tests on pancreas of the three groups, labelling the pancreas sections with an antibody anti-insulin.

At first, we used hematoxylin and eosin stains to mark nucleus and extracellular matrix and cytoplasm, respectively. This way, we were able to verify structure, shape and surroundings of the islets and, therefore, to compare pancreas between groups. In fact, animals from the control group (Figure 23A) presented well-defined structures, with a round-shape and islets very well delimited. Moreover, we observe many nuclei, appearing that the organ was totally functional a healthy. Even though that the WHFD pancreas (Figure 23B) seems to present a slight decrease in the number of nuclei and some changes on the tissue to fibrous connective on the islet (represented by white lines), its general shape and composition is quite similar to the control group.

However, the last image, concerning the WHFDSTZ group (Figure 23C), presents not only a few breaks in the structure, with unmistakable fibrosis, but also a disorganized shape. Therefore, we can easily presume that β-cells, among the other cells which constitute the islet, are changed. Nevertheless, such images only represent a first instance referent to this part of the study, providing good material of comparison for further discussion.

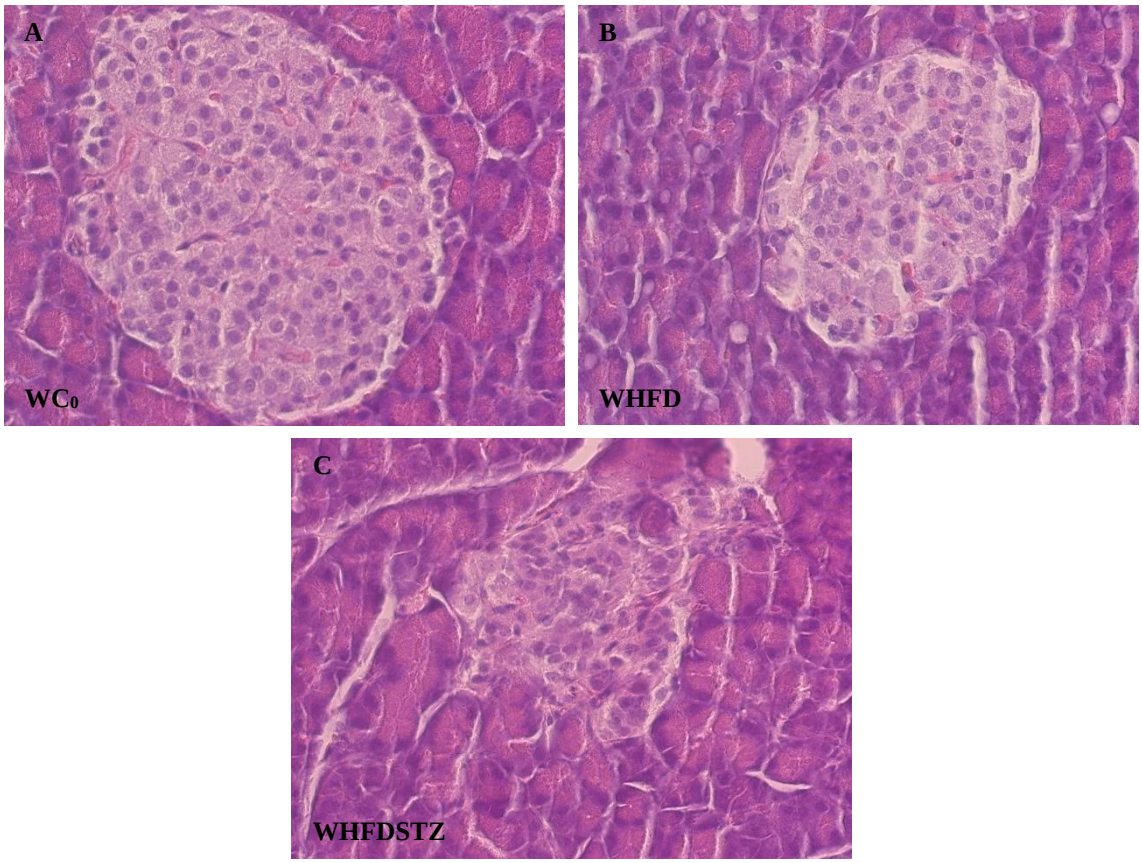

Figure 23: H&E staining procedure on islets of Langerhans in all WC_0, WHFD and WHFDSTZ groups (40x; n=3-4).

The immunohistochemistry procedure performed next marked the islets for the hormone insulin, using an antibody anti-insulin. Therefore, we expected to observe a reduction in β-cells mass. Nonetheless, we were also focused on shape and surrounding of each islet of the section. On the image of the control group (Figure 24A) we can observe four islets totally marked for the hormone insulin. As it was observed before with the 40x amplification, the islets are very well conserved and organized. Therefore, β-cells are labelled with the antibody anti-insulin and represent the majority of the cells of the islet, as expected.

On the other hand, the WHFD group (Figure 24B) shows islets with some tissue alteration, as seen on Figure 22B, some cell destruction inside the structure (appointed with the arrow) and a reduction in marked insulin. This way, we can deduce that, although high-fat diet-treated animals present some loss of β-cells, the most of it are still producing the rightful amount of the hormone.

Finally, the images obtained from the STZ-treated group had an abrupt decrease on the number of β-cells, as well as very disorganized islets. There can be noticed many tissue alterations on the structure (the islet is outlined on Figure 24C) and, as expected, a reduction of insulin labelling. This data demonstrates that we successfully induced a state of type 2 diabetes on Wistar rats due to the partial reduction of β-cell mass.

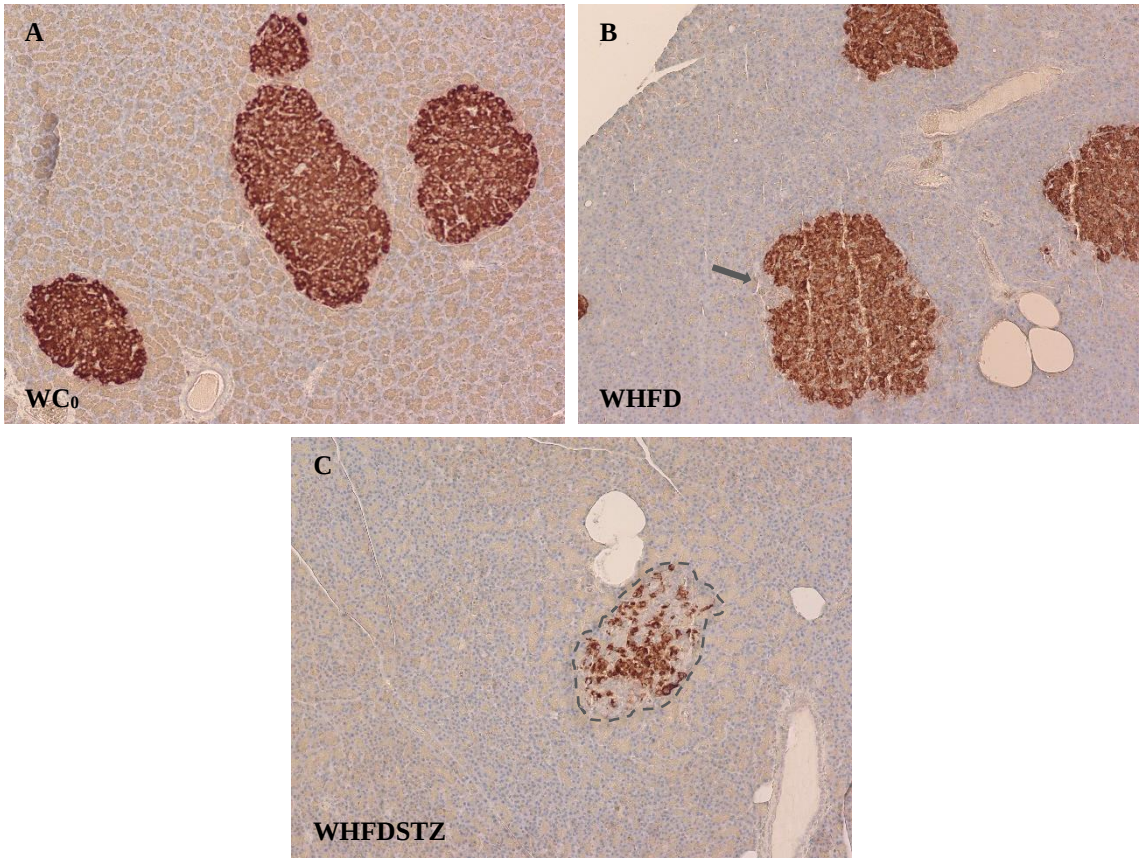

Figure 24: Detection of islets of Langerhans in all WC_0, WHFD and WHFDSTZ groups (10x; n=3-4). The arrow appoints to a loss of cell mass; the outline encircles one islet of Langerhans.

Furthermore, with a 40x microscopic objective, it is possible to comply the results previously demonstrated. In fact, a decrease in β-cells *per* islet, on WHFD group pancreas (represented by the arrow on Figure 25B), is slightly visible, when compared to WC_0 (Figure 25A). In the same way, the image of WHFDSTZ pancreas, demonstrates a very disorganized islet (outlined on Figure 25C) with, apparently, less than 50 % of β-cells.

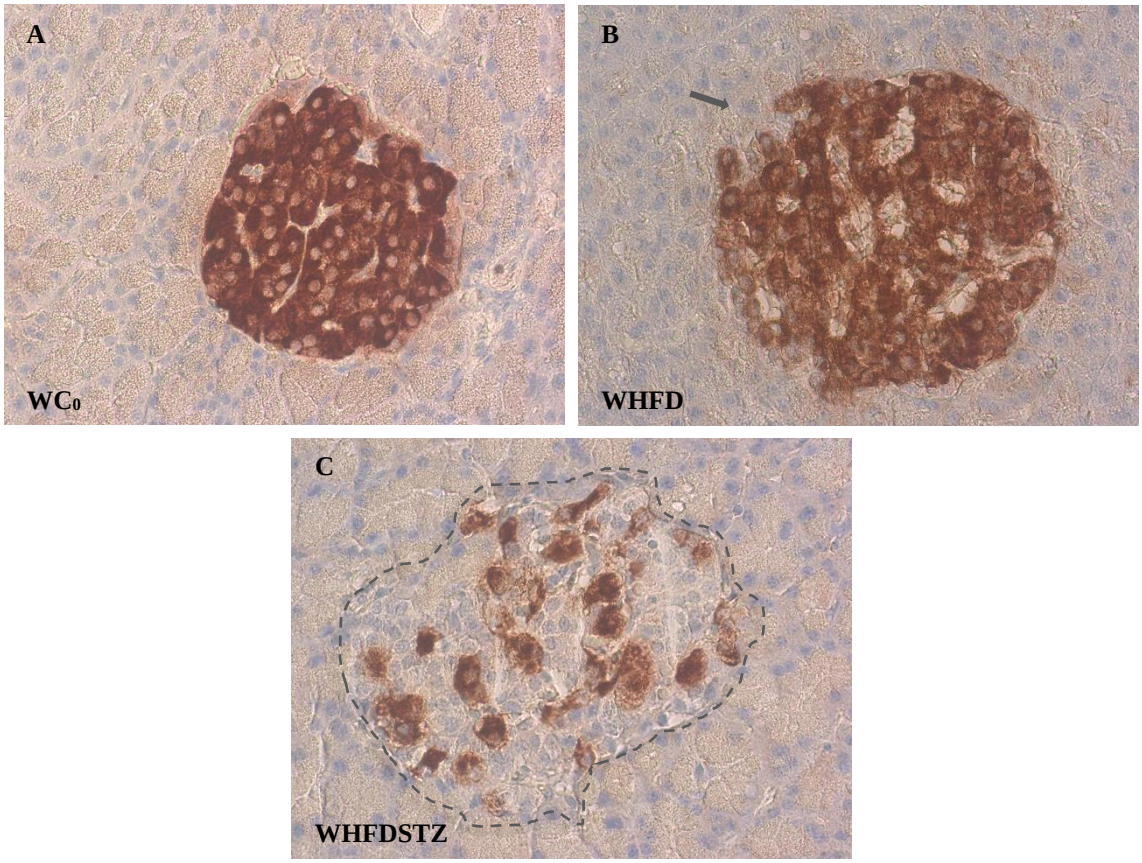

Figure 25: Detection of the islets of Langerhans in all WC_0, WHFD and WHFDSTZ groups (40x; n=3-4), with visible decrease in β-cells mass. The arrow appoints to a loss of cell mass; the outline encircles one islet of Langerhans.

Comparing WC_0 to WHFD, it is nearly assured that the diet had certain effects on the structure, in general. Although, given the quantification graph on Figure 26, which is a measurement of intensity of insulin, it is evident that the high-fat diet group did not show any difference in the maximum intensity of the marked hormone relatively to WC_0. In addition, the intensity observed on islets of the STZ-treated group decreased about 50 % from the other two (p<0,001), proving quantitative evidence for the reduction in the number of β-cells *per* islet and confirming that we were able to induce type 2 diabetes on this group of Wistar rats.

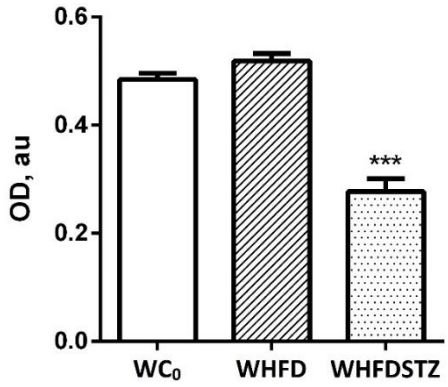

Figure 26: Quantification of insulin stain intensity on islets of Langerhans in all WC_0, WHFD and WHFDSTZ groups (n=3-4). Brown staining was quantified using ImageJ (1.40 g, NIH).

3.1.8. *In situ* liver examination

Beyond biochemical measurements of enzymes related to liver damage, right after the sacrifice of Wistar rats, the general aspect of the organ was examined. In fact, we observed that the HFD itself developed a significant hepatocellular injury, since the organ was visually swollen and its color turning yellow (Figure 27B), which is quite different from the normal liver aspect on the WC_0 group (Figure 27A). Moreover, we can see that the liver in STZ-treated animals has a light color and an increased on its size (Figure 27C).

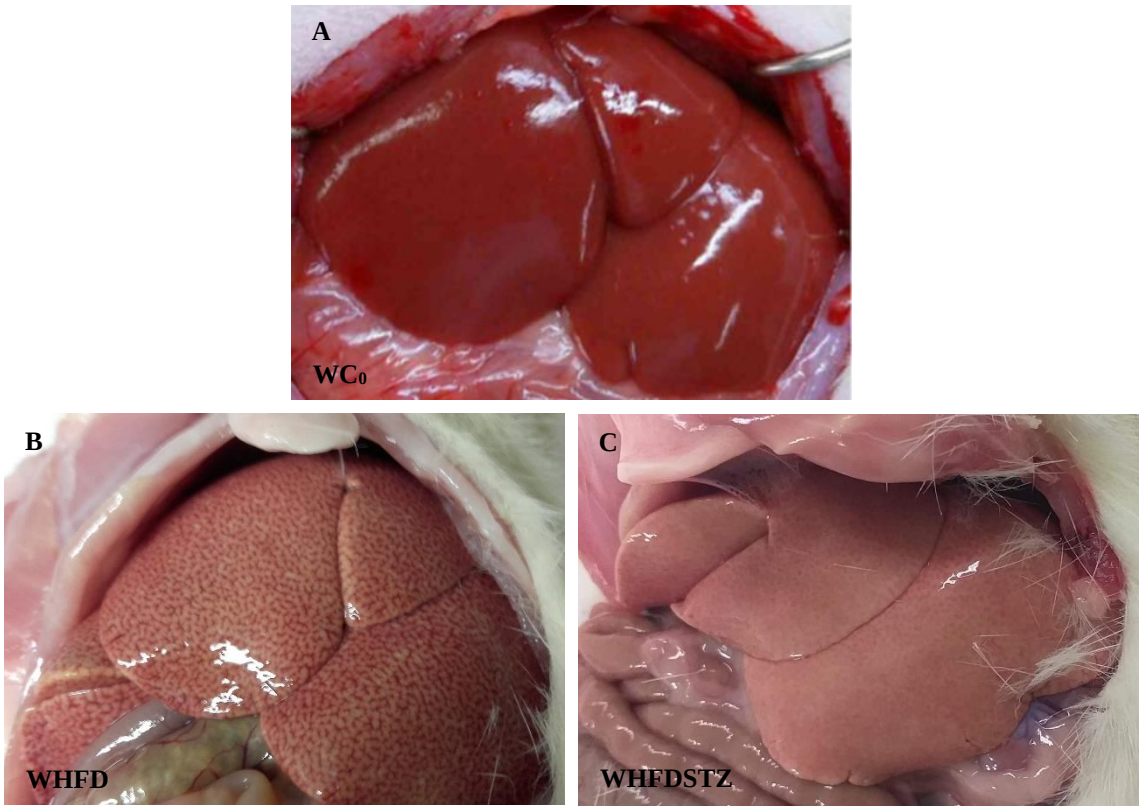

Figure 27: *In situ* examination of the liver in all WC_0, WHFD and WHFDSTZ groups.

3.2. High-fat diet MG-treated animal model

3.2.1. Body weight

For this study, three groups of animals were used: the control group (WC_0), which was fed with normal diet, the group fed with high-fat diet (WHFD) and the group fed with high-fat diet and treated with methylglyoxal (MG) for three months (WHFDMG). The groups WHFD and WHFDMG started the high-fat diet at two months-old, to prevent adaptation to the diet. Therefore, their body weight evolution was monitored, for four months. Additionally, after the third month, it was given a daily solution of increasing concentration of MG, to the WHFDMG group, with a final concentration of 75 mg/kg, as expressed on Figure 7.

Analyzing the range of weight (Table 11), we can verify that both control Wistar and Wistar fed with high-fat diet have a constant increasing weight profile and that WHFD has the highest values of body weight. Between these two groups, it is possible to notice the greatest difference at five months-old (p<0,001).

Regarding the WHFDMG group, we can notice a constant weight gain, quite similar to the other groups. At five months-old, however, there is a statistically significant difference (p<0,05), when compared to the WHFD group. Although not statistically noteworthy, on the sixth month the WHFDMG did not gain as much weight as the other animals, demonstrating a profile of the curve less accentuated (Figure 28).

Body weight (g)			
	WC_0 (n=18)	**WHFD (n=18)**	**WHFDMG (n=4)**
3 months	-	367 ± 6,13	386 ± 8,95
4 months	436 ± 5,10	424 ± 10,30	434 ± 15,77
5 months	460 ± 6,49	515 ± 3,59 §§§	459 ± 18,16 ^{ϕ}
6 months	515 ± 14,28	532 ± 12,75	493 ± 18,77

Table 11: Body weight profile of all Wistar rats used in this section of the study, expressed in g. Data are mean ± SEM (standard error of the mean; n=4-18). ^{ϕ} p<0,05 in comparison with WHFD; §§§ p<0,001 in comparison with WC_0. Data about the weight at 3 months-old from WC_0 group is not available.

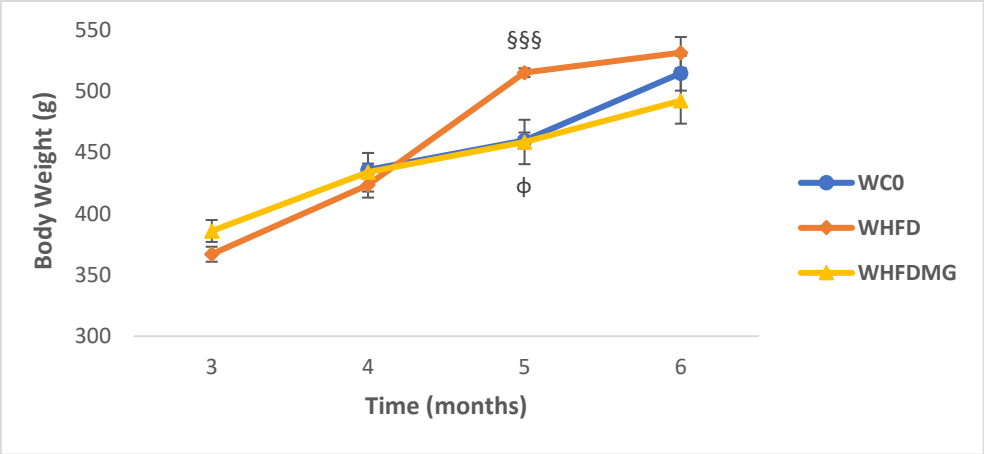

Figure 28: Evolution of body weight at 3, 4, 5 and 6 months-old, expressed in g. Data are mean ± SEM (standard error of the mean; n=4-18). ^{ϕ} p<0,05 in comparison with WHFD; §§§ p<0,001 in comparison with WC_0. Data about the weight at 3 months-old from WC_0 group is not available.

3.2.2. Lipid profile

a. Serum cholesterol levels and atherogenic index

As animals were fed with high-fat diet, it is convenient to evaluate their blood lipid profile. For such purpose, after the sacrifice the blood serum was collected and analyzed.

Concerning HDL levels after four months of an increased lipid intake, the group of WHFD presents significant lower levels when compared to the control group (p<0,001). As expected, in terms of total cholesterol, it is possible to notice a slight enhancement (Figure 29B), due to an increased value of non-HDL cholesterol (Table 12).

Similarly, the levels of total cholesterol are increased in WHFDMG (p<0,05), but, surprisingly, the levels of HDL are very low when compared to WC_0 (p<0,001) and also quite low comparing to WHFD (p<0,01). Wistar rats treated with fat diet already presented lower HDL levels relative to controls, that are exacerbated by methylglyoxal (Figure 29A).

	WC_0 (n=12)	WHFD (n=15)	WHFDMG (n=4)
HDL Cholesterol (mg/dL)	49 ± 1,51	23 ± 1,07 §§§	16 ± 1,08 ^{***ϕϕ}
Total Cholesterol (mg/dL)	83 ± 3,53	112 ± 15,68	133 ± 16,07 *

Table 12: Serum cholesterol levels, expressed in mg/dL. Data are mean ± SEM (standard error of the mean; n=4-15). ^{ϕϕ} p<0,01 in comparison with WHFD; * p<0,05 in comparison with WC_0; *** p<0,001 in comparison with WC_0; §§§ p<0,001 in comparison with WC_0.

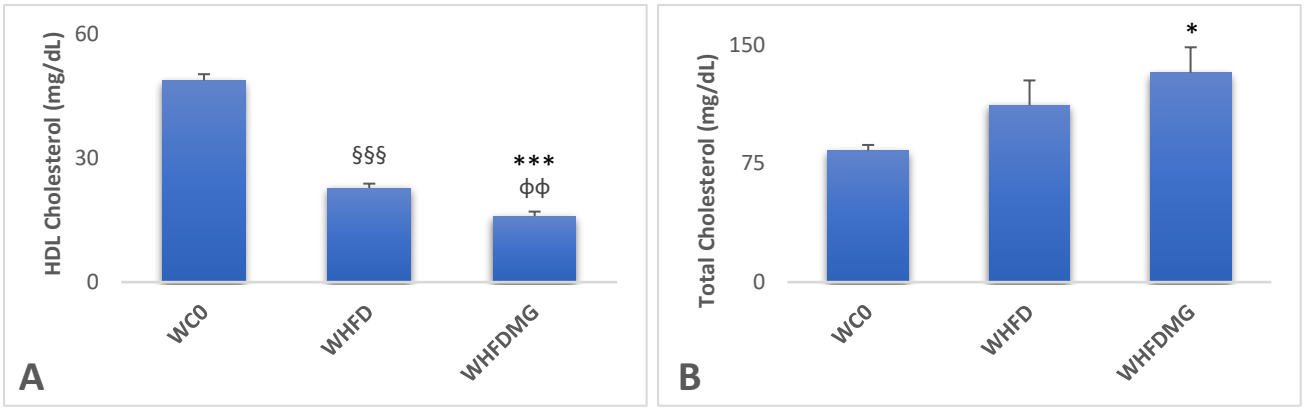

Figure 29: Serum cholesterol levels, expressed in mg/dL, of the three groups of study. Data are mean ± SEM (standard error of the mean; n=4-15). $^{\phi\phi}$ p<0,01 in comparison with WHFD; * p<0,05 in comparison with WC_0; *** p<0,001 in comparison with WC_0; §§§ p<0,001 in comparison with WC_0.

Representing the relationship between HDL and total cholesterol, the atherogenic index (AI; given by the ratio total cholesterol/HDL) is a strong marker to predict the risk of atherosclerosis. As expected, it is higher in animals fed with high-fat diet than those fed with normal diet (Figure 30). Therefore, there is a prominent difference of AI between WHFD and the control group (p<0,001).

MG-treated rats have an atherogenic index statistically different from the control group (p<0,05) and from WHFD (p<0,01). In fact, a high value was expected considering that, in WHFDMG, HDL cholesterol is very low, we understand the increase of AI.

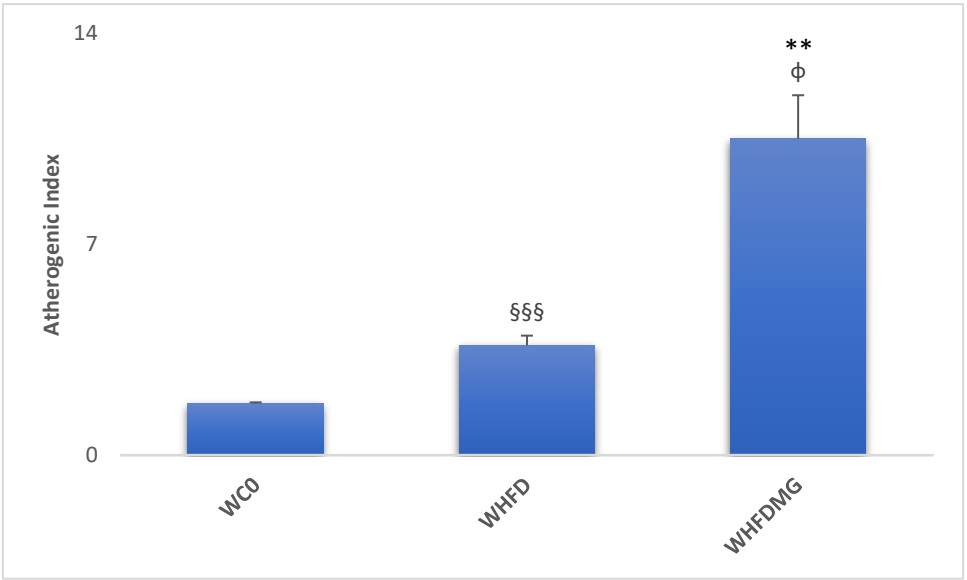

Figure 30: Atherogenic index of the three groups of study. Data are mean ± SEM (standard error of the mean; n=4-12). $^{\phi}$ p<0,05 in comparison with WHFD; ** p<0,01 in comparison with WC_0; §§§ p<0,001 in comparison with WC_0.

b. Triglycerides and phospholipids

As part of the lipid profile, triglycerides were also analyzed and WHFD had similar levels compared to WC_0. It is also visible that WHFDMG presented levels of triglycerides much higher than WC_0 (p<0,01) and WHFD (p<0,05), as expected.

In addition, the phospholipids level is only significantly different from the control group (p<0,05) and rather similar to the WHFD group. Unsurprisingly, both parameters are increased in MG-treated rats (Table 13).

	WC_0 (n=11)	WHFD (n=12)	WHFDMG (n=5)
Triglycerides (mg/dL)	75 ± 5,69	86 ± 10,13	152 ± 13,89 $^{**\phi}$
Phospholipids (mg/dL)	137 ± 4,80	142 ± 6,19	170 ± 9,47 *

Table 13: Triglycerides and phospholipids levels, expressed in mg/dL. Data are mean ± SEM (standard error of the mean; n=5-12). $^{\phi}$ p<0,05 in comparison with WHFD; * p<0,05 in comparison with WC_0; ** p<0,01 in comparison with WC_0.

3.2.3. Liver function tests

a. Transaminase levels and AST/ALT ratio

Levels of both liver enzymes alanine transaminase (ALT) and aspartate transaminase (AST) were measured and their ratio calculated through the formula AST/ALT.

As a specific marker of liver damage, extracted from serum, ALT (Figure 31A) is significantly increased in WHFD group when compared to the control (p<0,05) and, similarly, so does the WHFDMG (p<0,001).

Moreover, as a marker of other inflammatory processes, AST levels (Figure 31B) are also important to determine liver damage. Relating WHFD group with the control (Table 14), it is possible to understand that there is a slight, although significant (p<0,05), difference on this transaminase level. Similarly, MG-treated Wistar rats show an increased value of AST when compared to the other WC_0 group (p<0,05).

The hepatocellular injury may be reflected on the ratio of these two enzymes (Figure 31C). The MG-treated group does not reveal any statistically significant difference from neither WC_0 nor WHFD groups (Table 14 and Figure 30). However, it is visible the increment associated with the levels of both enzymes.

	WC_0 (n=12)	WHFD (n=14)	WHFDMG (n=4)
ALT (U/L)	50 ± 2,22	64 ± 3,11 §	91 ± 18,12 ***
AST (U/L)	114 ± 5,45	141 ± 12,54 §	177 ± 21,98 *
ratio	2,28	2,22	1,90

Table 14: Transaminases levels, expressed in U/L, and corresponding ratio. Data are mean ± SEM (standard error of the mean; n=4-14). * $p<0,05$ in comparison with WC_0; *** $p<0,001$ in comparison with WC_0; § $p<0,05$ in comparison with WC_0.

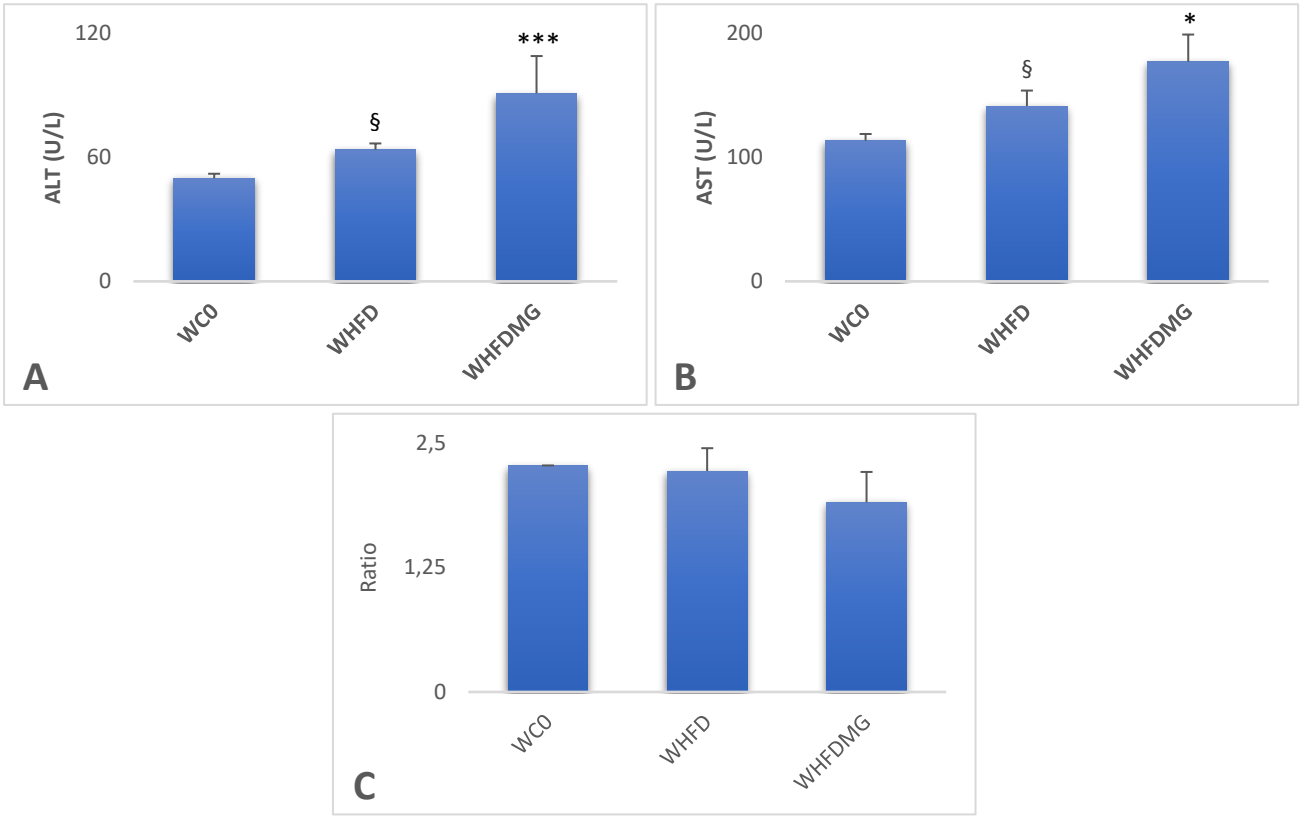

Figure 31: Transaminases levels, expressed in U/L, and corresponding ratio of the three groups of study. Data are mean ± SEM (standard error of the mean; n=4-14). * $p<0,05$ in comparison with WC_0; *** $p<0,001$ in comparison with WC_0; § $p<0,05$ in comparison with WC_0.

b. Levels of alkaline phosphatase and gamma-GT

More biomarkers of liver damage were analyzed to determine the extent of harm, on the organ, in methylglyoxal-treated Wistar rats. Concerning the alkaline phosphatase, we can observe that the levels increased (Figure 32A) when comparing both WHFD and WHFDMG to the control group (p<0,001). Although, the level of this enzyme is lower, in MG-treated animals than the value observed in WHFD (p<0,01), which was not predictable (Table 15).

Similarly, the gamma-glutamyl transferase level, also reflecting the pathological condition in the liver (Figure 32B), is, on WHFDMG group, higher than the other two groups. Although, there are no relevant differences to mention.

	WC_0 (n=12)	WHFD (n=14)	WHFDMG (n=5)
Alkaline Phosphatase (U/L)	84 ± 5,69	172 ± 18,51 §§§	118 ± 3,36 ^{***ϕϕ}
Gamma-GT (U/L)	1	1,11 ± 0,11	1,2 ± 0,20

Table 15: Values of alkaline phosphatase and gamma-GT, expressed in U/L. Data are mean ± SEM (standard error of the mean; n=5-14). ^{ϕϕ} p<0,01 in comparison with WHFD; *** p<0,001 in comparison with WC_0; §§§ p<0,001 in comparison with WC_0.

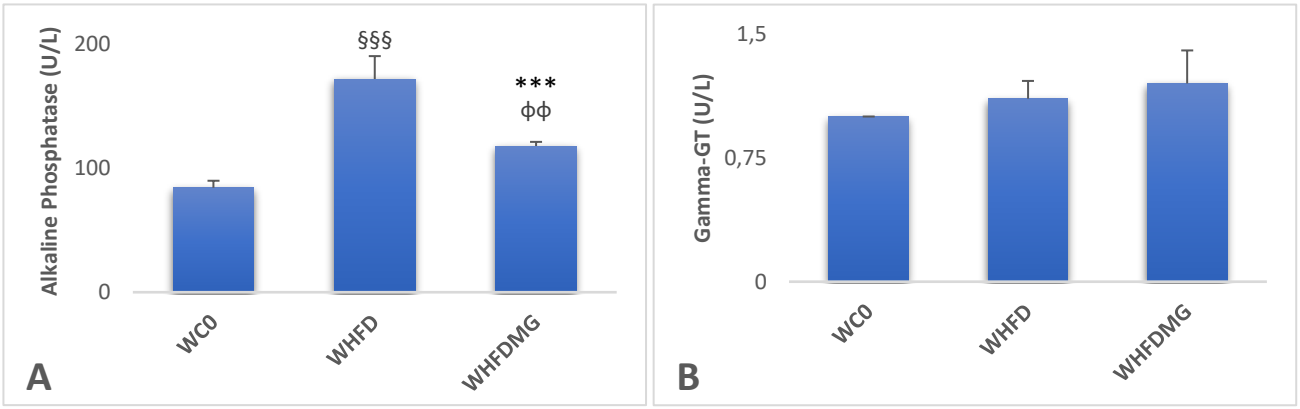

Figure 32: Levels of alkaline phosphatase and gamma-GT, expressed in U/L, of the three groups of study. Data are mean ± SEM (standard error of the mean; n=5-14). ^{ϕϕ} p<0,01 in comparison with WHFD; *** p<0,001 in comparison with WC_0; §§§ p<0,001 in comparison with WC_0.

3.2.4. Glucose Tolerance Test (GTT) and Insulin Tolerance Test (ITT)

Insulin resistance is an inherent feature of endothelial dysfunction and, therefore, it is crucial for the present study. These two tests, performed one week before the sacrifices and a week apart, are proof of the glucose intolerance and insulin resistance state in this animal model, respectively. The GTT is given to determine how quickly glucose is cleared from the blood and it is quite important to prove an impaired beta cell function. Similarly, the ITT is used to evaluate the insulin sensitivity.

For the first test, GTT, the WC_0 group is the control model of glucose tolerance, therefore fulfilled the expected metabolic profile, since it indicates proper glucose utilization.

As expected, the high-fat diet, by itself, creates a certain degree of glucose intolerance, showed by statistically significant differences (Table 16), when compared to the control group, with normal diet, at the beginning of the test (fasting glucose; $p<0,05$), one and two hours after a glucose load ($p<0,01$).

It is tempting to assume, right away, that MG-treated rats had impaired glucose tolerance (Figure 33). In general, the levels of glycemia are higher in WHFDMG than WC_0 and WHFD ($p<0,01$) before the beginning of the test. One hour after the injection of glucose, glycemia is significantly higher than the control ($p<0,01$) and WHFD rats ($p<0,05$). Finally, and to prove glucose intolerance, the values two hours after the injection are significantly higher from WC_0 ($p<0,001$) and from WHFD ($p<0,01$). The area under the curve is significantly higher in WHFD (261 ± 12.7) and WHFDMG (333 ± 15.6) compared with WC_0 group (220 ± 4.8).

Glycemia (mg/dL)			
Time (min)	**WC_0 (n=11)**	**WHFD (n=14)**	**WHFDSMG (n=5)**
0	66 ± 1,13	74 ± 2,82 §	91 ± 3,49 $^{**\phi\phi}$
60	138 ± 5,14	165 ± 13,30 §§	214 ± 14,22 $^{**\phi}$
120	98 ± 2,99	118 ± 5,88 §§	147 ± 6,91 $^{***\phi\phi}$

Table 16: Glucose tolerance test, where glycemia expressed in mg/dL. Data are mean ± SEM (standard error of the mean; n=5-14). $^{\phi}$ $p<0,05$ in comparison with WHFD; $^{\phi\phi}$ $p<0,01$ in comparison with WHFD; ** $p<0,01$ in comparison with WC_0; *** $p<0,001$ in comparison with WC_0; § $p<0,05$ in comparison with WC_0; §§ $p<0,01$ in comparison with WC_0.

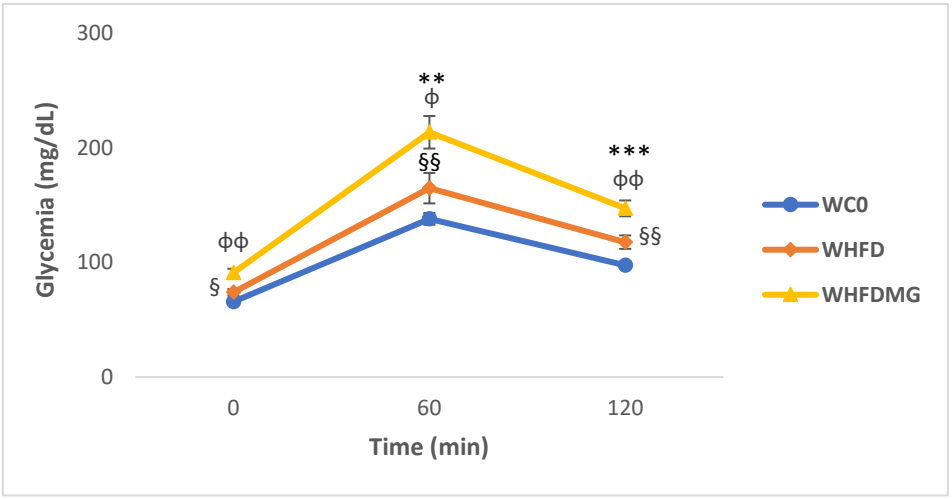

Figure 33: Glucose tolerance test, with glycemia expressed in mg/dL, of the three groups in study. Data are mean ± SEM (standard error of the mean; n=5-14). ^{ϕ} p<0,05 in comparison with WHFD; ^{ϕϕ} p<0,01 in comparison with WHFD; ** p<0,01 in comparison with WC_0; *** p<0,001 in comparison with WC_0; § p<0,05 in comparison with WC_0; §§ p<0,01 in comparison with WC_0.

In the insulin tolerance test, the degree to which blood glucose concentrations fall following insulin administration represent the efficiency of insulin action. First, we must test the theory that the HFD, itself, has some effect on insulin resistance. We can see the significant difference from the WHFD to WC_0 at the beginning and after 15 minutes of the test (p<0,001). At 30 minutes there is still a slight increment in the glucose levels (p<0,01), but it is only after 45 minutes that we observe equal levels of glucose between the two groups (Table 17).

Concerning the WHFDMG, only before the insulin injection we can notice some similarity of values with WHFD, and a variance when compared to WC_0 (p<0,01). The following results indicate a great statistic difference from the control group at 15, 30 and 45 minutes (p<0,001), leaving 60 and 120 minutes with a significance of p<0,01 (Figure 34). In fact, this group is insulin resistant, since the glucose clearance from the blood is quite delayed.

When compared to the high-fat diet group, the values of glycemia for 15, 45, 60 and 120 minutes have a significance of p<0,001. Only at minute 30 the statistic difference is lower (p<0,01).

Glycemia (mg/dL)			
Time (min)	**WC_0 (n=9)**	**WHFD (n=11)**	**WHFDMG (n=5)**
0	81 ± 1,80	93 ± 2,30 §§§	97 ± 3,05 **
15	75 ± 1,07	93 ± 1,45 §§§	122 ± 1,84 ^{***ϕϕϕ}
30	65 ± 1,87	80 ± 3,52 §§	105 ± 4,82 ^{***ϕϕ}
45	66 ± 2,72	68 ± 2,85	99 ± 4,14 ^{***ϕϕϕ}
60	65 ± 2,15	65 ± 2,95	93 ± 4,51 ^{**ϕϕϕ}
120	67 ± 2,30	63 ± 3,06	87 ± 3,38 ^{**ϕϕϕ}

Table 17: Insulin tolerance test, with glycemia expressed in mg/dL. Data are mean ± SEM (standard error of the mean; n=5-11). ^{ϕϕ} p<0,01 in comparison with WHFD; ^{ϕϕϕ} p<0,001 in comparison with WHFD; ** p<0,01 in comparison with WC_0; *** p<0,001 in comparison with WC_0; §§ p<0,01 in comparison with WC_0; §§§ p<0,001 in comparison with WC_0.

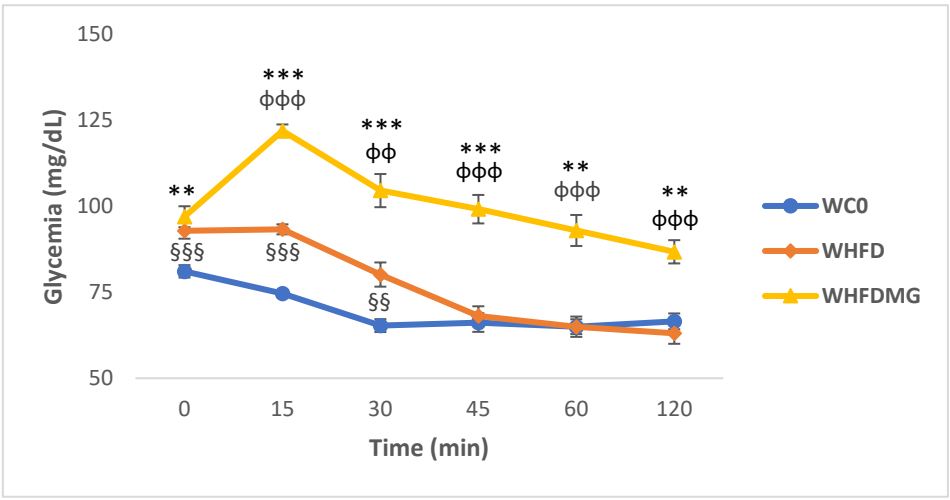

Figure 34: Insulin tolerance test, with glycemia expressed in mg/dL, of the three groups in study. Data are mean ± SEM (standard error of the mean; n=5-11). ^{ϕϕ} p<0,01 in comparison with WHFD; ^{ϕϕϕ} p<0,001 in comparison with WHFD; ** p<0,01 in comparison with WC_0; *** p<0,001 in comparison with WC_0; §§ p<0,01 in comparison with WC_0; §§§ p<0,001 in comparison with WC_0.

3.2.5. Isometric tension studies

The following studies of isometric tension intend to demonstrate the effect of the treatment with HFD and HFD+MG at the vascular level, in thoracic aorta. Therefore, three parts of the subsequent protocol were performed to evaluate the endothelium and smooth muscle cells response to different vasodilator factors, both dependent and independent from the endothelium, and one part is meant to evaluate their response to a contractile factor. The comparison of HFD-fed animals with WC_0 will give us quantitative and qualitative information about the degree of endothelium dysfunction.

At first, the vasodilation dependent from the endothelium was examined. The procedure involves contraction with phenylephrine (PHE), a α-1 adrenergic agonist, followed by a dose-response to increasing concentrations of acetylcholine (ACh). In fact, the control group shows a vascular relaxation of about 80 % (Figure 35). In contrast, WHFD group has about 10 % less relaxation (p<0,01 and p<0,001) and lower sensitivity to ACh, with a shift in the dose-response to the right.

Adding methylglyoxal to the drinking water, WHFDMG group, displayed 30 % of maximum relaxation, which is quite different from the other two (p<0,001 in general), including the shape of the curve. This way, we can predict that the glycation, as consequence of the treatment with MG, affects the endothelium response to ACh, significantly diminishing the endothelial function.

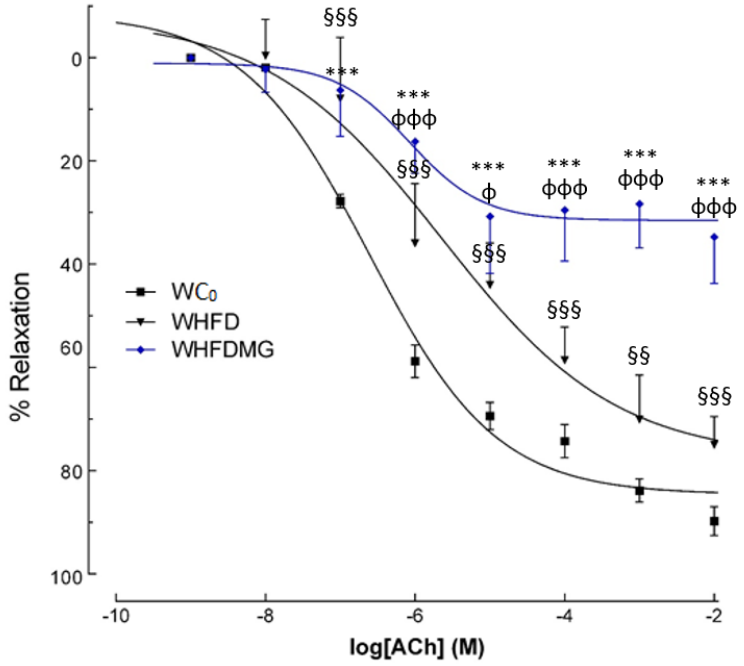

Figure 35: Dose-response curves to ACh of the three groups in study after contraction with PHE. Data are mean ± SEM (standard error of the mean; n=4-12). ^{ϕ} p<0,05 in comparison with WHFD; ^{ϕϕϕ} p<0,001 in comparison with WHFD; *** p<0,001 in comparison with WC_0; §§ p<0,01 in comparison with WC_0; §§§ p<0,001 in comparison with WC_0.

To evaluate the role of perivascular adipose tissue on endothelial function, aortic rings were mounted with and without PVAT. On Figure 36, we first compare the control group with the group fed with HFD. In fact, there are no significant differences on WC_0 with and without PVAT. Moreover, the curve of WC_0+PVAT shows an apparent 5 % increment in maximum relaxation relative to WC_0-PVAT. In reality, there are no significant differences in these curves.

Concerning the WHFD group, we can observe that the curve regarding the presence of PVAT has a profile which indicates that, after the fourth concentration of ACh, the tissue does not respond to any increased concentration of the relaxing factor, leaving WHFD+PVAT with a maximum relaxation of 50 %. In comparison with the absence of perivascular adipose tissue, there is a variance between the curves of about 25 %, with differences of $p<0,01$, on third and sixth concentrations, and $p<0,001$, on seventh and eighth concentrations. In addition, there are also statistically significant differences from the control group with PVAT ($p<0,01$ on the fourth concentration and $p<0,001$ after the fifth concentration).

Moreover, there are some differences between WC_0+PVAT and WHFD-PVAT, and WC_0-PVAT and WHFD+PVAT, yet we do not intend to compare groups with distinct conditions, since the perivascular adipose tissue creates a different environment.

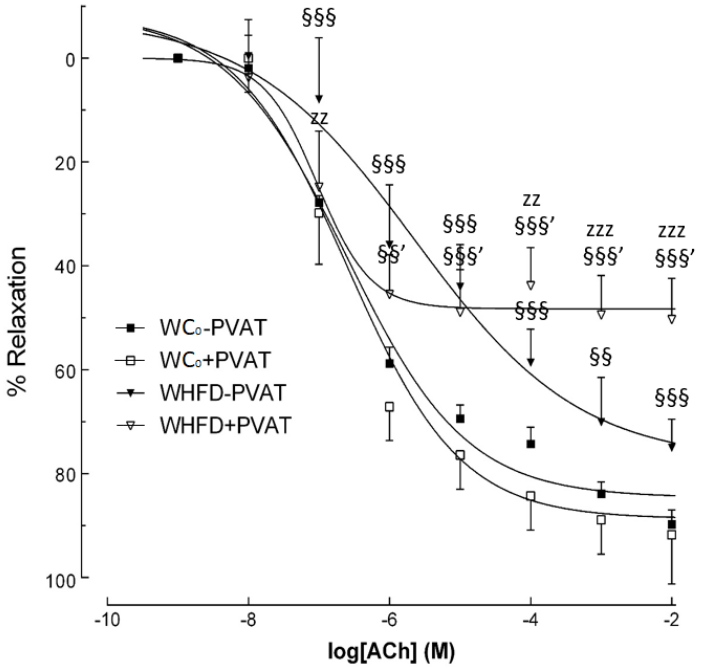

Figure 36: Dose-response curves to ACh of WC_0 and WHFD after contraction with PHE. Data are mean ± SEM (standard error of the mean; n=4-12). §§ $p<0,01$ in comparison with WC_0-PVAT; §§§ $p<0,001$ in comparison with WC_0-PVAT; $^{§§'}$ $p<0,01$ in comparison with WC_0+PVAT; $^{§§§'}$ $p<0,001$ in comparison with WC_0+PVAT; ^{zz} $p<0,01$ in comparison with WHFD-PVAT; ^{zzz} $p<0,001$ in comparison with WHFD-PVAT.

The same protocol was applied to MG-treated group (Figure 37). It is possible to verify that the curve corresponding to WHFDMG+PVAT reaches 20 % of relaxation, about 15 % less than WHFDMG-PVAT. In fact, there are some significant differences on the last two concentrations (p<0,001). This aggravation of endothelial function is possibly due to the severe damage on perivascular adipose tissue, that seems to have lost its beneficial properties.

In addition, we can verify some discrepancies when comparing the MG-treated group to WHFD. As mentioned before, there are statistically significant differences in the absence of perivascular adipose tissue (p<0,05 on the fifth concentration and p<0,001 in general). Moreover, since the beginning of the dose-response, the WHFDMG+PVAT group is shown to be very different from WHFD+PVAT (p<0,001) in terms of shape of the curve, since it stabilizes faster for lower concentrations and has less sensitivity to acetylcholine.

To note, data regarding any comparison with the WC_0 is not expressed on the graph simply because we would like to compare the HFD-fed animals, which have similar curve profiles. Although, it is noticed a very high discrepancy compared to the MG-treated group.

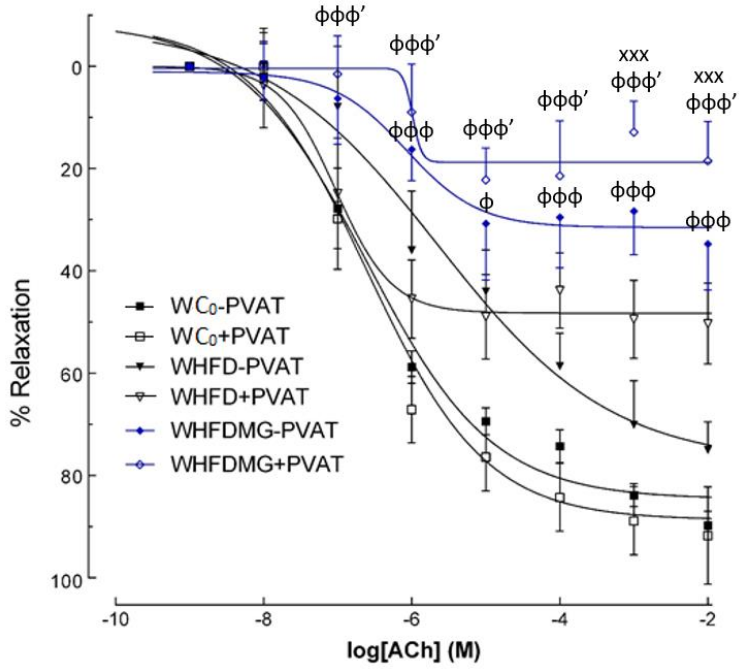

Figure 37: Dose-response curves to ACh of the three groups in study after contraction with PHE. Data are mean ± SEM (standard error of the mean; n=4-12). $^{\phi}$ p<0,05 in comparison with WHFD-PVAT; $^{\phi\phi\phi}$ p<0,001 in comparison with WHFD-PVAT; $^{\phi\phi\phi'}$ p<0,001 in comparison with WHFD+PVAT; ^{xxx} p<0,001 in comparison with WHFDMG-PVAT.

Concerning the endothelium-independent vasodilation to evaluate vascular smooth muscle integrity, the method included contraction with phenylephrine, followed by a dose-response to a powerful nitric oxide donor, sodium nitroprusside (SNP).

All three groups fulfil the prognostic: the vasodilation was almost total (Figure 38). As the compound is very potent and its action quite extensive, the expected results were, indeed, a full relaxation of the artery. Observing the curves on the control group, WC_0+PVAT appears to have a slightly faster relaxation compared to WC_0-PVAT, which is the expected result, since the perivascular adipose tissue integrity is intact and, consequently, its anticontractile effect can be noticed. Although, a small statistically significant difference between these two curves was observed on the fourth concentration ($p<0,05$).

Similarly, the curves of WHFD-PVAT and WHFD+PVAT also have the same profile as those from the control group, where the presence of PVAT requires less concentration of SNP for the same percentage of relaxation of WHFD-PVAT. Although, the maximum vasodilation is achieved by the aorta without the perivascular adipose tissue. In addition, there are some significant differences between the curves along the dose-response ($p<0,05$ on the third concentration and $p<0,001$ in general). Also, some points reveal the variance from the control group, in both absence ($p<0,01$ on the seventh concentration) and presence of PVAT ($p<0,05$ on the eighth concentration).

In respect to the MG-treated group, we observe a different behavior of the curves when compared to the two other groups. In this case, WHFDMG-PVAT has a rapid reaction to SNP, while the response of WHFDMG+PVAT is delayed. In fact, data indicates some statistically significant differences between these two curves ($p<0,05$ on the fifth, $p<0,01$ on the third and $p<0,001$ on the fourth concentration). Comparing to WC_0, there are differences between the curves in the absence ($p<0,01$ on the second and $p<0,001$ on following concentrations) and the presence of PVAT ($p<0,05$ on sixth and seventh concentrations and $p<0,01$ on the fifth concentration). Likewise, comparing to WHFD, there are also differences with the absence ($p<0,05$ on the sixth and $p<0,001$ on third, fourth and fifth concentrations) and the presence of PVAT ($p<0,05$ only on the sixth and $p<0,001$ on seventh and eighth concentrations).

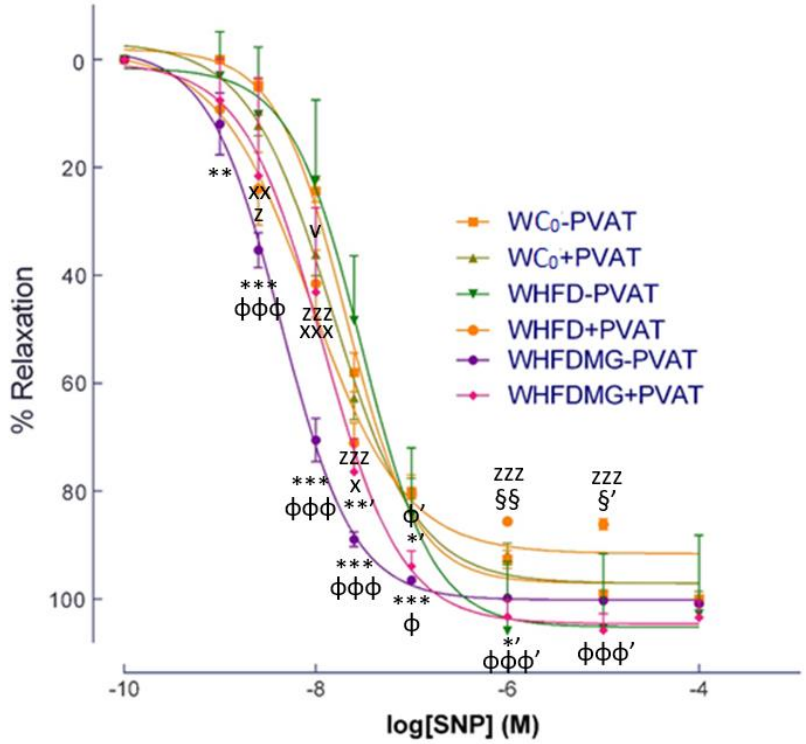

Figure 38: Dose-response curves to SNP of the three groups in study after contraction with PHE. Data are mean ± SEM (standard error of the mean; n=4-12). $^{\phi}$ p<0,05 in comparison with WHFD-PVAT; $^{\phi\phi\phi}$ p<0,001 in comparison with WHFD-PVAT; ** p<0,01 in comparison with WC_0-PVAT; *** p<0,001 in comparison with WC_0-PVAT; §§ p<0,01 in comparison with WC_0-PVAT; $^{\phi'}$ p<0,05 in comparison with WHFD+PVAT; $^{\phi\phi\phi'}$ p<0,001 in comparison with WHFD+PVAT; $^{*'}$ p<0,05 in comparison with WC_0+PVAT; $^{**'}$ p<0,01 in comparison with WC_0+PVAT; $^{\S'}$ p<0,05 in comparison with WC_0+PVAT; ^{v} p<0,05 in comparison with WC_0-PVAT; ^{x} p<0,05 in comparison with WHFDMG-PVAT; ^{xx} p<0,01 in comparison with WHFDMG-PVAT; ^{xxx} p<0,001 in comparison with WHFDMG-PVAT; ^{z} p<0,05 in comparison with WHFD-PVAT; ^{zzz} p<0,001 in comparison with WHFD-PVAT.

Next, we studied the effect of L-NAME, an inhibitor of the enzyme NOS, incubated with indomethacin, a cyclooxygenase inhibitor, with the purpose to evaluate the vasodilation independent of direct actions of NO and prostaglandins, especially PGI2 (Figure 39). To note, the increase, in almost every point, of contraction between the first and the second concentration is due to the prevailing contractile conditions of L-NAME, Indo and PHE, which are not revertible by the first addition of a small concentration of ACh.

The WC_0-PVAT group presents a constant relaxation, providing us the expected dose-response to acetylcholine after contraction with phenylephrine, on an environment with L-NAME and indomethacin. Nevertheless, some differences can be noticed when studying the WC_0+PVAT curve. In fact, the perivascular adipose tissue leads to a late response to ACh, demonstrating that it is affected by L-NAME and indomethacin (p<0,05 on the third and p<0,001

on the following concentrations). Similarly, the behavior of the curves on WHFD rats shows that PVAT is affected by the substances used on this study and, consequently, affects smooth muscle relaxation. In fact, it does not appear to have any relaxation at all, creating statistically significant differences with the curve WHFD-PVAT (p<0,05 on the fourth, p<0,001 on fifth and sixth, and p<0,01 on the last two concentrations). In fact, there are also points where the difference is important when comparing to WC_0-PVAT (p<0,01 on the sixth and p<0,001 on the seventh concentration) and to WC_0+PVAT (p<0,01 on the seventh concentration of ACh).

Regarding the MG-treated group, there is quite a similarity between the curves WHFDMG-PVAT and WHFDMG+PVAT, since they do not seem to relax, except with the addition of the most concentrated dose of ACh. Although, in that point we can observe a maximum relaxation on WHFD-PVAT, with a significant difference from the other curve (p<0,01). Along the dose-response, we can notice variances when comparing to WC_0-PVAT (p<0,01 on the third and p<0,001 on the following concentrations). Even though the curves, in the absence of PVAT, of WHFD and WHFDMG are quite similar and have identical profiles, some differences can be appointed, especially in the middle of the procedure (p<0,05 and p<0,01).

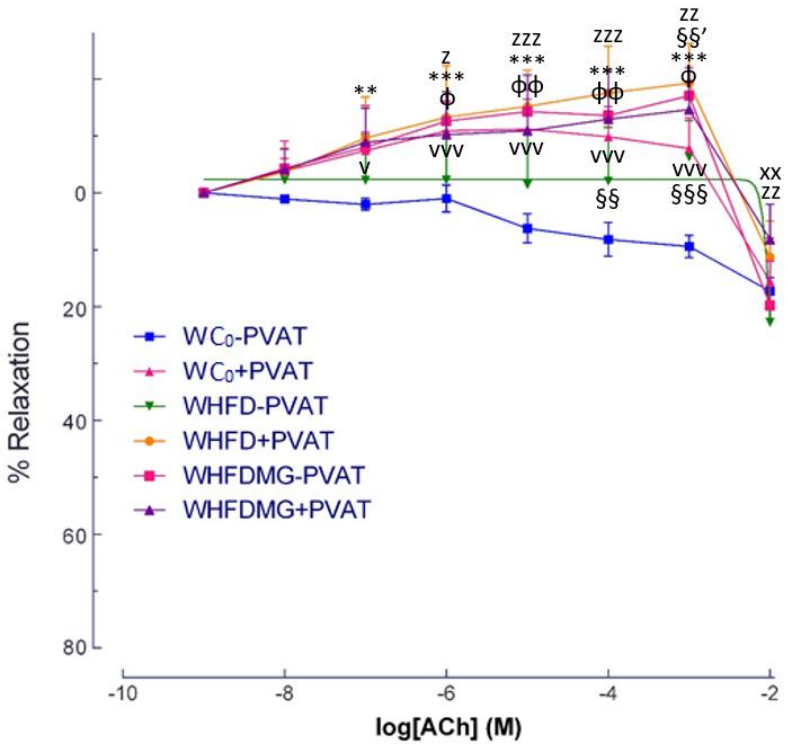

Figure 39: Dose-response curves to ACh of the three groups in study after incubation with L-NAME+Indo and contraction with PHE. Data are mean ± SEM (standard error of the mean; n=4-12). $^{\phi}$ p<0,05 in comparison with WHFD-PVAT; $^{\phi\phi}$ p<0,01 in comparison with WHFD-PVAT; ** p<0,01 in comparison with WC_0-PVAT; *** p<0,001 in comparison with WC_0-PVAT; §§ p<0,01 in comparison with WC_0-PVAT; §§§ p<0,001 in comparison with WC_0-PVAT; $^{\S\S'}$ p<0,01 in comparison with WC_0+PVAT; ^{v} p<0,05 in comparison with WC_0-PVAT; ^{vvv} p<0,001 in comparison with WC_0-PVAT; ^{xx} p<0,01 in comparison with WHFDMG-PVAT; ^{z} p<0,05 in comparison with WHFD-PVAT; ^{zz} p<0,01 in comparison with WHFD-PVAT; ^{zzz} p<0,001 in comparison with WHFD-PVAT.

At last, a study of the vasoconstriction was performed, through a dose-response to the potent vasoconstrictor endothelin-1 (ET-1).

Analyzing the behavior of the curves on the control group (Figure 40), we can verify that WC_0-PVAT has a higher contraction than WC_0+PVAT, as expected due to the anticontractile effect of this tissue. Yet, some differences between these curves in the presence and the absence of perivascular adipose tissue can be appointed for third, fourth and fifth concentrations (p<0,001).

Similarly, the group fed with high-fat diet demonstrates a higher contraction level on the aorta with PVAT than on the one without the tissue, also showing some difference between the curves (p<0,001 on fourth and last concentrations). Although, WHFD-PVAT can contract slightly more than WC_0-PVAT, possibly because subjects with diet rich in lipids have higher production of contractile substances, thus it is not significantly different.

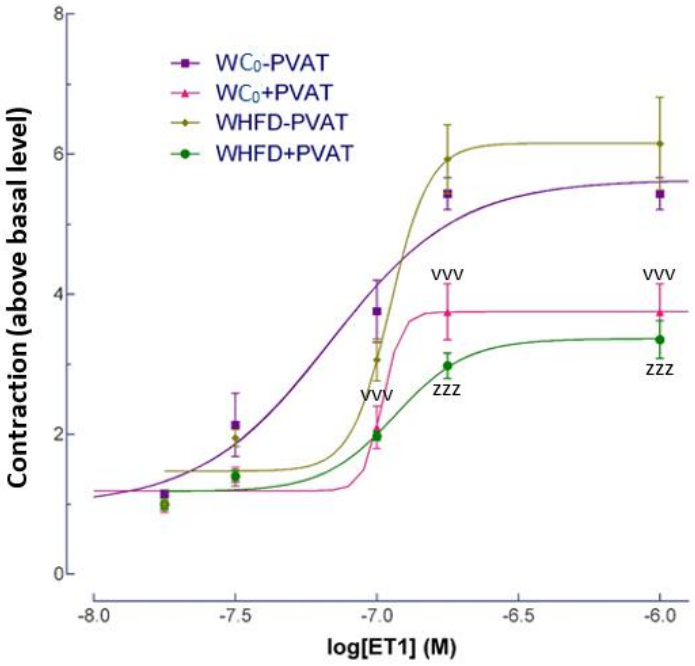

Figure 40: Dose-response curves to ET-1 of WC_0 and WHFD. Data are mean ± SEM (standard error of the mean; n=4-12). ^{vvv} p<0,001 in comparison with WC_0-PVAT; ^{zzz} p<0,001 in comparison with WHFD-PVAT.

When adding WHFDMG to the comparison (Figure 41), we can see that the curves regarding this group are quite similar to the curves of WHFD group.

In fact, the maximum contraction, in WHFDMG-PVAT, reaches almost the same level as WHFD-PVAT, with a small significant difference (p<0,01). Moreover, the three curves regarding the presence of the perivascular adipose tissue are so similar between each other that we can predict that endothelin-1 does not seem to be enough to prove that the anticontractile effect has been lost in neither WHFD nor WHFDMG. In addition, the curves of MG-treated Wistar rats appear to have a normal behavior, compared to the control group, and, so, some differences between the curves with and without PVAT can be noticed (p<0,05 on third and fourth and p<0,001 on the fifth concentration).

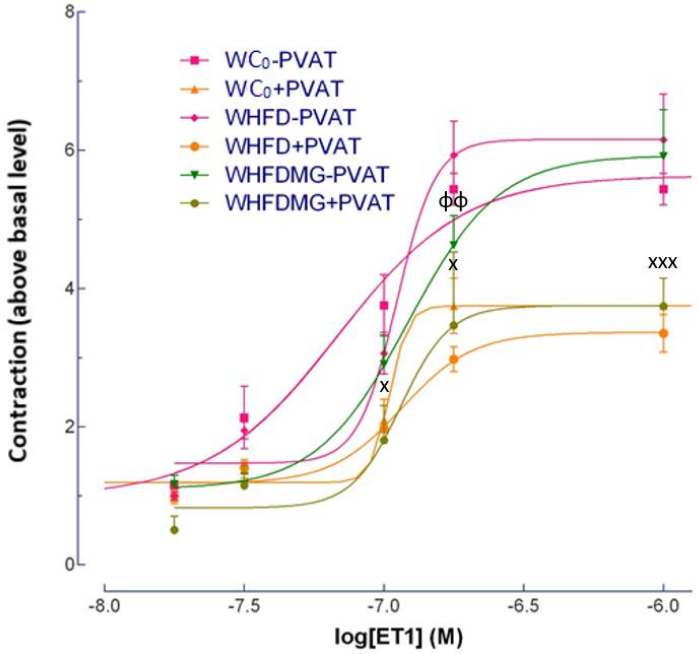

Figure 41: Dose-response curves to ET-1 of the three groups in study. Data are mean ± SEM (standard error of the mean; n=4-12). $^{\phi\phi}$ p<0,01 in comparison with WHFD-PVAT; ^{x} p<0,05 in comparison with WHFDMG+PVAT; ^{xxx} p<0,001 in comparison with WHFDMG+PVAT.

3.2.6. *In situ* liver examination

Beyond biochemical measurements of enzymes related to liver damage, right after the sacrifice of Wistar rats, the general aspect of the organ was examined. In fact, we observed that the HFD itself developed a significant hepatocellular injury, since the organ was visually swollen and its color turning yellow (Figure 42B), which is quite different from the normal liver aspect on the WC_0 group (Figure 42A). Moreover, we can see that the liver in MG-treated animals has a light color and an increased on its size (Figure 42C).

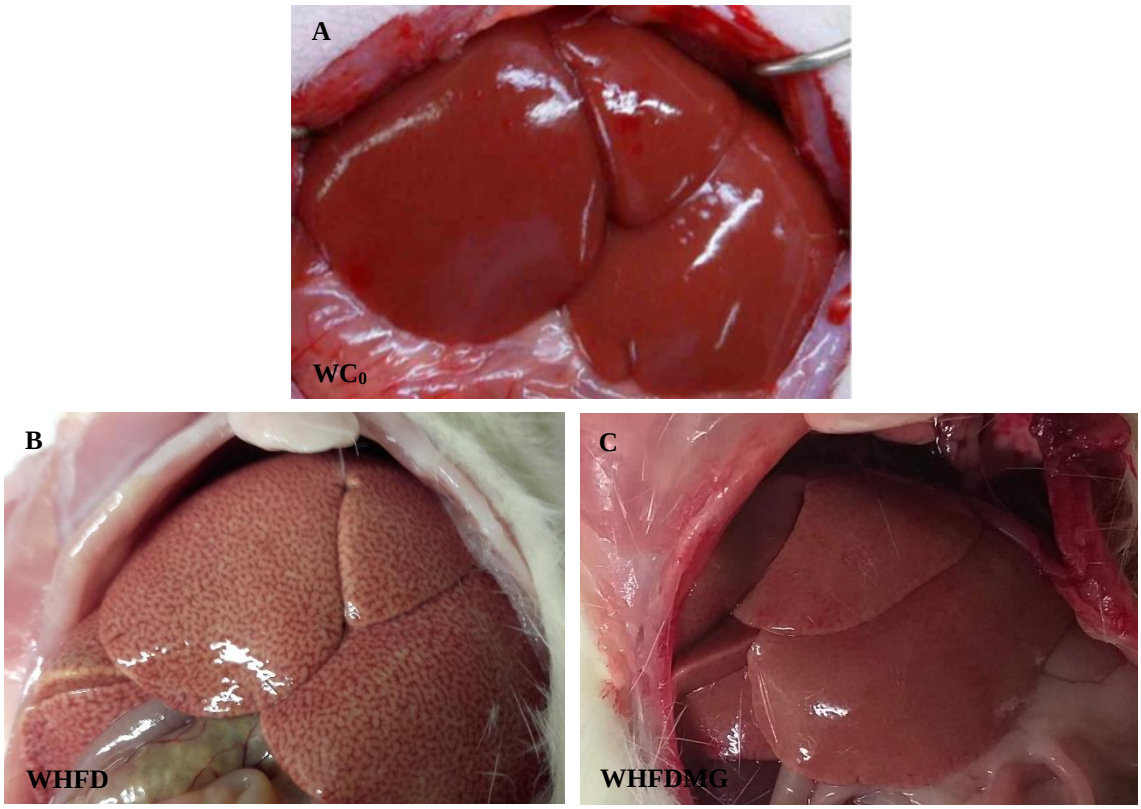

Figure 42: *In situ* examination of the liver in all WC_0, WHFD and WHFDMG groups.

Chapter 4

Discussion

Chapter 4: Discussion

Diabetes *mellitus* is a chronic metabolic disorder, with an increasing number of cases, described as a combination of low amounts of insulin production from pancreatic β-cells and peripheral insulin resistance (Al-Goblan *et al.*, 2014). Moreover, is it well known that type 2 diabetes causes, among others, endothelial cell dysfunction, amplification of the atherosclerotic process, glycosylation of extracellular matrix proteins, and vascular denervation (Kolluru *et al*., 2011). The most common risk factor for the development of type 2 diabetes is, indeed, obesity, which is a prevalent problem of western societies (Cade, 2008). By definition, obesity results from an imbalance between food intake and energy expenditure, which leads to an excessive accumulation of adipose tissue. Consequently, enlarged adipose tissue results in infiltration of macrophages and unbalance of pro- and anti-inflammatory factors, which leads to progressive metabolic complications (Jung and Choi, 2014).

Obesity not only induces a prediabetic state on the organism, but it also develops a vascular dysfunction. Methylglyoxal is a molecule formed, mainly, by glycolysis that has been implicated in the molecular events that lead to endothelial dysfunction (Sena *et al.*, 2012). In fact, it begins affecting the microvasculature but, with progressive dysfunction, MG is able to create major harmful effects on the vasculature. Moreover, it usually runs along type 2 diabetes to implicate the whole system, leading, together, to endothelium dysfunction, insulin resistance and impaired β-cells function (Rodrigues *et al.*, 2017).

Endothelial dysfunction is a systemic pathological condition associated with diabetes and it can be broadly defined as an imbalance between vasodilating and vasoconstricting substances produced by the endothelium. Importantly, endothelial dysfunction has been shown to be of prognostic significance in predicting vascular events, therefore endothelial function testing may potentiate the detection of cardiovascular diseases such as myocardial infarction and ischemic stroke (Kolluru *et al.*, 2011). Experimental evidence indicates that almost the totality of cardiovascular risk factors, such as aging and hypertension, are characterized by the presence of endothelial dysfunction, which is mainly induced by the production and release of oxygen-derived free radicals, which cause NO breakdown (Taddei *et al.*, 2001).

In this study, not only we worked towards the effects that high-fat diet and methylglyoxal have on endothelial function in a normal animal model, as we include a new vision that, for many years, was disregarded. Recent studies demonstrate that perivascular adipose tissue (PVAT, a tissue that surrounds the endothelial layer) relates to endothelium-dependent vasoregulation and inflammation by secreting a variety of substances that affect vascular tone and infiltration of inflammatory cells (Qi *et al.*, 2018). Because this tissue is related to insulin resistance, controls vascular function and is located within insulin target tissues, it may well contribute to the pathogenesis of type 2 diabetes (Meijer *et al.*, 2011). In fact, adipokines and inflammatory products of adipose tissue associated with the vasculature, denominated PVAT, have been shown to control insulin sensitivity and vascular function (Gollasch, 2012).

Recent evidence suggests that PVAT alters the balance between endothelium-dependent vasodilator and vasoconstrictor substances, such as NO and endothelin-1. In fact, PVAT could modify vascular reactivity by secreting adipokines, some of which are known to influence vasoreactivity (Meijer *et al.*, 2011). For example, leptin is a hormone, released from the adipose tissue, that can influence both endothelium-dependent and independent vasodilation; adiponectin is also a hormone responsible for vasorelaxation, either by stimulating NO production or by activating potassium channels, which cause hyperpolarization accompanied by reduced influx of extracellular calcium into smooth muscle cells, therefore decreasing contraction (Lohn *et al.*, 2002); and IL-6 is a cytokine that reduces the vasorelaxant effect of PVAT due to increased ROS and decreased NO production (Maenhaut and Voorde, 2011).

Although, obesity affects the homeostasis of adipose tissues, among other effects. With this disorder, perivascular adipocytes increase in size, creating a hypoxic environment, which attenuates the anticontractile properties that are subliminal to PVAT (Meijer *et al.*, 2011). Therefore, we suggest that PVAT may hold one of the keys to effective future treatment or prevention of both insulin resistance and cardiovascular disease in obesity.

Another factor involved on the inflammatory process of the endothelium is, as mentioned before, endothelin-1, which stimulates the production of inflammatory cytokines, increases oxidative stress and influences several crucial steps in the inflammatory component of atherosclerosis (Maenhaut and Voorde, 2011). Moreover, this includes increasing the release of various cytokines from monocytes and enhancing the uptake of LDL cholesterol by these cells, promoting a phenotypic change in foam cells. Cytokines released from monocytes/macrophages, in turn, stimulate ET-1 production, providing positive feedback for further cytokine production. It has been well documented that vascular endothelin-1 production is elevated in atherosclerosis, an inflammatory disease, and influences the development of atherosclerotic lesions through a variety of mechanisms (Schneider *et al.*, 2007).

In a normal and healthy situation, ET-1 acts on ET_A receptors, mainly located on vascular smooth muscle cells, increasing arterial blood pressure and causing potent and long-lasting vasoconstriction in pulmonary, renal, splanchnic, myocardial, and skeletal muscle vasculatures. Similarly, activation of ET_B receptors on endothelial cells cause release of NO and PGI2 but, in contrast, stimulation of the vascular smooth muscle cell ET_B receptor results in vasoconstriction. On the other hand, plasma ET-1 concentrations have been reported to be elevated in patients with hypertension and type 2 diabetes and have been demonstrated to activate macrophages, resulting in the release of TNF-α, IL-1, IL-6 and IL-8, which are related to the atherosclerotic process (Böhm and Pernow, 2007).

Looking forward to adding new insights on PVAT and its connection with endothelial dysfunction, we worked on two different models. On the first one, we induced a diabetic state on Wistar rats and evaluated the role of the perivascular adipose tissue on this disease, while on the second one we induced protein glycation that, expectedly, promotes endothelial dysfunction. Moreover, it was used, for our study, high-fat diet that not only causes the visible adiposity and obesity, but it also induces temporal changes in structural membrane lipids, suggesting dynamic alterations in physical membrane bilayer properties in the liver. These effects might have an impact on the physiology of cells and cell organelles, on cellular energy metabolism and, thereby, contribute to insulin resistance. Previous studies indicate that alterations on the respiratory chain complex activity or mitochondrial β-oxidation capacity in liver, produced by a fat-rich diet have been linked to the development of hepatosteatosis, hepatic insulin resistance, and type 2 diabetes (Kahle *et al.*, 2014).

Several factors may contribute to alterations in lipid metabolism, including insulin deficiency or resistance, adipokines, and hyperglycemia. Insulin resistance activates intracellular hormone-sensitive lipase which, by several of the following processes, leads to cholesterol efflux contributing, therefore, for the development of atherosclerotic plaques (Schofield *et al.*, 2016). The high-fat diet itself, given to Wistar rats on our study, increased adiposity and promoted vascular dysfunction. As expected, the animals had a fast increment of body weight and a severe decrease of HDL cholesterol, accompanied by a slight rise of total cholesterol. This way, levels of LDL cholesterol were increased and, most likely, induced endothelial dysfunction, contributing to inflammation in the endothelium (Kolluru *et al.*, 2011).

Levels of triglycerides and phospholipids were increased on WHFD especially due to the diet effect. In addition, exposure to chronic fat intake expands hepatic lipid stores and impairs hepatic insulin action, therefore leading to hepatic insulin resistance (Kahle *et al.*, 2014). In fact, the group WHFD has shown increased values of AST, ALT, alkaline phosphatase and

gamma-GT, which are enzymes that reflect liver damage and inflammation and, the last one, oxidative stress (Ko *et al.*, 2015).

Moreover, GTT and ITT were performed in order to determine glucose and insulin tolerance, reflecting impaired β-cell function and insulin resistance (Nagy and Einwallner, 2018). In fact, WHFD demonstrated a slight level of intolerance, presumably due to the harmful effect obesity has in general system inflammation, especially in the liver.

On isometric tension studies, the high-fat diet-fed group induced macrovascular dysfunction. Previous studies have shown that diet-induced obesity results in hypertension associated with elevated systemic concentrations of angiotensin peptides, therefore enhancing responsiveness of the artery to various contractile agonists (Kari *et al.*, 2007). Moreover, we were able to demonstrate that HFD alone was able to induce a significant decrement in ACh-induced vasodilation, with minor effects on the dose-response to endothelin-1.

When testing the action of inhibitors of vasorelaxant factors (such as nitric oxide and PGI2), using L-NAME + indomethacin, we verified that both WC_0 and WHFD groups were able to release vasorelaxant compounds, therefore suggesting that about 20 % of relaxation is due to substances other than NO and PGI2 (Kellogg *et al.*, 2005). Although, this data is also proof that the main vasodilator acting on smooth muscle cells is nitric oxide.

Regarding the effect of PVAT, it is already known that, in healthy subjects, it exerts anticontractile properties due to release of substances such as NO, leptin and adiponectin (Oriowo, 2015). One of our goals was to determine at which point the high-fat diet itself would have harmful effects on the normal PVAT activity. In fact, on WC_0, the presence of PVAT conferred 5 % more relaxation on endothelium-dependent vasodilation, indicating that this adipose tissue secreted vasodilating molecules to enhance the relaxation. Although, regarding the PVAT response to ACh, after contraction with phenylephrine, we observe that its anticontractile functions are lost on WHFD group, possibly due to a reduction in PVAT-derived adiponectin release. HFD-induced obesity likely impairs PVAT-mediated anticontractile effects by promoting proinflammatory shift in cytokines and chemokines associated with oxidative stress in this tissue (Gil-Ortega *et al.*, 2015).

In endothelium-independent vasodilation, mediated by SNP, it seems that PVAT presence does not affect vascular smooth muscle function. Besides the fact that SNP is a very potent inducer of vasodilation, it is also important to notice that the mechanism in which PVAT exerts its anticontractile properties involves hydrogen peroxide, that can easily diffuse to underlying smooth muscle cells and induce vasodilatation (Xia and Li, 2017). Moreover, H_2O_2 is one of the ROS that is enhanced in obesity, so there is no decrease in its bioavailability (Aprioku, 2013). Even so, PVAT does not seem to affect endothelium-independent vasodilation in WHFD.

Incubation of the aortic rings with L-NAME and indomethacin and comparing the dose-responses to ACh with previous contractions with PHE enable to inhibit the NO and PGI2 vasodilation component in the different groups. In fact, we observe a relaxation of less than 20 %, on WC_0+PVAT, with the effect of L-NAME and indomethacin. Such data can lead us to conclude that PVAT-induced vasodilation is very dependent on NO-bioavailability and synthesis. Moreover, the dose-response to ACh in aortic rings mounted with PVAT has been shown to be impaired in WHFD group, which is also consistent with the data from the NO-independent vasodilation.

Finally, we tested the effect of a potent vasoconstrictor, endothelin-1, on PVAT and concluded that this tissue only resembles beneficial properties on healthy subjects, since it prevented aortic rings from WC_0 to have an enhanced contraction. Although, a similar effect can be observed on WHFD+PVAT. In fact, the presence of PVAT on this group protected the aortic ring from an accentuated contraction. We believe that, since PVAT-derived ET-1 is enhanced due to the high-fat diet, the tissue does not have a very increased reaction to this substance, therefore leaving the contraction level near the basal. Moreover, we must also consider that, due to increased levels of H_2O_2, a ROS, the vascular contraction is attenuated.

At the end, we strongly associate high-fat diet, which has become a classic western type diet, to insulin resistance and endothelial dysfunction. Furthermore, the induced overweight on Wistar rats did cause liver inflammation (increased transaminases and alkaline phosphatase), glucose and insulin intolerance and a great predisposition for the development of atherosclerosis. Besides, the HFD itself was able to cause increase and subsequent dysfunction of the perivascular adipose tissue, which has been shown to participate in mechanisms of vascular regulation. While, in healthy subjects, this tissue displays anticontractile actions, by releasing vasodilating molecules, in obese subjects it causes impaired release of vasoactive compounds. As a cycle, dysfunctional PVAT causes enhanced endothelial dysfunction.

Finally, we were able to determine the conditions involved on the switch from beneficial to harmful effects of PVAT: the high fat diet was the determinant factor that led to endothelial dysfunction and possibly, among others, increase of adipose tissue, causing hypoxia followed by macrophage infiltration, and insulin resistance, therefore being responsible for low-grade inflammation.

4.1. High-fat low STZ dose-induced diabetes model

We developed an animal model of type 2 diabetes with a high-fat diet and low doses of STZ. In fact, the model had common and different features relative to others previously described. As mentioned earlier, Wistar rats started the high-fat diet at two months-old, since early changes of diet can cause adaptations and minor changes to the overall phenotype. After the fourth month, and with two weeks in between, we performed three intraperitoneal injections of streptozotocin (STZ) with a concentration of 35 mg/kg. In result, we successfully induced type 2 diabetes in these animals.

We assumed, at first, that our model led to a destruction on β-pancreatic cells higher than the expected for type 2 diabetes. In fact, results indicate a fast gain of weight on animals treated with high-fat diet, as expected, but, surprisingly, as soon as the treatment with streptozotocin began on the WHFDSTZ group, the animals started to lose weight. Accordingly, we presumed that β-cells destruction was such that we induced type 1 diabetes instead, therefore leading to muscle, protein and adipose tissue breakdown, which would cause weight loss. Nevertheless, we were able to associate this harm to the toxic effects of the compound.

As previously mentioned, type 2 diabetes *mellitus* causes amplification of the atherosclerotic process, which is intimately related to elevated cholesterol levels and insulin resistance (Kolluru *et al.*, 2011). In fact, both WHFD and WHFDSTZ had increased level of total cholesterol, while presenting a reduction on HDL levels. On WHFDSTZ, the percentage of non-HDL cholesterol is quite elevated, providing a greater predisposition for atherosclerosis. Furthermore, the ratio between HDL and total cholesterol, represented by the atherogenic index, demonstrates a great predisposition for the development of atherosclerosis.

The diabetic model presented high levels of triglycerides. In fact, accumulation of triglycerides in liver and muscle are considered a major contributor to insulin resistance in these organs, and triglycerides stored in the pancreas may cause the inability of the β-cell to fully compensate for insulin resistance, therefore resulting in amplification of type 2 diabetes-like damage (Burhans *et al.*, 2019). In terms of phospholipids, it is known that they influence insulin action in many ways, including regulating insulin secretion in pancreatic cells, mediating insulin action on skeletal muscle and adipocytes and modulating gene expression related glucose uptake, as well as controlling mitochondrial dynamics (Chang *et al.*, 2018). Therefore, it is understandable that high-fat diet causes insulin resistance and glucose tolerance.

Our data demonstrates, not only by biochemical methods but also by observing the steatosis in livers (clearly observed by a macroscopic change in color and accumulation of fat), that these Wistar rats have developed severe liver damage caused, mostly, by the STZ treatment

and high-fat diet. Accordingly, high levels of liver enzymes ALT, AST, alkaline phosphatase and gamma-GT are predictive of several disease and all-cause mortality and can reflect liver injury, fatty liver and oxidative stress (Beek *et al.*, 2013). AST and ALT blood levels increase when the liver cell membrane is damaged and, thus, mark hepatocellular injury, which is exactly what was observed on STZ-treated group, where the levels were tremendously higher compared to WC_0 and WHFD and the liver was visually swollen. In addition, the levels of the two other biomarkers, alkaline phosphatase and gamma-GT, also extensively increased in WHFDSTZ, indicate severe liver damage.

To make sure we successfully induced type 2 diabetes in this Wistar rat group, a few tests were performed. Random glycemia was measured and was, in fact, much higher that 200 mg/dL, which is consistent with diabetes. Moreover, fasting glycemia also confirms diabetes, since it was higher than 126 mg/dL. In addition, glucose and insulin tolerance tests were also important not only to reinforce the diabetic state, but also to verify impaired glucose and insulin tolerance. Alterations in the normal function of pancreas and liver are shown by GTT through delayed reaction in insulin secretion from the pancreas, with consequent delayed absorption of glucose; and by ITT through the curve on which blood glucose concentrations fall after insulin administration, which showed a slow and ineffective glucose uptake, by peripheral tissues, 2h after the test. In conclusion, WHFDSTZ group was, indeed, diabetic with an elevated degree of insulin resistance.

An important feature of endothelial dysfunction is the inability of arteries to optimally dilate in response to an appropriate stimulus by vasodilators acting on smooth muscle. This endothelial dysfunction is especially associated with decreased NO bioavailability, as explained before (Kolluru *et al.,* 2011). Isometric tension studies were performed comparing the different groups.

On endothelium-dependent vasodilation, the maximum relaxation observed in response to ACh is around 50%, corroborating this state of endothelial dysfunction in WHFDSTZ. Furthermore, the presence of perivascular adipose tissue worsened the response to this signaling molecule, as the curve of WHFDSTZ+PVAT has a maximum relaxation of 30 %. Therefore, we can notice that the presence of PVAT decreases endothelial function, with following pejorative consequences on vessels. In addition, vascular inflammation is a prominent feature of diabetes and it has been reported that macrophages accumulate in the vascular wall, creating a cycle of cause-effect of endothelial dysfunction. It is quite possible that the reduced vasodilation observed in the presence of PVAT, in dysfunctional animals, is due to an accumulation of pro-inflammatory factors released by the macrophages, such as TNF-α, which then exerts a pro-contractile effect by a mechanism involving generation of reactive oxygen species and angiotensin II (Oriowo, 2015).

Only small differences were observed on the endothelium-independent vasodilation, mediated by SNP. Moreover, the EC_{50} value is lower for WHFDSTZ-PVAT, when comparing to WHFDSTZ+PVAT, unlike WC_0 and WHFD groups. Therefore, we hypothesize that, regarding PVAT, high-fat diet is not enough to cause changes in endothelium-independent vasodilation, but diabetes is. Furthermore, we can conclude that the perivascular adipose tissue secretes vasocontractile factors under a diabetic state, therefore delaying SNP-mediated vasodilation.

Concerning the L-NAME + indomethacin inhibition protocol, it is possible to notice that, even with a delayed response to ACh, WHFDSTZ-PVAT achieves the same level of maximum relaxation as the other two groups, which is about 25 %. This way, we can say that about one quarter of the vasodilation on this group is mediated by molecules other than NO and PGI2. Furthermore, these results also indicate that such molecules can still be produced and act on smooth muscle cells in animals with diabetes *mellitus*. Moreover, the presence of PVAT on this group completely abolished the relaxation, demonstrating that only vasoconstrictor substances were released from this tissue, even in response to acetylcholine.

In type 2 diabetes *mellitus*, there is an increased production of vasoconstrictor molecules rather than vasodilators. This way, high levels of contraction are expected, when performing a dose-response to ET-1, on the STZ-treated group. However, we observed the opposite effect, where the curve WHFDSTZ-PVAT reaches the least contraction, compared to WC_0 and WHFD. In fact, previous studies have demonstrated that it is possible that high glucose concentrations, which occur in diabetes, may affect responsiveness to ET-1. Indeed, it is possible that the reduced response to ET-1 may be a manifestation of an adaption of the vasculature to high levels of circulating blood glucose (Hodgson and King, 1992). Moreover, it is also possible that the decreased contractile response to ET-1 may be due, primarily, to a desensitization of ET_A receptors, possibly due to elevation in the plasma endothelin-1 level (Makino and Kamata, 1998). Similarly, the perivascular adipose tissue does not intensify the response to endothelin-1, as expected from a dysfunctional PVAT. In fact, we presume that there is such damage on this tissue explaining its responsiveness to this stimulus.

Adequate and proper β-cell function is critical for the appropriate metabolism of insulin. Data from literature suggest that, in type 2 diabetes, the decrease in β-cell mass is around 40 to 60 % (Leibowitz *et al.*, 2011; Cerf, 2013). Therefore, we expected that our STZ-induced type 2 diabetes would not exceed nor be inferior to those values of β-cell destruction. Although, not only this percentage is important to understand the effects of streptozotocin, but also the general aspect of the endocrine pancreas.

All shape, surrounding and composition of each islet of Langerhans, on WC_0 group, are well-defined. Moreover, marked cells with the antibody anti-insulin show an intensified labeling for this hormone, as expected on a healthy group of animals. On WHFD we noticed a few differences from the control group. In fact, the labeling of insulin is not affected, possibly due to the primary effect that hyperglycemia has on pancreas, which includes hyperplasia and hypertrophy in order to compensate for the insulin resistance that this group exhibits. Although, islets structures have changed to fibrous connective tissue. In fact, according to the literature, long-term HFD intake increases the concentration of TAGs in the pancreas, which are further broken down to produce FFAs, that, in turn, can obstruct the pancreatic capillary network, cause vascular endothelial injury and stimulate collagen synthesis (Ye *et al.*, 2018; Zhang *et al.*, 2008).

On the images obtained from WHFDSTZ pancreas, we can observe that the physiological compensation mechanism did regress, leading to islets destruction, in general, and decreased insulin labeling. In fact, the structure of islets of Langerhans, on this group, is visually disorganized, with fibrous tissue and decrease in β-cells mass. Moreover, our data indicates that we induced a destruction of nearly 50 % on these cells, observed by the quantification of the intensity of the brown staining for insulin.

At the end, we were able to develop a new model of induced type 2 diabetes in Wistar rats, which had a significant reduction of about 50 % of β-cell mass. Furthermore, hyperglycemia, dyslipidemia, endothelial dysfunction and severe liver damage were major features observed in our animal model. Importantly, insulin resistance is a condition strongly associated with diabetes *mellitus* and related to endothelial dysfunction. Moreover, in insulin resistance, the main pathway involved in insulin signaling transduction is the MAPK pathway, which is responsible for stimulating secretion of ET-1 and ROS, therefore leading to enhanced vasoconstriction and oxidative stress, respectively. Together with endothelial dysfunction, these conditions initiate vascular dysfunction, which may result in macrovascular complications, such as cardiovascular disease. In fact, the most important contributor factor is reduced NO bioavailability.

We were able to determine that, in type 2 diabetes, arteries mounted with PVAT displayed 30 % of maximum relaxation in response to ACh, a dramatic decrement in comparison with healthy controls. Importantly, we could verify that PVAT harms endothelium and vascular structure and properties, in this dysfunctional diabetic state. The anticontractile-like feature observed was on the dose-response do endothelin-1 remains, probably due to the adaptation to already increased plasma ET-1 concentrations. PVAT has shown to be totally dysfunctional in type 2 diabetes, creating a positive feedback on several factors acting on the endothelium.

4.2. Animals models treated with MG

The present study shows that exogenous administration of methylglyoxal leads to significant damage on the vasculature, therefore being responsible for endothelial dysfunction. Moreover, MG induces glycation in major matrix proteins, increasing the extracellular matrix area and protein crosslinking, which results in increased stiffness of the vasculature. In addition, this compound also affects proteins in adipose tissue, impairing secretion of hormones and vascular modulators (Singh *et al.*, 2014).

It was mentioned before that dietary advanced glycation-end products (AGEs) can cause liver inflammation, and consequently, loss of the organ essential properties, accompanied by increased levels of triglycerides and LDL (Patel *et al.*, 2012). Moreover, accumulation of AGEs is associated with impaired insulin signaling, which is related to decreased glucose tolerance, increased FFAs and insulin resistance. Therefore, we expected to observe diabetes-like complications. However, it is important to say that methylglyoxal supplementation (frequently occurring with western type diets) and high-fat diet separately had no major effects on insulin receptor levels. In contrast, together they induced a significant decrease of the activated insulin receptor form (Rodrigues *et al.*, 2017).

Methylglyoxal supplementation, accompanied by high-fat diet, led to a constant increasing weight on Wistar rats. In terms of cholesterol, levels of HDL abruptly decreased, while total cholesterol raised. This way, we can associate this increase of non-HDL cholesterol to the harmful role that AGEs play in the liver. The ratio between HDL and total cholesterol, which reflects the predisposition for the development of atherosclerosis, AI, is quite elevated, compared to the normal values on the control group, and even compared to the WHFD group. Furthermore, we can conclude that MG has an emphasized effect on the atherosclerotic process.

As MG is an important AGEs precursor, and together with high-fat diet, it is responsible for liver inflammation. Understandable, besides increased levels of non-HDL and AI, triglycerides and phospholipids also behold an increment. Similarly, liver damage markers, AST, ALT and gamma-GT, were increased on WHFDMG group. Interestingly, alkaline phosphatase was higher than WC_0, but lower than WHFD group. In fact, Baskaran and Balasubramanian, 1990, had proven that methylglyoxal decreases alkaline phosphatase activity, by interfering with protein thiol and amino groups.

Glucose tolerance test reveals a certain unbalance on glucose homeostasis but, more importantly, insulin tolerance test proves a delayed insulin action, thereby proving that MG supplementation is responsible for insulin resistance. Next, studies to determine endothelial dysfunction were done.

The endothelium-dependent vasodilation is quite affected by methylglyoxal, since the maximum relaxation obtained in response to ACh for WHFDMG group was about 30 %. Although, this data is not all surprising, as it is already known that AGEs can decrease NO synthesis and bioavailability by several pathways (Liu *et al.,* 2017; Brouwers *et al.,* 2010). In addition, the presence of perivascular adipose tissue leads to an endothelial-dependent relaxation much more compromised than WC_0 or even WHFD groups, with a maximum relaxation of 20 %. This way, we can immediately conclude that, in MG-treated Wistar rats fed with high-fat diet, PVAT is very dysfunctional. According to the literature, glycation impairs adipose tissue capillarization and blood flow, hampering its expandability during a high-fat diet-treatment and leading to hypoxia and insulin resistance (Rodrigues *et al.*, 2017). Therefore, the benefic properties that PVAT has proven to own are impaired with both HFD and MG-treatment.

Concerning the endothelium-independent vasodilation, we noticed that the lower value of EC_{50} is given to WHFDMG-PVAT. In fact, the absence of the perivascular adipose tissue leads to rapid and maximum vasodilation, demonstrating great sensitivity to the NO-donor, SNP. Although, the presence of PVAT reflects its pro-contractile function on the MG-treated group. Furthermore, on WHFD+PVAT we did not observe any difference on the curve profile when comparing to WC_0+PVAT, therefore leading us to conclude that high-fat diet did not cause impaired endothelium-independent vasodilation. Although, as WHFDMG+PVAT seems to have a different profile than these other two curves, indicating that the perivascular adipose tissue secretes vasocontractile factors under advanced glycation, and other consequences from MG-supplementation, therefore delaying SNP-mediated vasorelaxation.

When testing the inhibition of vasodilating factors, such as NO and PGI2, we noticed that the maximum relaxation obtained on WHFDMG group were 20 and 10 % for the absence and presence of PVAT, respectively. Since the values of final arterial dilation did not change much from the endothelium-dependent vasodilation, we can conclude that only a very small portion is due to vasodilation induced by NO, and the majority is mediated by other factors. NO-bioavailability and synthesis are remarkably affected on this group. Moreover, since PVAT secretes vasoconstrictor factors under pathological situations, the result obtained on its decreased vasorelaxation was already expected.

Performing the dose-response do endothelin-1, we were able to notice many similarities between all the groups involved. In fact, the curve WHFDMG-PVAT is slightly above the control group and under the high-fat diet group, inferring that methylglyoxal does not seem to have marked effects. Indeed, decreased NO and PGI2 production seem to have more effect than direct increased ET-1 expression on endothelial cells. Moreover, the presence of PVAT does not appear

to affect the ET-1-mediated vasoconstriction, since WHFDMG+PVAT has the same profile and maximum contraction as the WC_0+PVAT.

At the end, we were able to associate accumulation of glycation-end products, induced by MG, to endothelial dysfunction. It was already known that this compound could cause stiffness of the vasculature, but the exact mechanisms through which it could induce endothelial and PVAT changes were still unclear. As mentioned before, high-fat diet itself seems to be enough to cause damage on PVAT, but we assume that the use of additives like MG inducing AGEs formation might lead to irreversible loss of PVAT features.

MG was responsible for an abrupt enhanced atherogenic index, dyslipidemia, liver inflammation and insulin resistance. Moreover, it impaired vascular normal vasodilation by 50 % and, comparing to the previously impaired vascular dilation (on the high-fat diet-fed rats), MG worsen the relaxation by 40 %. Therefore, we could conclude that NO-mediated vasodilation is significantly impaired on rats with MG supplementation, by at least more than half of its bioavailability. Furthermore, the presence of PVAT decreases the response to vasodilating factors, therefore we believe that the tissue reflects, now, pro-contractile features. In conclusion, we had proven that MG causes PVAT dysfunction more accentuated that only HFD. Moreover, methylglyoxal affects especially NO-mediated vasorelaxation.

Previous studies have shown that MG supplementation on diet increases the formation of stable MG adducts that are partially absorbed to the bloodstream, accumulate in different tissues and cause diabetes-like microvascular lesions (Rodrigues *et al.*, 2017). Curiously, the effects produced by this compound on the endothelium layer are quite similar to those on the diabetic model induced by streptozotocin.

Liver damage was more pronounced on the diabetic model, a conclusion not only stated based on the values of liver damage markers, but also from the hepatosteatosis observed *post-mortem.* Nevertheless, MG-treated rats also presented hepatomegaly (swollen liver) and steatosis aspect. Moreover, we believe that insulin resistance in association with an atherogenic lipid profile were the trigger that, in both models, developed endothelial complications. Although, NO-mediated vasodilation was 20 % more affected on WHFDMG, demonstrating that AGEs are quite effective at decreasing NO bioavailability and also to reduce PGI2 production and increase ET-1 expression. In terms of PVAT features, both models aggravated endothelial dysfunction, though it seems to be worsened in type 2 diabetes. In conclusion, both models demonstrate severe endothelial and perivascular adipose tissue dysfunction, caused by persistent either hyperglycemia or glycation-end products.

Chapter 5

Conclusions

Type 2 diabetes, as it is well known, causes intensification of the atherosclerotic process, endothelial cell dysfunction and glycosylation of extracellular matrix proteins, due to chronic hyperglycemia (Kolluru *et al.*, 2011). Advances in understanding the vascular pathology of diabetes have made it clear that the pathogenesis of diabetic vascular complications is determined by a balance between molecular mechanisms of injury and endogenous protective factors (Madsen and King, 2013). Moreover, dysfunction of the endothelium can be worsened by obesity, which is classified as an increase of total body weight mostly due to growth of adipose tissue. In fact, the largest proportion is attributed to white adipose tissue (WAT) which, under this condition of hyperplasia and hypertrophy, produces large amounts of inflammatory molecules and creates resistance to hormones like insulin and leptin.

In obesity, perivascular adipose tissue (PVAT) is also increased in volume and the environment here developed involves hypoxia, oxidative stress and infiltration of immune cells with production of pro-inflammatory adipokines, cytokines and chemokines. Hence, these substances contribute to the progress of atherosclerosis, reflecting the endothelial cell dysfunction. For a long time, the main function of PVAT was thought to be providing mechanical support to the vessels. Moreover, recent studies indicate that the tissue actually regulates vascular homeostasis, since it attenuates agonist-induced vasoconstriction on the endothelium. Due to its capacity of producing a large number of vasorelaxant molecules, including hydrogen peroxide, angiotensin 1-7, adiponectin, NO and leptin, PVAT is known for its anticontractile properties on vessels. However, under stress conditions, such as hyperglycemia, chronic inflammation, hypoxia and others, this tissue tends to lose its qualities and reverse its beneficial effects to harmful effects.

Therefore, one of the aims of this study relied on characterizing PVAT and identifying the conditions necessary for the switch from positive to negative effects on vascular function. Furthermore, we proposed to understand the potential pathogenic effect of PVAT on the vasculature and its long-term effects. For such purpose, we used two models, both fed with high-fat diet, in which 1) we induced type 2 diabetes and 2) we gave a supplement of methylglyoxal, that induced diabetes-like vascular lesions.

The presence of perivascular adipose tissue on vessels demonstrated, in our study, advantageous anticontractile properties on control group. In fact, the relaxation observed with dose-responses to ACh and SNP was higher than in the aorta without PVAT, proving the right balance between vasodilators and vasoconstrictors secreted by this tissue. On the other hand, the high-fat diet induced an intensified insulin resistance and consequent endothelial dysfunction. Our results show that, in the presence of PVAT, the arterial rings have 30 % less relaxation than the PVAT-free aorta. Therefore, we can conclude that this high-fat diet induced PVAT modifications able to promote vascular dysfunction just by itself. In fact, we proved that the

high-fat diet was the switch on PVAT from beneficial to harmful properties. Therefore, this type of western type food has shown to be behind obesity, diabetes-like complications and microvascular problems that might be irreversible with increased intake of HFD and sedentary lifestyle. Unsurprisingly, overweight and disease associated with endothelial dysfunction are increasing worldwide mostly because of the processed food that, almost inevitable, we consume.

The model we developed with high-fat diet and low doses of STZ-induced type 2 diabetes was successful and the animals developed insulin resistance and further complications, that enable the studies of endothelial and PVAT dysfunction. Aortic rings extracted from WHFDSTZ had impaired vascular functions, since the endothelium was quite dysfunctional. Moreover, we were able to determine, both quantitatively and qualitatively, the consequences that a dysfunctional PVAT has on the endothelium and the progressive damages it can cause.

On WHFDMG we induced diabetes-like vascular complications, such as oxidative stress, endothelial dysfunction, atherogenic profile, insulin resistance, among others. Consequently, these factors contribute to systemic alterations and that was exactly what we observed. In fact, AGEs induced an extensive decrease in NO bioavailability by many mechanisms and favored a constriction environment. Therefore, we proved that MG causes endothelial dysfunction at a higher level than type 2 diabetes. Moreover, the perivascular adipose tissue changed its phenotype and became dysfunctional on MG-treated Wistar rats, so we assume that AGEs formation in adipose tissue is responsible, in addition, to insulin resistance and obesity.

Finally, we could notice a few similarities between the STZ-induced diabetes and the MG-treated models. In these animals, the decrease in vasorelaxation dependent on the endothelium is quite visible in arteries mounted with and without PVAT, revealing a condition of endothelial cell dysfunction that is worsened by the presence of damaged perivascular adipose tissue. Indeed, the unbalance between the production of NO and vasoconstrictors on PVAT exacerbates the vascular dysfunction.

In sum, we were able to determine the extent of damage that diabetes and diabetes-like vascular complications can cause on endothelial cells and perivascular adipose tissue. Indeed, PVAT plays a very important role on endothelium function with its vascular protective properties. However, the physiologic beneficial features can turn into a reversible metabolically active tissue that synthesizes pro-inflammatory cytokines and that it is related to vascular inflammation, playing a key role in vascular disease. In fact, we learned that the balance between positive and negative characteristics of PVAT is very sensitive, to the point of turning to a dangerous tissue after long periods of fat intake. We believe that increasing the knowledge about perivascular adipose tissue may, eventually, be used to develop therapies concerning diabetes or obesity-related pathologies.

Reference list

American Diabetes Association. (2020). Standards of medical care in diabetes- 2020. *Diabetes Care*. **43**: 14-31.

Al-Goblan, A., Al-Alfi, M. and Khan, M. (2014). Mechanism linking diabetes *mellitus* and obesity. *Diabetes, Metabolic Syndrome and Obesity: Targets and Therapy.* **7**: 587-591.

Aprioku, J. (2013). Pharmacology of free radicals and the impact of reactive oxygen species on the thesis. *Journal of Reproduction and Infertility*. **14:** 158-172.

Barthel, S., Gavino, J., Descheny, L. and Dimitroff, C. (2008). Targeting selectins and selectin ligands in inflammation and cancer. *Expert Opinion on Therapeutic Targets.* **11:** 1473-1491.

Baskaran, S. and Balasubramanian, K. (1990). Effect of methylglyoxal on protein thiol and amino groups in isolated rat enterocytes and colonocytes and activity of various brush border enzymes. *Indian Journal of Biochemistry and Biophysics.* **27:** 13-17.

Beek, J., Moor, M., Geus, E., Lubke, G., Vink, J., Willemsen, G. and Boomsma, D. (2013). The genetic architecture of liver enzyme levels: GGT, ALT and AST. *Behavior Genetics*. **43**: 329-339.

Bento, C., Fernandes, R., Matafome, P., Sena, C. Seiça, R. and Pereira, P. (2010). Methylglyoxal-induced imbalance in the ratio of vascular endothelial growth factor to angiopoietin 2 secreted by retinal pigment epithelial cells leads to endotelial dysfunction. *Experimental Physiology*. **95**: 955-970.

Berg, J., Tymoczko, J. and Stryer, L. (2012). *Biochemistry*. 7th edition, W. H. Freeman and Company. New York.

Bluestone, J., Herold, K. and Eisenbarth, G. (2010). Genetics, pathogenesis and clinical interventions in type 1 diabetes. *Nature*. **464**: 1293-1300.

Boden, G., She, P., Mozzoli, M., Cheung, P., Gumireddy, K., Reddy, P., Xiang, X., Luo, Z. and Ruderman, N. (2005). Free fatty acids produce insulin resistance and activate the proinflammatory nuclear factor-kappaB pathway in rat liver. *Diabetes*. **54**: 3458-3465.

Böhm, F. and Pernow, J. (2007). The importance of endothelin-1 for vascular dysfunction in cardiovascular disease. *Cardiovascular Research.* **76:** 8-18.

Bongarzone, S., Savickas, V., Luzi, F. and Gee, A. (2017). Targeting the receptor for advanced glycation end products (RAGE): a medicinal chemistry perspective. *Journal of Medicinal Chemistry*. **60:** 7213-7232.

Boucher, J., Kleinridders, A. and Kahn, C. (2014). Insulin receptor signaling in normal and insulin-resistant states. *Cold Spring Harbor Perspectives in Biology.* **6:** 1-12.

Brouwers, O., Niessen, P., Haenen, G., Miyata, T., Brownlee, M., Stehouwer, C., Mey, J. and Schalkwijk, C. (2010). Hyperglycemia-induced impairment of endothelium-dependent vasorelaxation in rat mesenteric arteries is mediated by intracellular methylglyoxal levels in a pathway dependent on oxidative stress. *Diabetologia*. **53**: 989-1000.

Brown, N., Zhou, Z., Zhang, J., Zeng, R., Wu, J., Eitzman, D., Chen, Y. and Chang, L. (2014). Perivascular adipose tissue in vascular function and disease: a review of current research and animal models. *Arteriosclerosis, Thrombosis, and Vascular Biology*. **34**: 1621-1630.

Cade, W. (2008). Diabetes-related microvascular and macrovascular diseases in the physical therapy setting. *Physical Therapy*. **88:** 1322-1335.

Cantley, J. and Ashcroft, F. (2015). Q&A: insulin secretion and type 2 diabetes: why do β-cells fail? *BCM Biology.* **13:** 33-40.

Cerf, M. (2013). Beta cell dysfunction and insulin resistance. *Frontiers in Endocrinology*. **4:** 37-49.

Chang, W., Hatch, G., Wang, Y., Yu, F. and Wang, M. (2018). The relationship between phospholipids and insulin resistance: from clinical to experimental studies. *Journal of Cellular and Molecular Medicine*. **23:** 702-710.

Chawla, A., Chawla, R. and Jaggi, S. (2016). Microvasular and macrovascular complications in diabetes *mellitus*: Distinct or continuum? *Indian Journal of Endocrinology and Metabolism.* **20:** 546-551.

Coelho, M., Oliveira, T. and Fernandes, R. (2013). Biochemistry of adipose tissue: an endocrine organ. *Archives of Medical Science*. **9**: 191-200.

Collier, B., Dossett, L., May, A. and Diaz, J. (2008). Glucose control and the inflammatory response. *Nutrition in Clinical Practice*. **23**: 3-15.

Czech, M., Tencerova, M., Pedersen, D. and Aouadi, M. (2013). Insulin signalling mechanisms for triacylglycerol storage. *Diabetologia*. **56:** 949-964.

Dam, A., Boon, M., Berbée, J., Rensen, P. and Harmelen, V. (2017). Targeting white, brown and perivascular adipose tissue in atherosclerosis development. *European Journal of Pharmacology*. **816**: 82-92.

Damjanov, I. (2008). *Pathophysiology*. 1st edition, Saunders, China.

Deryugina, E. and Quigley, J. (2012). Cell surface remodeling by plasmin: a new function for an old enzyme. *Journal of Biomedicine and Biotechnology*. **2012:** 1-21.

Dhar, A., Dhar, I., Jiang, B., Desai, K. and Wu, L. (2011). Chronic methylglyoxal infusion by minipump causes pancreatic β-cell dysfunction and induces type 2 Diabetes in Sprague-Dawley rats. *Diabetes*. **60:** 899-908.

Duncan, R., Ahmadian, M., Jaworski, K., Nagy, E. and Sul, H. (2010). Regulation of lipolysis in adipocytes. *Annual Review of Nutrition.* **27:** 79-101.

Fayfman, M., Pasquel, F. and Umpierrez, G. (2017). Management of hyperglycemic crises: diabetic ketoacidosis and hyperglycemic hyperosmolar state. *Medical Clinics of North America.* **101:** 587-606.

Fournet, M., Bonté, F. and Desmoulière, A. (2018). Glycation damage: a possible hub for major pathophysiological disorders and aging. *Aging and Disease.* **9:** 880-900.

Galley, H. and Webster, N. (2004). Physiology of the endothelium. *British Journal of Anaesthesia.* **93:** 105-118.

Genge, A., Blocki, A., Franke, R. and Jung, F. (2019). Vascular endothelial cell biology: an update. *International Journal of Molecular Sciences.* **20:** 4411-4433.

Gil-Ortega, M., Somoza, B., Huang, Y., Gollasch, M. and Fernández-Alfonso, M. (2015). Regional differences in perivascular adipose tissue impacting vascular homeostasis. *Trends in Endocrinology & Metabolism*. **26**: 367-375.

Gkogkolou, P. and Böhm, M. (2012). Advanced glycation end products: key players in skin aging? *Dermato-Endocrinology*. **4**: 259-270.

Gollasch, M. (2012). Vasodilator signals from perivascular adipose tissue. *British Journal of Pharmacology*. **165:** 633-642.

Guilherme, A., Virbasius, J., Puri, V. and Czech, M. (2008). Adipocyte dysfunctions linking obesity to insulin resistance and type 2 diabetes. *Nature Reviews Molecular Cell Biology.* **9**: 367-377.

Herder, C., Roden, M. (2010). Genetics of type 2 diabetes: pathophysiologic and clinical relevance. *European Journal of Clinical Investigation*. **41**: 679-692.

Hernández, A., Beneit, N., Castroverde, S. and Escribano, O. (2016). Differential role of adipose tissues in obesity and related metabolic and vascular complications. *International Journal of Endocrinology*. **2016**: 1-15.

Hildebrand, S., Stümer, J. and Pfeifer, A. (2018). PVAT and its relation to brown, beige, and white adipose tissue in development and function. *Frontiers in Physiology.* **9:** 70-80.

Hinsbergh, V. (2012). Endothelium- role in regulation of coagulation and inflammation. *Seminars in Immunopathology.* **34:** 93-106.

Hodgson, W. and King, R. (1992). Effects of glucose, insulin or aldose reductase inhibition on responses to endothelin-1 of aortic rings from streptozotocin-induced diabetic rats. *British Journal of Pharmacology*. **106:** 644-649.

Houten, S. and Wanders, R. (2010). A general introduction to the biochemistry of mitochondrial fatty acid β-oxidation. *Journal of Inherited Metabolic Disease.* **33:** 469-477.

International Diabetes Federation. (2019). *Diabetes Atlas*. 9th edition.

Itoh, M., Suganami, T., Hachiya, R. and Ogawa, Y. (2011). Adipose tissue remodeling as homeostatic inflammation. *International Journal of Inflammation*. **2011**: 720926-720934.

Jung, U. and Choi, M. (2014). Obesity and its metabolic complications: the role of adipokines and the relationship between obesity, inflammation, insulin resistance, dyslipidemia and nonalcoholic fatty liver disease. *International Journal of Molecular Sciences.* **15:** 6184-6223.

Kahle, M., Schäfer, A., Seelig, A., Schultheiß, J., Wu, M., Aichler, M., Leonhardt, J., Rathkolb, B., Rozman, J., Sarioglu, H., Hauck, S., Ueffing, M., Wolf, E., Kastenmueller, G., Adamski, J., Walch, A., Hrabé de Angelis, M. and Neschen, S. (2014). High-fat diet-induced modifications in membrane lipid and mitochondrial-membrane protein signatures precede the development of hepatic insulin resistance in mice. *Molecular Metabolism*. **4**: 39-50.

Kalapos, M. (1999). Methylglyoxal in living organisms: chemistry, biochemistry, toxicology and biological implications. *Toxicology Letters.* **110**: 145-175.

Kari, C., Gong, M., Akers, W., Guo, Z. and Cassis, L. (2007). Enhanced vascular contractility and diminished coronary artery flow in rats made hypertensive from diet-induced obesity. *International Journal of Obesity*. **31:** 1652-1659.

Kellogg, D., Zhao, J., Coey, U. and Green, J. (2005). Acetylcholine-induced vasodilation is mediated by nitric oxide and prostaglandins in human skin. *Journal of Applied Physiology*. **98:** 629-632.

Kitabchi, A., Umpierrez, G., Miles, J. and Fisher, J. (2009). Hyperglycemic crises in adult patients with diabetes. *Diabetes Care*. **32**: 1335-1343.

Ko, S., Baeg, M., Han, K., Ko, S. and Ahn, Y. (2015). Increased liver markers are associated with higher risk of type 2 diabetes. *World Journal of Gastroenterology*. **21**: 7478-7487.

Kolluru, G., Bir, S. and Kevil, C. (2011). Endothelial Dysfunction and Diabetes: Effects on angiogenesis, vascular remodeling, and wound healing. *International Journal of Vascular Medicine*. **2012**: 1-30.

Kubisz, P., Stančiaková, L., Staško, J., Galajda, P. and Mokáň, M. (2015). Endothelial and platelet markers in diabetes *mellitus* type 2. *World Journal of Diabetes*. **6**: 423-431.

Leibowitz, G., Kaiser, N. and Cerasi, E. (2011). β-cell failure in type 2 diabetes. *Journal of Diabetes Investigation.* **2:** 82-92.

Leon, B. and Maddox, T. (2015). Diabetes and cardiovascular disease: epidemiology, biological mechanisms, treatment recommendations and future research. *World Journal of Diabetes*. **6:** 1246-1258.

Liao, Y. and Hung, M. (2010). Physiological regulation of Akt activity and stability. *American Journal of Translation Research.* **2:** 19-42.

Liu, T., Zhang, L., Joo, D. and Sun, S. (2017). NF-κB signaling in inflammation. *Signal Transduction and Targeted Therapy*. **2:** 17023-17032.

Lohn, M., Dubrovska, G. and Lauterbach, B. (2002). Periadventitial fat releases a vascular relaxing factor. *The FASEB Journal*. **16**: 1057-1063.

Longo, M., Zatterale, F., Naderi, J., Parrillo, L., Formisano, P., Raciti, G., Beguinot, F. And Miele, C. (2019). Adipose tissue dysfunction as determinant of obesity-associated metabolic complications. *International Journal of Molecular Sciences*. **20**: 2358-2381.

Luévano-Contrera, C., Gómez-Ojeda, A., Macías-Cervantes, M. and Garay-Sevilla, M. (2017). Dietary advanced glycation end products and cardiometabolic risk. *Current Diabetes Reports*. **17**: 63-74.

Madsen, C. and King, G. (2013). Vascular complications of diabetes: mechanisms of injury and protective factors. *Cell Metabolism*. **17:** 20-33.

Maenhaut, N. and Voorde, J. (2011). Regulation of vascular tone. *BCM Medicine*. **9:** 25-37.

Majed, B. and Khalil, R. (2012). Molecular mechanisms regulating the vascular prostacyclin pathways and their adaptation during pregnancy and in the newborn. *Pharmacological Reviews.* **64:** 540-582.

Makino, A. and Kamata, K. (1998). Elevated plasma endothelin-1 level in streptozotocin-induced diabetic rats and responsiveness of the mesenteric arterial bed to endothelin-1. *British Journal of Pharmacology*. **123:** 1065-1072.

Manrique, C., Lastra, G. and Sowers, J. (2014). New insights into insulin action and resistance in the vasculature. *Annals of the New York Academy of Sciences*. **1311**: 138-150.

Martins, A., Nachbar, R., Gorjao, R., Vinolo, M., Festuccia, W., Lambertucci, R., Boaventura, M., Silveira, L., Curi, R., Hirabara, S. (2012). Mechanisms underlying skeletal muscle insulin resistance induced by fatty acids: importance of mitochondrial function. *Lipids in Health and Disease*. **11:** 30-41.

Meijer, R., Serne, E., Smulders, Y., Hinsbergh, V., Yudkin, J. and Eringa, E. (2011). Perivascular adipose tissue and its role in type 2 diabetes and cardiovascular disease. *Current Diabetes Report*. **11**: 211-217.

Michel, T. and Vanhoutte, P. (2010). Cellular signaling and NO production. *Pflugers Archiv: European Journal of Physiology*. **459:** 807-816.

Morón, E., Jiménez, Z., Marañón, A., Iannantuoni, F., López, I., Domènech, S., Salom, C., Jover, A., Mora, V., Roldan, I., Solá, E., Rocha, M. and Víctor, V. (2019). Relationship between oxidative stress, ER stress and Inflammation in type 2 diabetes: the battle continues. *Journal of Clinical Medicine*. **8**: 1385-1407.

Mueckler, M. and Thorens, B. (2013). The SLC2 (GLUT) family of membrane transporters. *Molecular Aspects of Medicine*. **34:** 121-138

Muniyappa, R. and Sowers, J. (2013). Role of insulin resistance in endothelial dysfunction. *Reviews in Endocrine and Metabolic Disorders.* **14**: 5-12.

Nagy, C. and Einwallner, E. (2018). Study of in vivo glucose metabolism in high-fat diet-fed mice using Oral Glucose Tolerance Test (OGTT) and Insulin Tolerance Test (ITT). *Journal of Visualized Experiments.* **131:** 1-12.

Natali, A., Toschi, E., Baldeweg, S., Ciociaro, D., Favilla, S., Saccà, L. and Ferrannini, E. (2006). Clustering of insulin resistance with vascular dysfunction and low-grade inflammation in type 2 diabetes. *Diabetes.* **55**:1133-1140.

Newsholme, P., Haber, P., Hirabara, S., Rebelato, E., Procopio, J., Morgan, D., Oliveira-Emilio, H., Carpinelli, A. and Curi, R. (2007). Diabetes associated cell stress and dysfunction: role of mitochondrial and non-mitochondrial ROS production and activity. *The Journal of Physiology*. **583:** 9-24.

Nigro, C., Leone, A., Fiory, F., Prevenzano, I., Nicolò, A., Mirra, P., Beguinot, F. and Miele, C. (2019). Dicarbonyl stress at crossroads of healthy and unhealthy aging. *Cells*. **8:** 749-776.

Nosalski, R. and Guzik, T. (2017). Perivascular adipose tissue inflammation in vascular disease. *British Journal of Pharmacology*. **174**: 3496-3513.

Oriowo, M. (2015). Perivascular adipose tissue, vascular reactivity and hypertension. *Medical Principles and Practice*. **24**: 29-37.

Ormazabal, V., Nair, S., Elfeky, O., Aguayo, C., Salomon, C. And Zuñiga, F. (2018). Association between insulin resistance and the development of cardiovascular disease. *Cardiovascular Diabetology*. **17:** 122-136.

Park, H. and Ahima, R. (2015). Physiology of leptin: energy homeostasis, neuroendocrine function and metabolism. *Metabolism*. **64**: 24-34.

Patel, R., Baker, S., Liu, W., Desai, S., Alkhouri, R., Kozielski, R., Mastrandrea, L., Sarfraz, A., Cai, W., Vlassara, H., Patel, M., Baker, R. and Zhu, L. (2012). Effect of Dietary Advanced Glycation End Products on Mouse Liver. *PLOS ONE*. **7:** 1-7.

Pessin, J. and Saltiel, A. (2000). Signaling pathways in insulin action: molecular targets of insulin resistance. *The Journal of Clinical Investigation*. **106**: 165-169.

Petrie, J., Guzik, T. and Touyz, R. (2018). Diabetes, hypertension, and cardiovascular disease: clinical insights and vascular mechanisms. *Canadian Journal of Cardiology*. **34:** 575-584.

Pitocco, D., Tesauro, M., Alessandro, R., Ghirlanda, G. and Cardillo, C. (2013). Oxidative stress in diabetes: implications for vascular and other complications. *International Journal of Molecular Sciences*. **14:** 21525-21550.

Potenza, M., Gagliardi, S., Nacci, C., Carratu, M. and Montagnani, M. (2009). Endothelial dysfunction in diabetes: from mechanisms to therapeutic targets. *Current Medicinal Chemistry*. **16**: 94-112.

Privratsky, J., Newman, D. and Newman, P. (2010). PECAM-1: conflicts of interest in inflammation. *Life Sciences*. **87:** 69-82.

Qi, X., Qu, S., Xiong, W., Rom, O., Chang, L. and Jiang, Z. (2018). Perivascular adipose tissue (PVAT) in atherosclerosis: a double-edged sword. Cardiovascular Diabetology. **17:** 134-154.

Rashid, G., Benchetrit, S., Fishman, D. and Bernheim, J. (2004). Effect of advanced glycation end-products on gene expression and synthesis of TNF-α and endothelial nitric oxide synthase by endothelial cells. *Kidney International*. **66**: 1099-1106.

Ravussin, E. and Galgani, J. (2015). The implication of brown adipose tissue for humans. *Annual Review of Nutrition*. **31:** 33-47.

Röder, P., Wu, B., Liu, Y. and Han, W. (2016). Pancreatic regulation of glucose homeostasis. *Experimental & Molecular Medicine*. **48:** 219-228.

Rodrigues, L., Matafome, P., Crisóstomo, J., Santos-Silva, D., Sena, C., Pereira, P. and Seiça, R. (2014). Advanced glycation end products and diabetic nephropathy: a comparative study using diabetic and normal rats with methylglyoxal-induced glycation. *Journal of Physiology and Biochemistry*. **70**: 173-184.

Rodrigues, T., Matafome, P., Sereno, J., Almeida, J., Castelhano, J., Gamas, L., Neves, C., Gonçalves, S., Carvalho, C., Arslanagic, A., Wilcken, E., Fonseca, R., Simões, I., Conde, S., Castelo-Branco, M. and Seiça, R. (2017). Methylglyoxal-induced glycation changes adipose tissue vascular architecture, flow and expansion, leading to insulin resistance. *Scientific Reports*. **7**: 1698-1711.

Romero, C., Sadidi, M. and Feldman, E. (2014). Mechanisms of disease: the oxidative stress theory of diabetic neuropathy. *Reviews in Endocrine and Metabolic Disorders*. **9:** 301-314.

Rui, L. (2014). Energy metabolism in the liver. *Comprehensive Physiology.* **4:** 177-197.

Samuel, V. and Shulman, G. (2016). The pathogenesis of insulin resistance: integrating signaling pathways and substrate flux. *The Journal of Clinical Investigation*. **126:** 12-22.

Saponaro, C., Gaggini, M., Carli, F. and Gastaldelli, A. (2015). The subtle balance between lipolysis and lipogenesis: a critical point in metabolic homeostasis. *Nutrients.* **7**: 9453-9474.

Sena, C., Leandro, A., Azul, L., Seiça, R. and Perry, G. (2018). Vascular oxidative stress: impact and therapeutic approaches. *Frontiers in Physiology*. **9**: 1668.

Sena, C., Matafome, P., Crisóstomo, J., Rodrigues, L., Fernandes, R., Pereira, P. and Seiça, R. (2012). Methylglyoxal promotes oxidative stress and endothelial dysfunction. *Pharmacological Research*. **65**: 497-506.

Sena, C., Pereira, A. and Seiça, R. (2013). Endothelial dysfunction - a major mediator of diabetic vascular disease. *Molecular Basis of Disease*. **1832**: 2216-2231.

Schneider, M., Boesen, E., Pollock, D. (2007). Contrasting actions of endothelin ET_A and ET_B receptors in cardiovascular disease. *National Institute of Health*. **47**: 731-759.

Schofield, J., Liu, Y., Rao-Balakrishna, P., Malik, R. and Soran, H. (2016). Diabetes dyslipidemia. *Diabetes Therapy.* **7:** 203-219.

Singh, V., Bali, A., Singh, N. and Jaggi, A. (2014). Advanced glycation end products and diabetic complications. *The Korean Journal of Physiology and Pharmacology.* **18:** 1-14.

Surmi, B. And Hasty, A. (2008). Macrophage infiltration into adipose tissue: initiation, propagation and remodeling. *Future Lipidol*. **3:** 545-556.

Szasz, T. and Webb, R. (2012). Perivascular adipose tissue: more than just structural support. *Clinical Science*. **122:** 1-12.

Taddei, S., Virdis, A., Ghiadoni, L., Salvetti, G., Bernini, G., Magagna, A. and Salvetti, A. (2001). Age-related reduction of NO availability and oxidative stress in humans. *Hypertension.* **38**: 274-279.

Tkacs, N., Herrmann, L. and Johnson, R. (2020). *Advanced physiology and pathophysiology-essencials for clinical practice*. 1st edition. Springer Publishing Company. United States of America.

Umpierrez, G., Murphy, M. and Kitabchi, A. (2002). Diabetic ketoacidosis and hyperglycemic hyperosmolar syndrome. *Diabetes Spectrum.* **15:** 28-36.

Villarroya, F., Cereijo, R., Gavaldà-Navarro, A., Villarroya, J. and Giralt, M. (2018). Inflammation of brown/beige adipose tissues in obesity and metabolic disease. *Journal of Internal Medicine*. **284**: 492-504.

Walker, C., Liu, N. and Xu, X. (2013). PTEN/PI3K and MAPK signaling in protection and pathology following CNS injuries. *Frontiers Biology.* **8:** 421-433.

Wilcox, G. (2005). Insulin and insulin resistance. *Clinical Biochemist Reviews.* **26:** 19-39.

World Health Organization. (2016). *Global Report on Diabetes*. France.

World Health Organization. (2020). Obesity and overweight. *WHO* https://www.who.int/news-room/fact-sheets/detail/obesity-and-overweight.

Xavier, G. (2018). The Cells of the Islets of Langerhans. Journal of Clinical Medicine. **7:** 54-71.

Xia, N. and Li, H. (2017). The role of perivascular adipose tissue in obesity-induced vascular dysfunction. *British Journal of Pharmacology*. **174**: 3425-3442.

Xu, B., Chibber, R., Ruggiero, D., Kohner, E., Ritter, J. and Ferro, A. (2003). Impairment of vascular endothelial nitric oxide synthase activity by advanced glycation end products. *The FASEB Journal*. **17**: 1289-1291.

Yao, D., Taguchi, T., Matsumura, T., Pestell, R., Edelstein, D., Giardino, I., Suske, G., Rabbani, N., Thornalley, P., Sarthy, V., Hammes, H. and Brownlee, M. (2007). High glucose increases angiopoietin-2 transcription in microvascular endothelial cells through methylglyoxal modification of mSin3A. *Journal of Biological Chemistry*. **282**: 31038-31045.

Yau, J., Teoh, H. and Verma, S. (2015). Endothelial cell control of thrombosis. *BCM Cardiovascular Disorders.* **15:** 130-141.

Ye, T., Chen, Y., Gao, J., Wang, X., Qiang, O., Tang, C. and Liu, R. (2018). Effect of octreotide on pancreatic fibrosis in rats with high-fat diet-induced obesity. *International Journal of Clinical and Experimental Pathology*. **11:** 4784-4794.

Zhang, D., Jiao, R. and Kong, L. (2017). High dietary fructose: direct or indirect dangerous factors disturbing tissue and organ functions. *Nutrients*. **9**: 335-360.

Zhang, H., Dellsperger, K. and Zhang, C. (2012). The link between metabolic abnormalities and endothelial dysfunction in type 2 diabetes: an update. *Basic Research in Cardiology*. **107:** 237-256.

Zhang, X., Cui, Y., Fang, L. and Li, F. (2008). Chronic high-fat diets induce oxide injuries and fibrogenesis of pancreatic cells in rats. *Pancreas*. **37:** 31-38.

Zhang, Z., Yan, J. and Shi, H. (2013). Hyperglycemia as a risk factor of ischemic stroke. *Journal of Drug Metabolism and Toxicology*. **4**: 153-165.